NPL

National Physical Laboratory

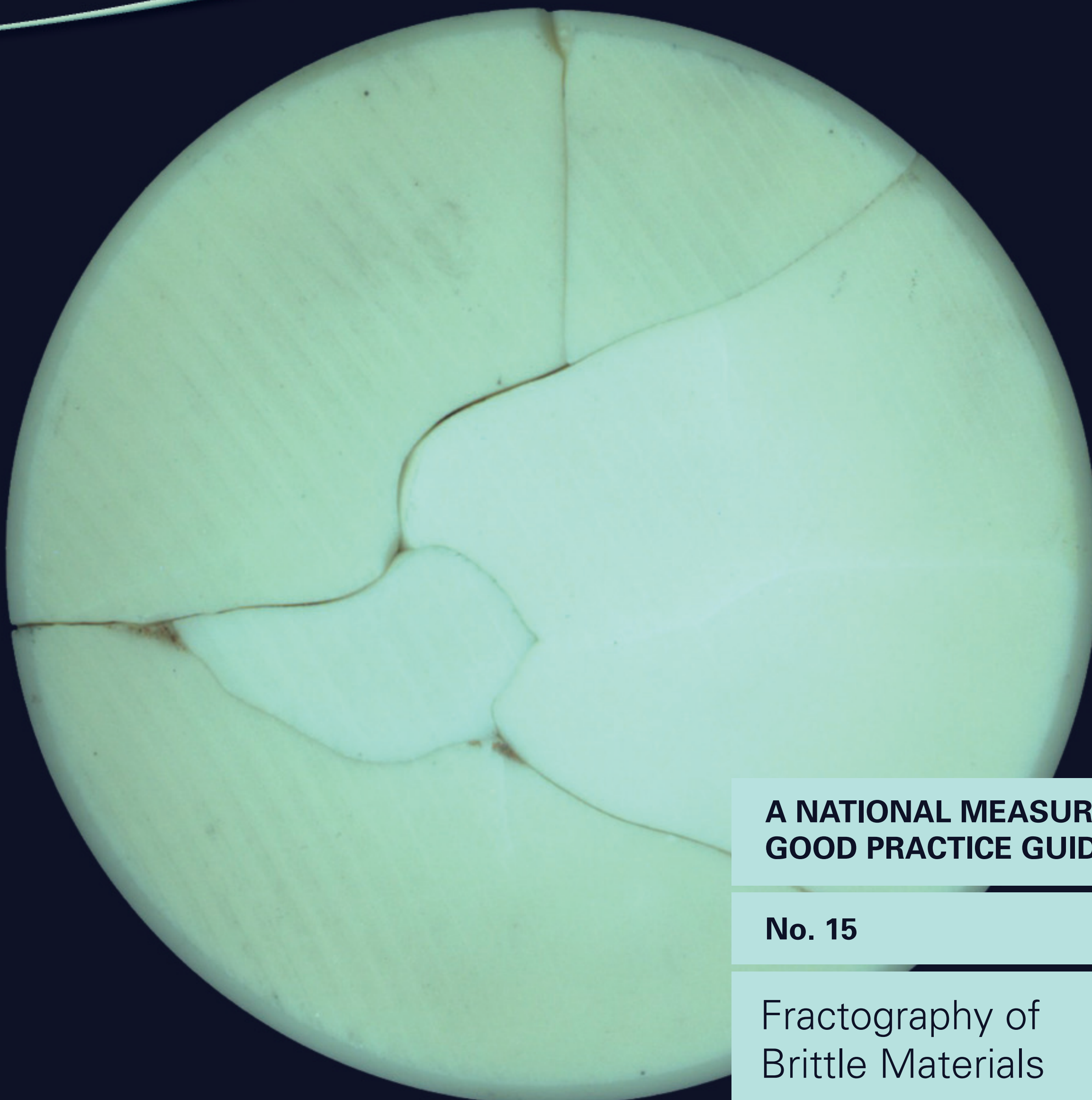

A NATIONAL MEASUREMENT GOOD PRACTICE GUIDE

No. 15

Fractography of Brittle Materials

Department for Innovation, Universities & Skills

Measurement Good Practice Guide No. 15

Fractography of Brittle Materials

Roger Morrell

Centre for Materials Measurement and Technology
National Physical Laboratory

Abstract: Fractography can tell us why something broke. It can help us understand material or processing limitations, what features of materials need to be removed in order to improve their mechanical properties, and, sometimes, who is to blame for something going wrong. However, although fractography is backed up by the science of fracture, there are aspects which are down to skill and knowledge of the person undertaking the study, particularly the ability to recognise fracture markings. Different people may come to different conclusions, based on their approach to examining fragments and their experience. This guide is intended to lay down the basis for observing the pattern of cracks and features on fracture surfaces of broken test-pieces and components made of brittle materials such as ceramics and hardmetals. It provides a simple procedure in the form of a series of steps to be adopted, and provides a wide range of examples of applying fractography to test-pieces and components.

ISSN 1386-6550

February 1999
(This electronic version created February 2008.)

National Physical Laboratory
Teddington, Middlesex, UK, TW11 0LW

Acknowledgements

This guide has been produced in a *Characterisation of Advanced Materials* project, part of the *Materials Measurement* programme sponsored by the Engineering Industries Directorate of the Department of Trade and Industry. The advice and steer from the Ceramics and Hardmetals Industrial Advisory Group in reviewing the guide are gratefully acknowledged.

The author would also like to acknowledge collaborations with George D. Quinn of the Ceramics Division, National Institute of Standards and Technology, Gaithersburg, Maryland, USA, and formerly of US Army Materials Laboratory, Watertown, Mass., USA, concerning earlier VAMAS round robin activities and the development of ASTM and CEN standards. Bryan Roebuck (NPL) is thanked for providing examples of hardmetal fracture surfaces. Lewis Lay and Simone Taylor (NPL) are thanked for assistance with preparing photographic material, for reviewing the manuscript and for offering helpful suggestions.

Particular thanks are due to Ray Wallis of John Crane UK Ltd for permitting Example A.4.4 to be included in this guide, and to those other organisations contributing examples, the sources of which must remain anonymous.

For further information on *Materials Measurement* contact the Materials Enquiry Point at the National Physical Laboratory:

Tel: 0181 943 6701
Fax: 0181 943 7160
E-mail: materials@npl.co.uk

Fractography of Brittle Materials

Contents

Executive summary

1. Objectives 1

2. Brittle fracture 1

3. Fracture origins 2

3.1 Introduction 2
3.2 Normal microstructure 3
3.3 Cracked grain boundaries 3
3.4 Abnormal microstructure 3
3.4.1 Large grains 3
3.4.2 Pores 5
3.4.3 Porous region 5
3.4.4 Agglomerates 5
3.4.5 Compositional inhomogeneities 5
3.4.6 Foreign material 5
3.4.7 Delaminations 6
3.5 Surface (extrinsic) origins 6
3.5.1 Pits, pocks, pores 6
3.5.2 Machining damage 6
3.5.3 Adventitious mechanical damage 6
3.5.4 Corrosion/oxidation effects 7

4. Fracture paths 7

4.1 Intergranular and transgranular fracture 7
4.2 Subcritical crack growth 8
4.3 Micromorphology of fracture 8
4.4 Mesomorphology of fracture 10
4.4.1 Mirror, mist and hackle 10
4.4.2 Planes of fracture 14
4.5 Macromorphology of fracture 15
4.5.1 Introduction 15
4.5.2 Crack patterns under uniaxial flexural loading 16
4.5.3 Crack patterns under biaxial loading 16
4.5.4 Multiple origins 16
4.5.5 Longer range fracture markings 19
4.6 Fractal approaches 20
4.7 Concluding remarks 20

5. Fractography **21**
5.1 Purpose 21
5.2 Typical procedures 21
5.2.1 The fractographer's kit 21
5.2.2 Handling and storage of fragments 22
5.2.3 Photomicrography 24
5.3 Flow chart for fractography 24
5.4 Interpretation of fracture features 26
5.5 Reporting a fractographic study 27

6. Limitations and problems **28**

7. Practical examples **28**

8. Bibliography **29**
8.1 Specific references 29
8.2 General references on fractography 29

Annex A - Practical examples of fractography **31**
A.1 Introduction 31
A.2 Uniaxial flexural strength test-pieces 31
Example A.2.1 - silicon carbide 32
Example A.2.2 - silicon carbide 34
Example A.2.3 - silicon carbide 36
Example A.2.4 - high-strength, high-purity alumina 38
Example A.2.5 - high-strength alumina/zirconia 39
Example A.2.6 - medium-strength, refractory mullite porcelain 40
Example A.2.7 - sintered silicon nitride 42
Example A.2.8 - sintered silicon nitride 44
Example A.2.9 - sintered alumina-based hard particulate composite 46
Example A.2.10 - partially stabilized zirconia 48
Example A.2.11 - Y-TZP machining flaws 50
Example A.2.12 - hardmetal fracture origins 52
Example A.2.13 - misleading effects 60
A.3 Biaxial disc flexural strength test-pieces 62
Example A.3.1 - microwave dielectric ceramic (1) 62
Example A.3.2 - microwave dielectric ceramic (2) 64
A.4 Fractures in ceramic components 67
Example A.4.1 - ceramic machine base 67
Example A.4.2 - ceramic ball valve 70
Example A.4.3 - gas valve plate 72
Example A.4.4 - mechanical gas seal rings 76
Endnote 86

Executive summary

Brittle materials can fail unexpectedly from structural weaknesses which are almost impossible to see in a finished component. Finding out how and why a component fails can be crucial to improving the performance and reliability of a design, even to modifying the method of manufacturing the material. Fractography is the key observational skill for those involved in interpreting failure of brittle materials because it helps to identify whether causes of failure are intrinsic to the material, to the way it has been surface finished, or to the way it has been used. It can help pinpoint where improvements could be made.

This guide is an introduction to practical fractography of brittle materials, and is intended as a background document to support the development of formal standards[1] on fractography. Its intention is to aid the inexperienced fractographer by describing:

- what causes failures to occur, the different types of fracture origin that typically can be found in brittle materials, including ceramics and hardmetals;
- what to look for in the pattern of cracks when fragments are reassembled;
- the macroscopic features of fracture surfaces and how they arise;
- how to use the fracture surface features to identify the location of fracture origins;
- how to interpret origins when viewed using microscopy;
- the importance of cleanliness when working at high magnification;
- how to use fracture mechanical information to compute approximate fracture stresses;
- the types of material for which fractography is difficult or impossible.

The bibliography to the guide gives some recommended further reading for those who wish to delve deeper into the subject. The annex has a number of examples of applying fractography to deliberately broken flexural strength test-pieces and to accidentally fractured components. The emphasis is very much on the initial visual assessments made using the unaided eye or optical microscopy, rather than high-magnification scanning electron microscopy, because a correct interpretation at the early stages of examination is crucial in arriving at the correct conclusions.

The guide should be of value as a teaching aid and reference booklet to all those involved in

[1] ASTM C1322 has been published, following a VAMAS round robin on fractographic assessment, the results of which are reported by Swab and Quinn (1995) in VAMAS Report no. 19. A CEN standard EN 843-5 and is also now available.

material development in which strength is routinely measured, and to those involved in evaluating component failures in brittle materials.

1. Objectives

Brittle materials such as glasses, ceramics and hardmetals, as well as numerous other materials of all types, may fail without warning. Low values of fracture toughness mean that small irregularities of structure, either intrinsic to the intended microstructure or inadvertent, may act as pre-existing origins of fracture when a sufficient stress is applied. Once moving under stress, seldom is a crack in such a body halted quickly, and failure, often into many fragments, ensues.

While normally an application is designed to be reliable and successful, when things do go wrong and a component breaks, it is often necessary to find out why, and to try to interpret whether the problem lies with the basic material manufacture, or the component manufacture, or whether the conditions of use were abnormal. Equally, in materials development, determining the nature of fracture origins can often be useful in pin-pointing where process improvements are needed. In either case, the first step in this process is fractography, i.e. an examination of the broken fragments to find any evidence that will help provide a focus for the investigation.

To achieve success in fractography requires patience and an understanding of how to set about the task and how to interpret observed features. This guide provides an overview of the process of undertaking fractography, and gives a range of examples of how to piece together the evidence presented by the fragments. This is backed up by an explanation of how various types of feature arise in brittle materials. The guide is aimed principally at glass, ceramic and hardmetal materials, but the principles apply to other materials of low ductility, such as cast iron, semiconductors, rocks, concrete, ice, and some polymeric materials such as polymethylmethacrylate.

2. Brittle fracture

Sharp crack-like features[2] in materials act as local stress raisers, and limit the tensile strength of a brittle material. In contrast, in the presence of plasticity, such features would become blunt, and the stress concentration would be reduced. This effect is most simply described by the Griffith expression for the fracture strength, σ_f, given by:

$$\sigma_f = \left(\frac{E\gamma_i}{Ac}\right)^{1/2} \tag{1}$$

where E is Young's modulus, γ_i is the energy required to form unit new surface, or fracture surface energy, c is the crack length, and A is a constant which depends on the crack geometry. In most brittle materials, particularly those of high strength, the crack lengths are

[2] The term "flaw" is often found in scientific texts, and should be taken to imply a normal discontinuity in microstructure which may be strength-determining. No microstructure or surface is perfect. The use of this term is avoided in this Guide because employing it may convey the wrong impression about a class of materials which is perfectly usable in an engineering sense.

typically a few tens of micrometres in length. An alternative formulation of this is to use a stress intensity factor approach:

$$\sigma = \left(\frac{K_{Ic}}{Yc^{1/2}} \right) \quad (2)$$

where K_{Ic} is the critical stress intensity factor for rapid fracture (= $(2\gamma_i E(1 - \nu^2))^{1/2}$), ν is Poisson's ratio and Y is a constant dependent on crack shape.

Once the applied stress intensity reaches the critical value, the crack will accelerate away to relieve strain energy in the system, to be halted usually only by a meeting compressive stress field.

Often, a crack-like feature under high but insufficient tensile force to cause immediate fracture will slowly extend with time as a result of thermally or chemically active processes which progressively "unzip" the atomic bonds at the crack tip. This is known as **subcritical crack growth**. It is most well known for glasses, but can occur in most brittle materials. Under steady applied tensile force, as the crack grows, the residual strength declines and the stress intensity at the crack tip increases until the critical condition is reached. The phenomenon is variously known as **delayed failure** or **static fatigue**, although the latter term tends to be confusing to engineers since fatigue is usually associated with cyclic stressing.

The process of fracture that ensues involves the growth of the cracks under the influence of the prevailing tensile or shear stresses, and generally cracks will run perpendicular to the direction of maximum principal tensile stress, initially accelerating and then slowing down as the available elastic energy is consumed. They may bifurcate, and secondary cracks may be initiated from primary cracks. The macroscopic pattern of cracks reflects the stress distribution and stored energy, and often gives a clear pointer to the approximate position of the origin. The microscopic features on crack surfaces help to demonstrate sequences and directions of propagation, and to identify the precise position of the origin. Studying and interpreting crack patterns and crack surface features is the skill of **fractography**. The following sections explain this subject in more detail.

3. Fracture origins

3.1 Introduction

Table 1 lists some of the more obvious microstructural features that can act as fracture origins, and Figure 1 illustrates them schematically. They fall into two broad categories, those which are **intrinsic** to the microstructure of the material and result from the method of formulating, shaping and processing the material, and those which are **extrinsic** to the material or component and arise as a result of machining or using the component.

Table 1 - Types of fracture origin commonly encountered in brittle materials

Intrinsic origins	Extrinsic origins
Normal microstructure (grain boundaries) Single or groups of large grains Pores, or porous regions Delaminations Agglomerates (often with an associated partial delamination) Compositional inhomogeneities (local normal species concentrations) Contaminants (foreign material)	Surface pits, pocks Machining damage Scratches/abrasions Impact Oxidation pitting, voiding Corrosive attack

Of course, machining a component may expose internal, intrinsic types of potential fracture origins. So, whereas a fracture origin away from the surface would normally indicate an intrinsic cause, for surface origins clear observations of origin detail must be made to distinguish intrinsic or extrinsic causes.

3.2 Normal microstructure

Any microstructure comprised of close-packed individual grains has a limiting strength determined by the crystallographic structural type and the presence of discontinuities in it, such as grain boundaries or second phases. In most materials, other forms of intrinsic origin are usually more significant mechanically, but microstructural failure is sometimes met with in hardmetals which are substantially free from other potential origin types including surface damage. The mechanism is usually failure of a grain boundary, or several closely aligned grain boundaries. In a hardmetal, this may be due to the bonding cobalt metal phase yielding.

3.3 Cracked grain boundaries

Internal stresses can develop between individual grains on cooling from the maximum processing temperature as a result of inter-phase mismatch or crystallographic anisotropy in thermal expansion behaviour. In coarser grained materials, or in materials with high levels of elastic or thermal crystallographic anisotropy, the grain boundaries may crack spontaneously. Such cracks are distributed throughout the material, and generally lower the elastic modulus and strength. Locating a specific origin may be difficult, if not impossible, because there would be little to distinguish it from the normal microstructural appearance.

3.4 Abnormal microstructure

3.4.1 Large grains

Some materials suffer localised grain growth in which a few isolated grains grow much larger than surrounding grains. Materials such as β-alumina are well known for this. Since even in the absence of any thermal expansion anisotropy large grains can act as stress raisers, and

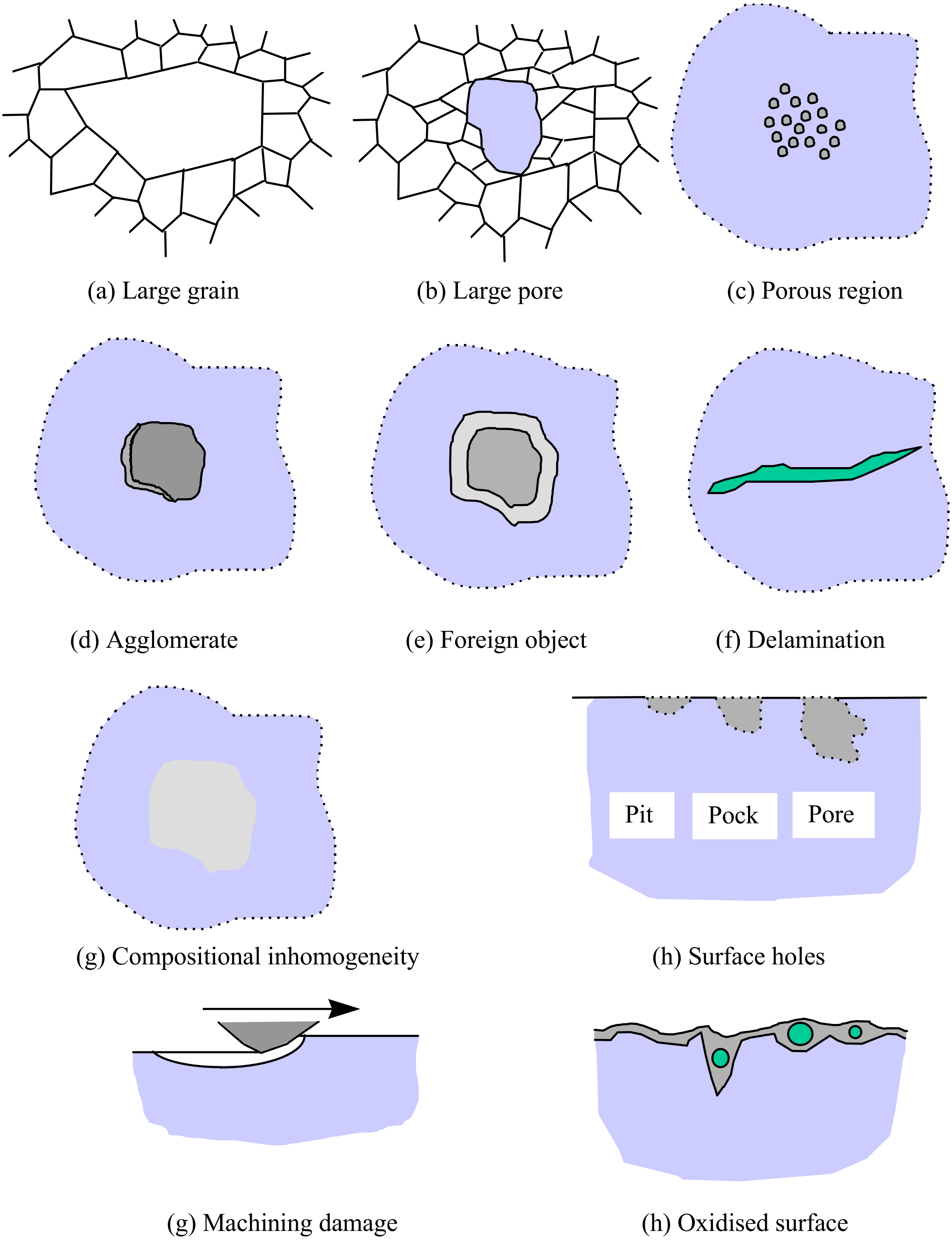

Figure 1 - Schematic representation of different fracture origin types.

may have reduced local toughness associated with them, they can become fracture origins. Because of their abnormal size, they are usually easy to identify under the microscope.

3.4.2 Pores

Pores result usually from incomplete densification of a powder-route processed material during sintering, or from a gas bubble developing inside an otherwise impervious body during processing. They act as stress raisers, and as they are often not spherical and have grain boundaries terminating at them, pores of say the grain size or larger can become fracture origins. Pores smaller than the grain size are usually difficult to identify as such on a fracture surface.

3.4.3 Porous region

Pores often appear in groups in powder route materials. One cause of this can be a localised concentration of an organic binder in the precursor powder batch. On firing the binder disappears, but leaves a region of relatively low density. Another cause can be incomplete collapse and compaction of granulates during pressing. Large arc or cap-shaped cusped pores denote the remnants of gaps between granulate particles, or the incomplete collapse of hollow granules. Fracture of material ligaments between pores occurs at a lower stress than for a fully dense material. A third cause is the existence of localised regions of poor original powder packing which are prevented from shrinking during firing because of the restraint of surrounding more densely packed material which shrinks less. Again, fracture of ligaments between pores occurs more readily than in dense material.

3.4.4 Agglomerates

These are hard close-packed accretions of particles which during sintering densify differently to material surrounding them and often tend to shrink away from the normal matrix. Again, cap-shaped continuous or discontinuous pores can result, and act as fracture origins.

3.4.5 Compositional inhomogeneities

In multicomponent materials, mixing processes should ensure homogeneity of the resulting microstructure. However, in practice, mixing may not be perfectly homogeneous, so the microstructure contains regions with locally abnormal compositional concentrations, which result in abnormal microstructure. Examples in ceramics include local glassy regions, phase concentrations, locally abnormal grain growth. Occasionally, such concentrations may be associated with pores, generated by locally different sintering behaviour. In hardmetals, regions rich in metallic binder phase or carbon may be produced.

3.4.6 Foreign material

Impurity concentrations are notorious for modifying the local microstructure, often associated with pores and leading to altered local toughness. Ferrous metal contamination from processing machinery is commonly encountered. Detailed local chemical analysis of this type of origin, typically by non-dispersive X-ray analysis in the scanning electron microscope, is usually needed to identify the cause.

3.4.7 Delaminations

In materials which are pressed from powders, delaminations or cracks can occur during pressing or on ejection from the pressing die, and these are generally not removed by subsequent sintering treatments. They act as extended pores. Typically they are of a size which is a substantial fraction of the component dimensions. Similar consequences can arise from organic contamination in powder processing, such as human skin flakes, which disappear on firing leaving a flat void.

3.5 Surface (extrinsic) origins

3.5.1 Pits, pocks, pores

These various descriptions of surface depressions in a brittle material reflect increasing depth, a pit being shallower than a pock, which in turn is shallower than a pore. (These are well defined in ASTM standard F109.) They can originate from the original processing of a component, such as pick-up of organic debris in a die during pressing, or adhesion and subsequent removal of inorganic debris, or simply the connection of a large natural pore, porous region or delamination with the surface.

3.5.2 Machining damage

Many brittle materials have to be machined, normally with diamond or other abrasive tools, to achieve accurate dimensions. The method of machining, the abrasive grit size, the sequence of depths of cut, the wheel speed, the traverse speed, the coolant used, and the machine rigidity all play a role in defining the effect of machining on the remaining surface. Abrasive machining is the process of gouging and localised fracturing of the surface of the material. A pattern of shallow cracks is developed, usually accompanied by surface compressive stress. The worst damage usually occurs during the rough grinding stage with coarse grits. Subsequent stages with finer grits induce less damage, but residual damage from a coarse grit grinding operation may not be completely removed if insufficient further material is removed with finer grit sizes. The pattern of remaining cracks may be closed off at the surface due to the induced compressive stress, and thus are not obvious, and may not be detectable using dye penetration tests. The tips of the cracks may well run through the compressive zone caused by machining damage, and when this occurs, they can act as fracture origins in preference to other defects, for example intrinsic ones. Since such cracks tend to be elongated in the surface, the detected fracture origin tends to be non-localised compared with pores or inclusions. Fracture markings may seem to come from a virtual focus outside the surface, and usually there are no obvious inhomogeneities unless, fortuitously, machining damage has interacted with a near surface intrinsic origin.

3.5.3 Adventitious mechanical damage

As with machining damage, hard materials can suffer localised cracking due to unintentional damage during handling or service. Scratches, impacts, indentations and abrasive wear can introduce small cracks into surfaces and, particularly, edges. Whereas machining damage is usually fairly general, leading to apparently non-localised origins, adventitious damage tends to be more localised in its effect, the crack directions are more random, and the fracture origin consequently more localised. The important clue is any evidence of damage to the external component surface which should be correlated with a suspected origin on the crack faces.

3.5.4 Corrosion/oxidation effects

Corrosion and oxidation processes can lead to localised pitting, or the development of crevices if a secondary phase is removed selectively, or to the development of a surface skin with modified microstructures containing glassy regions, voids or gas bubbles. Much will depend on the material type and the conditions of service. In extreme cases, degradation will be obvious from the fracture cross-section of the surface region, but in other cases, close inspection of the surface adjacent to the apparent origin will be needed to reveal the degree of damage.

4. Fracture paths

4.1 Intergranular and transgranular fracture

Cracks in brittle amorphous materials such as glass are not impeded by local microstructure, and propagate in a manner influenced only by the stress field applied. In contrast, cracks in brittle polycrystalline materials, once initiated, propagate in a way determined by both the overall applied stress field and the local microstructure. In particular, a crack can pass across grains, or pass around them along grain boundaries. Sometimes, both modes can occur in the same material, but this may depend on the speed of propagation, flipping from one mode to the other as the crack changes speed. Consequently, identification of the mode of crack propagation can be helpful in distinguishing mechanisms, or even crack propagation directions.

So what decides whether a crack prefers to jump across a grain or move round it? This is associated with the relative fracture energies of the different potential paths, coupled with the local stresses acting on the crack. It seems that, experimentally, if the material is of a single phase which has cubic crystalline structure, and hence reasonable mechanical and thermal isotropy and no local mismatch stresses between grains, the tendency is for transgranular fracture. The crack does not notice clean grain boundaries and is uninfluenced by them. Fracture toughness tends to be low. In contrast, if the material has internal thermal expansion anisotropy, or relatively weak or low toughness grain boundary phases, it is easier for the crack to propagate around the grain than across it, even though the crack face area may be larger. For example, pure alumina ceramics develop thermal expansion mismatch stresses between grains of different crystallographic orientations, and there is a strong tendency to obtain intergranular fracture, particularly in medium to coarse grained materials. In aluminas which contain a glassy secondary phase, the mismatch stresses may be changed by the presence of a less refractory, more compliant intergranular phase. This phase is also less tough, and transgranular or mixed fracture modes can be produced. In hardmetals, the interface between the carbide grains and the metal binder phase tends to be the favoured path, and transgranular fracture in carbide grains is rarely seen, except perhaps in coarse-grained materials.

Observation of the fracture surface at high magnification, usually using a scanning electron microscope, is the key to identifying the fracture mode. If the fracture surface is broadly planar, with fracture markings on each of the grains, then it is transgranular. If the grains show little or no marking, and the surface is microscopically rough with geometric grain shapes obvious, then the fracture is intergranular. If both forms of surface can be identified, then it is a mixed mode fracture.

4.2 Subcritical crack growth

A fracture origin subjected to static or varying tensile stress for a long period of time, or in a moist or corrosive atmosphere, may propagate slowly, weakening the object, but not in any obvious way. This is known as subcritical crack growth. This phenomenon is most marked in glassy materials, but also occurs in most oxide ceramics, and in some non-oxide based materials which contain oxide based secondary phases. It is much less apparent in other non-oxide materials, such as sintered silicon carbides and hardmetals.

When subcritical growth occurs, the microscale appearance of the fracture surface may be different from that occurring when growth is fast. If differences can be seen close to the origin, this can be an indication of a change in mode with increasing speed of propagation. If the characteristics of fracture of the material are known, this information can be used to identify the speed of crack propagation, and hence whether the stress field applied was high or low.

A classic case is when the article is subjected to alternating stress. Some waviness in fracture surface topography may result, giving a series of bands starting near the origin.

4.3 Micromorphology of fracture

From a fracture origin of a particular size and shape subjected to a particular stress field, a crack will commence its propagation from the position where the local stress concentration is greatest, and in a direction typically normal to the maximum principal tensile stress or parallel to the maximum shear stress. It will not necessarily propagate uniformly and radially from the origin. It may instead start at one side, and then move around the origin until the latter is surrounded by an annular crack (or a semiannular crack if the origin is at or close to the original surface). The result is often some asymmetry to the micro-scale appearance of the fracture surface near the origin, such as is shown diagrammatically in Figure 2. Even a pre-existing sharp semicircular flaw will not propagate uniformly radially, but tends to start at one side and to move round the tip.

If the origin is a particle of foreign material, such as a glassy inclusion, this may have associated with it much lower fracture toughness than the surrounding microstructure. A crack may start within this glassy region, run out to a surface, and then only later start moving into normal microstructure. The surface morphologies of the inclusion region and the normal microstructure may look very different. It pays to look carefully at the grain micromorphology. If the origin is a porous region, this presents less of a barrier to propagation than normal dense microstructure, and will have a different appearance.

Macro-features in flexural test bars:

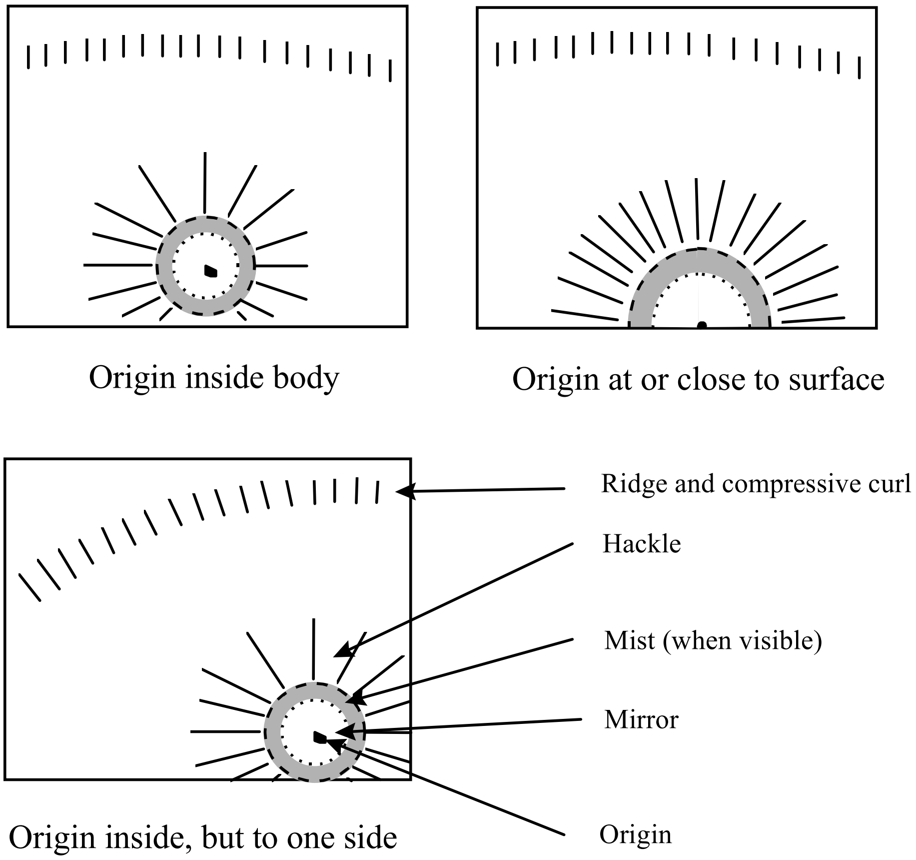

Features near fracture origins:

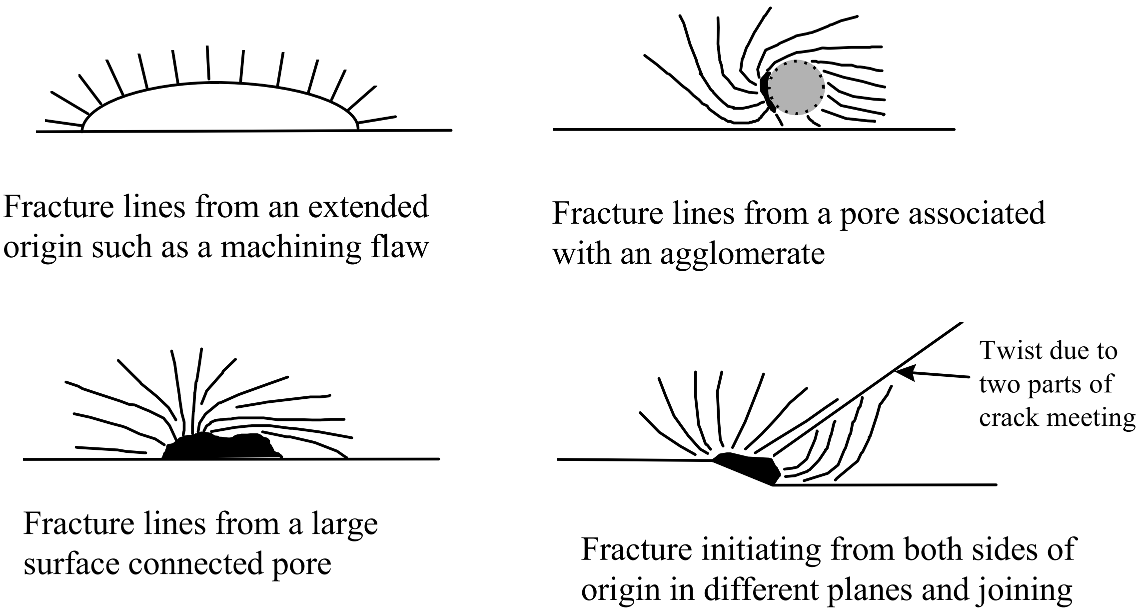

Figure 2 - Schematic appearances of the initial propagation of a crack from an origin.

Once the annular/semiannular crack is formed, propagation becomes radial and accelerates away from the origin.

4.4 Mesomorphology of fracture

4.4.1 Mirror, mist and hackle

With a glassy material, in which there are no microstructural factors to modify crack propagation, there is a classical appearance shown in Figure 3. The initial part of the fracture surface made as the crack accelerates is smooth and mirror-like, known as the ***mirror***. At a critical speed, usually considered to be at a velocity approaching 0.6 of the shear wave velocity (Congleton and Petch (1967)), the crack plane becomes unstable, and loses its mirror surface, becoming rougher. This region is called the ***mist***. Surrounding this region, parts of the advancing crack try to propagate in different directions, leading to radial striations known as ***hackle***. Beyond this, ***crack branching*** may occur, causing significant deviations of parts of the fracture surface from a common plane.

The origins of this behaviour are not absolutely clear, although the general consensus of opinion is that the limits of the mirror region occur when material just ahead of the crack tip starts to fracture in positions not in the crack plane (*e.g.* Congleton and Petch (1967)). This causes an increase in roughness of the fracture surface. The crack front is then moving at near its maximum possible velocity of about 0.6 of the elastic shear wave velocity in the material. The tendency to produce branching of the primary crack appears to be related to both crack velocity and to the rate of energy dissipation during fracture, and is more prevalent in high-energy (i.e. high-strength, small crack) fractures than in low energy ones.

With a material which is not glassy, but which has a granular microstructure dictating the micromorphology of fracture, similar fracture features are generally observed, but it may be difficult to identify these different zones in an unambiguous fashion. The finer the grain size and the greater the proportion of transgranular fracture, typically the easier it is to identify these zones. With coarse-grained materials, or with materials which show microstructural inhomogeneity left from processing, such as residual porosity effects of using a granulate, or with weak materials, the classical appearance is usually swamped by a general surface roughness. It has to be recognised that local properties of the material controlling fracture processes at the crack tip and generating the crack morphology may be very different from average properties normally measured.

The clarity with which these fracture boundaries can be seen also depends on the fracture stress, and hence the original flaw size. Rice (1984) has noted that the roughness associated with the feature boundaries tends to be fracture stress dependent, the markings becoming weaker as the boundary radii increase with reducing fracture stress. In fact, the absence of hackle or crack branching can sometimes be taken to imply that the fracture stress was low.

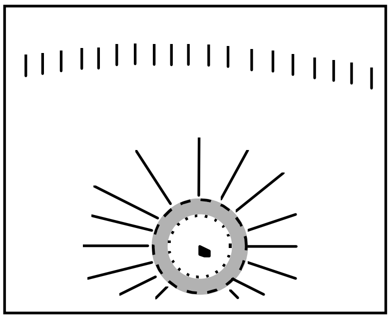

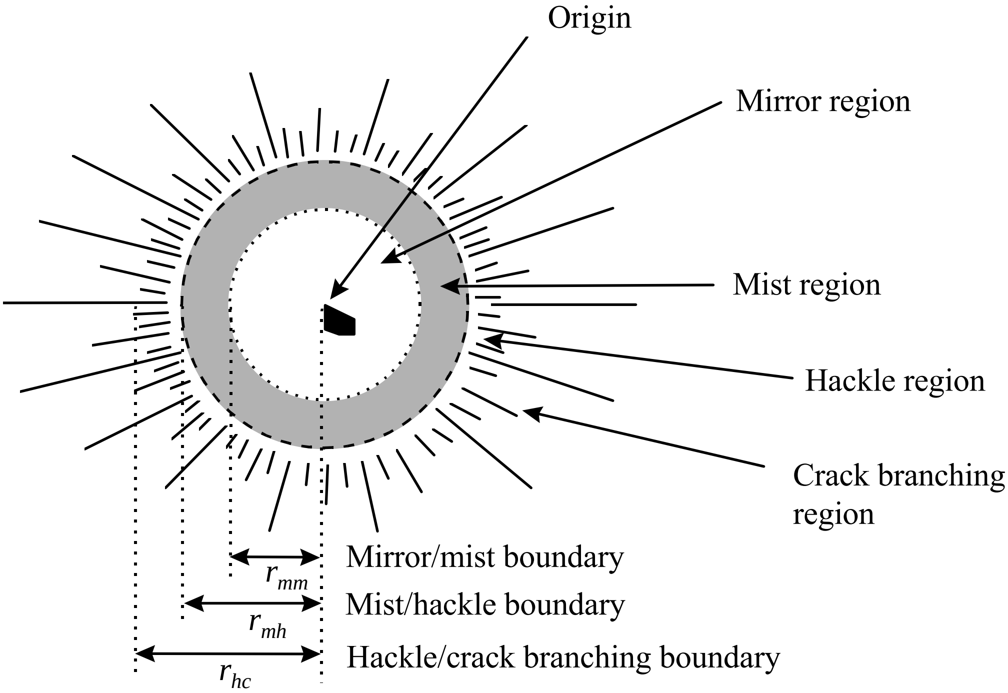

Figure 3 - Classical behaviour in fracture showing the evolution of the fracture surface through the mirror, mist, hackle and crack branching regimes. Not all regimes will necessarily be identifiable, especially in coarser-grained ceramic materials.

If they can be identified, the dimensions of the boundaries of these zones depend on the material properties and on the critical size of the origin. The smaller the origin, the smaller the radii of these boundaries. If the relationship is known mathematically, it is possible to estimate the stress at the point of fracture, which is a useful tool for the fractographer.

For a given material, and a given boundary between mirror, mist, hackle or crack branching, there is a relationship of the form (*e.g.* Mecholsky *et al.* (1974)):

$$\sigma_f \sqrt{R_i} = A_i \tag{3}$$

where the subscript i relates to the relevant boundary, σ_f is the fracture stress, R is the boundary radius, and A_i is a constant. Some constants for the mirror/mist boundary for various materials are given in Table 2.

In a study of hardmetals, Luyckx and Sannino (1988) found that mirror analysis was possible for all but the hardest and strongest grades where crack branching occurred immediately on fracture initiation. They found that the mirror constant was related linearly to the inverse of the hardness as a measure of toughness for 2 mm and 4 mm grain sizes.

This analysis assumes, of course, that the fracture initiation is circularly symmetrical. This may not always be the case. Rice (1984) gives some examples where the mirrors are distorted, or even doubled, for example when fracture initiates from two sides of an origin, and not uniformly around it. In cases where the stress field is not homogeneous on the scale of the expected mirror size, the mirror/mist boundary may not appear, or may appear only at the sides and not in the main crack propagation direction, for example in flexural strength test-pieces. Because there is a strong stress gradient through the test-piece thickness, this can lead to mirrors which are elliptical with the longer axis in the test-piece thickness direction. Mirror radii in such cases are best measured parallel with and a little below the test-piece surface (to avoid surface residual stress effects, see Rosenfield and Duckworth (1988)), rather than as a depth into the test-piece.

Table 2 - Typical fracture mirror/mist boundary constants

Material class	Range of vales of fracture mirror constant, *A*, MPa $m^{1/2}$
Glasses	1.8 - 2.4
"Pyroceram" glass-ceramics	5.7 - 6.5
Aluminas	8.0 - 10.4
Dense silicon nitrides	5.9 - 18.1
Porous silicon nitrides	4.2
Silicon carbides	10.7 - 11.9
Zirconias	7.4 - 15.2
Mullite	6.1
Boron carbide	9.3
WC/Co hardmetals	24 - 87

Source: ASTM C1322:1997

It will be noticed that the constants in Table 2 have the same units as those of stress intensity factor, i.e. MPa $m^{1/2}$, because the equation has a similar form. Taking this point further, the relationship between the initial origin size R_f and, say, the mirror/mist boundary size R_i, is given by:

$$\frac{R_i}{R_f} = \left(\frac{A_i}{Y K_{Ic}}\right)^2 \tag{4}$$

where K_{Ic} is the critical stress intensity factor or toughness, and Y is a flaw shape parameter, typically with a value between 1 and 2, depending on flaw geometry (see Table 3).

Using the data in Tables 2 and 3, and the above equations, two simple examples demonstrate the value of the analysis:

Table 3 - Flaw shape correction factors, *Y*

Bulk origins		Surface origins	
Shape	*Y*	Shape	*Y*
Circle, *c*/*a* = 1	1.13	Semicircle, *c*/*a* = 1	Centre: 1.17 Surface: 1.29
Ellipse, *c*/*a* = 1.4	1.26	Semiellipse, *c*/*a* = 1.4	Centre: 1.39 Surface: 1.29
Ellipse, *c*/*a* = 2	1.47	Semiellipse, *c*/*a* = 2	Centre: 1.59 Surface: 1.24
Long ellipse, *c*/*a* >> 4	1.77	Long ellipse, *c*/*a* a >> 4	Centre: 1.99

Example 1:
A component made from silicon nitride has failed from a surface crack. An examination of the fracture surface shows that the mirror radius is 200 µm. Using Equation 3 and the reported range of mirror constants for silicon nitride from Table 2, we calculate that the stress at the fracture origin was in the range 417 to 1279 MPa, figures that could be narrowed down by improved knowledge of mirror constant for the particular material type.

If we assume the upper stress, and we know that the fracture toughness of the silicon nitride is 4.7 MPa $m^{1/2}$, then, using Equation 4 for a semicircular flaw failing at its intersection with the surface (Y = 1.29 from Table 3), we would expect the starting crack radius R_f to be 22 µm. This is the approximate flaw size we should be looking for.

Example 2:
A standard size (3 x 4 x 40 mm) flexural strength test-piece made from boron carbide broke at a calculated stress of 200 MPa, but shows no mirror on the fracture surface. Using the mirror constant of 9.3 MPa $m^{1/2}$ from Table 2, the mirror radius should be 2.16 mm, and thus should be visible. However, this is calculated for uniform tensile stress, but the stress gradient through the thickness of a flexural strength test-piece means that the stress on the propagating crack has diminished significantly before the limit of the mirror region is reached, so explaining why no hackle appears.

Example 1 shows how mirror sizes can be used to track back to the stress at the time of failure, and with some knowledge of material properties, the approximate flaw size can also be determined. In contrast, example 2 shows how the analysis can be used to explain the absence of features on the fracture surface, when the fracture stress is known.

It should be noted that these calculations should be considered to produce only rough estimates for several reasons:

- existing data on mirror constants are sparse, and may not apply exactly to the material under examination

- flaw size estimates rely on a fracture toughness value which is appropriate for small flaws, and may not be known accurately

- the analysis assumes a uniform stress field which may not occur in practice.

Despite these limitations, the analysis can still be a valuable method of explaining what one sees.

4.4.2 Planes of fracture

The direction in which a crack front moves is dictated primarily by the direction of the applied stresses. Typically it runs in a plane perpendicular to the direction of maximum principal tensile stress. If the stress is equibiaxial tensile, the crack tends to wander, perturbations not being corrected. If the stress is torsional, the crack plane tends to be in the direction of maximum shear, and may twist. If the crack enters a region of compression, it will either be halted or deflected; the "compression curl" seen in flexural strength test-pieces is an example (see 4.4.1).

In high-strength materials, the shock of fracture can override applied stress fields. Elastic energy release during fracture sets up sonic waves which reflect off the surfaces of the article and interact with the advancing crack, enhancing branching effects and sometimes leading to multiple fractures and to fragmentation. Generally, the higher the elastic energy in the system, the higher the stress at fracture, and the lower the material toughness, the more fragments that are produced.

An example of this is given in Figure 4 in which the number of fragments produced in biaxial ring-on-ring disc strength tests on a high-strength alumina ceramic is plotted against the nominal fracture stress.

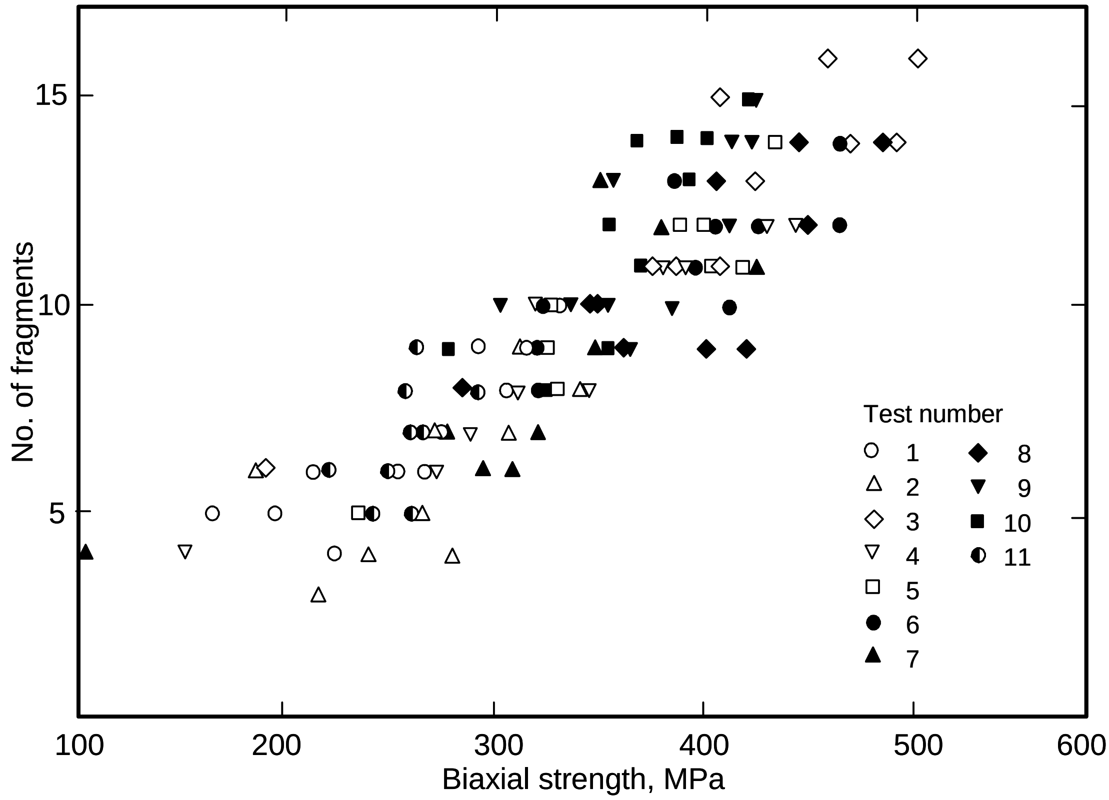

Figure 4 - Number of fragments as a function of nominal flexural stress in ring-on-ring strength tests of a high-strength alumina (from Byrne and Morrell (1990)).

4.5 Macromorphology of fracture

4.5.1 Introduction

The process of cracking is the release of elastic energy and its conversion into surface (fracture) energy and some kinetic energy of the fragments. As described above, the greater the amount of energy available in terms of both the stored elastic energy at the point of fracture and the energy associated with driving the fragments once fracture initiates, the greater the number of fragments. The directions of fracture depend on the stress field applied to the crack. The plane of the initiating feature at the origin may not be normal to the maximum tensile stress, but as it propagates into a crack, the plane quickly twists to become normal to the stress, and generally follows this orientation until the stress disappears. As the crack propagates, the stress field in the article may change, depending on the method of its application, and this too can influence fracture patterns, particularly in complex loading situations, and must be taken into account in analysis. Behaviour in some of the simpler geometries is given below.

4.5.2 Crack patterns under uniaxial flexural loading

Figure 5 shows typical positions and shapes of fracture occurring in flexural strength test-pieces. The higher the fracture force, the greater the energy available for fracture, and the more likely it becomes that multiple cracking will occur. Test-piece fragments may impact on the testing jig and suffer further damage. Note also that the stress field is highly inhomogeneous, and the crack propagating from the tensile side quickly runs into the compressive zone. In high-speed fracture when the compressive stress field does not relax fast enough as the crack advances, the crack can be slowed and deflected, giving the compression curl. This is a useful indicator for the post-test identification of the tensile faces of the test-piece if these were not marked as such before the test.

4.5.3 Crack patterns under biaxial loading

Figure 6 shows typical crack patterns in the equibiaxial fracture of discs. In this case, the disc normally starts to split into two fragments, each of which suffers further fractures using the available elastic energy. The fracture origin can usually be found by re-assembling the fragments and identifying the principal fracture line from which most of the other fractures initiate. The asymmetry of the pattern is an indicator of the origin, which is near the focus of the radiating secondary fractures. At high fracture stresses, the principal fracture line may bifurcate before crossing the test-piece.

Crack patterns obtained in flexural fracture are different from those obtained by applying thermal stress to a plate. If a ceramic plate is thermally shocked on the faces by, for example, water quenching, there is less elastic energy associated with the thermal stress than in the flexural case. Shallow surface cracks can be generated which meander across the face of the plate and which branch until the elastic energy is lost. If a plate is heated at its edge, but not in the central region, again, meandering cracks will be produced.

4.5.4 Multiple origins

In many components of complex shape there may be several fracture origins, depending on the geometry and the causes of fracture. For example, a plate with a hole through it subjected to flexural stress will fracture at the hole where there is a significant stress concentration. In order to break the plate into two pieces, fracture must initiate from both sides of the hole. The more severe origin breaks first, reducing the stiffness of the plate and permitting the stress concentration on the other side of the hole to build up until a second incipient origin starts to propagate. Casual observation will reveal two possible origins, but if the mirror sizes are measured, the larger one corresponds with the larger flaw and the lower stress, and is likely to be the one initiating the failure.

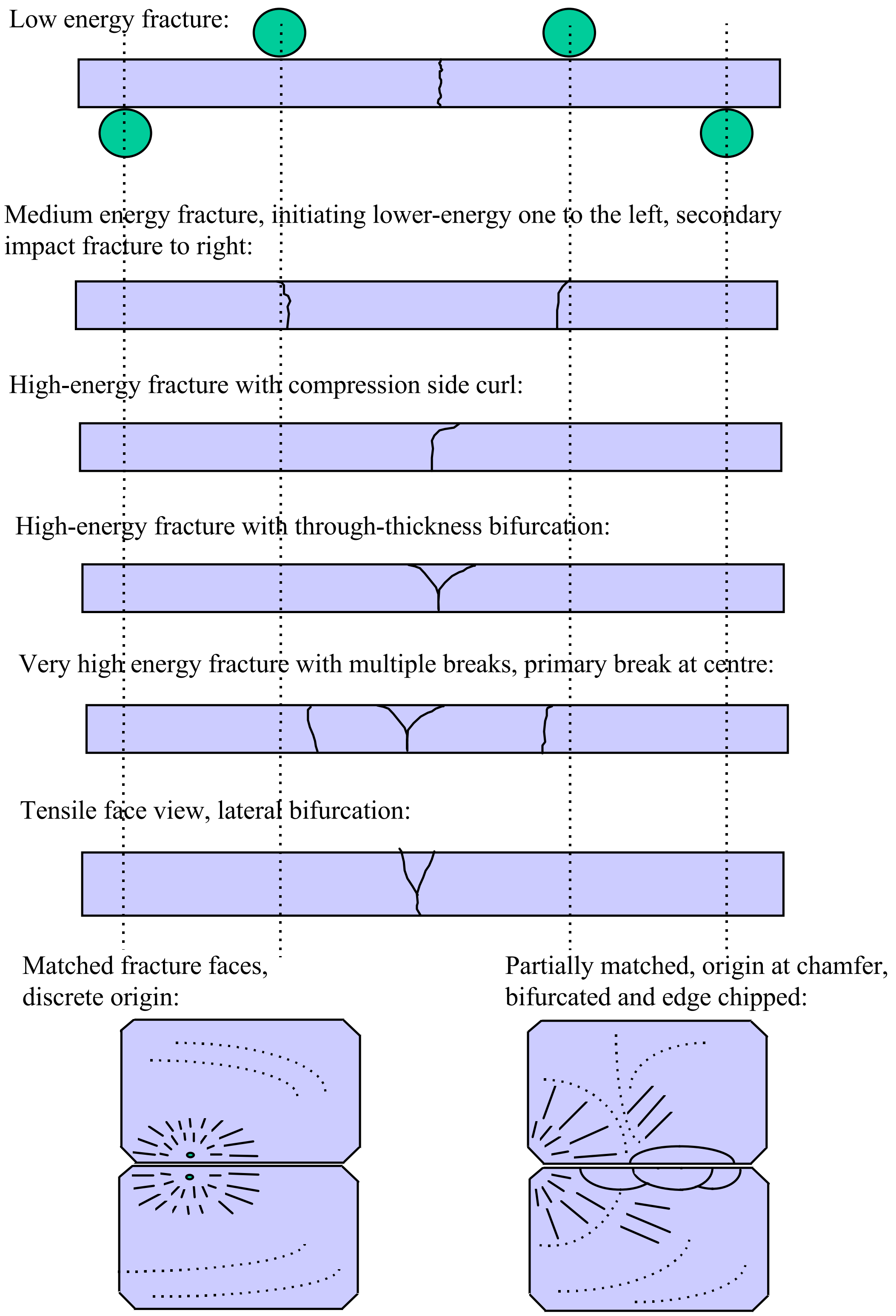

Figure 5 - Typical patterns of fracture in uniaxial flexural testing.

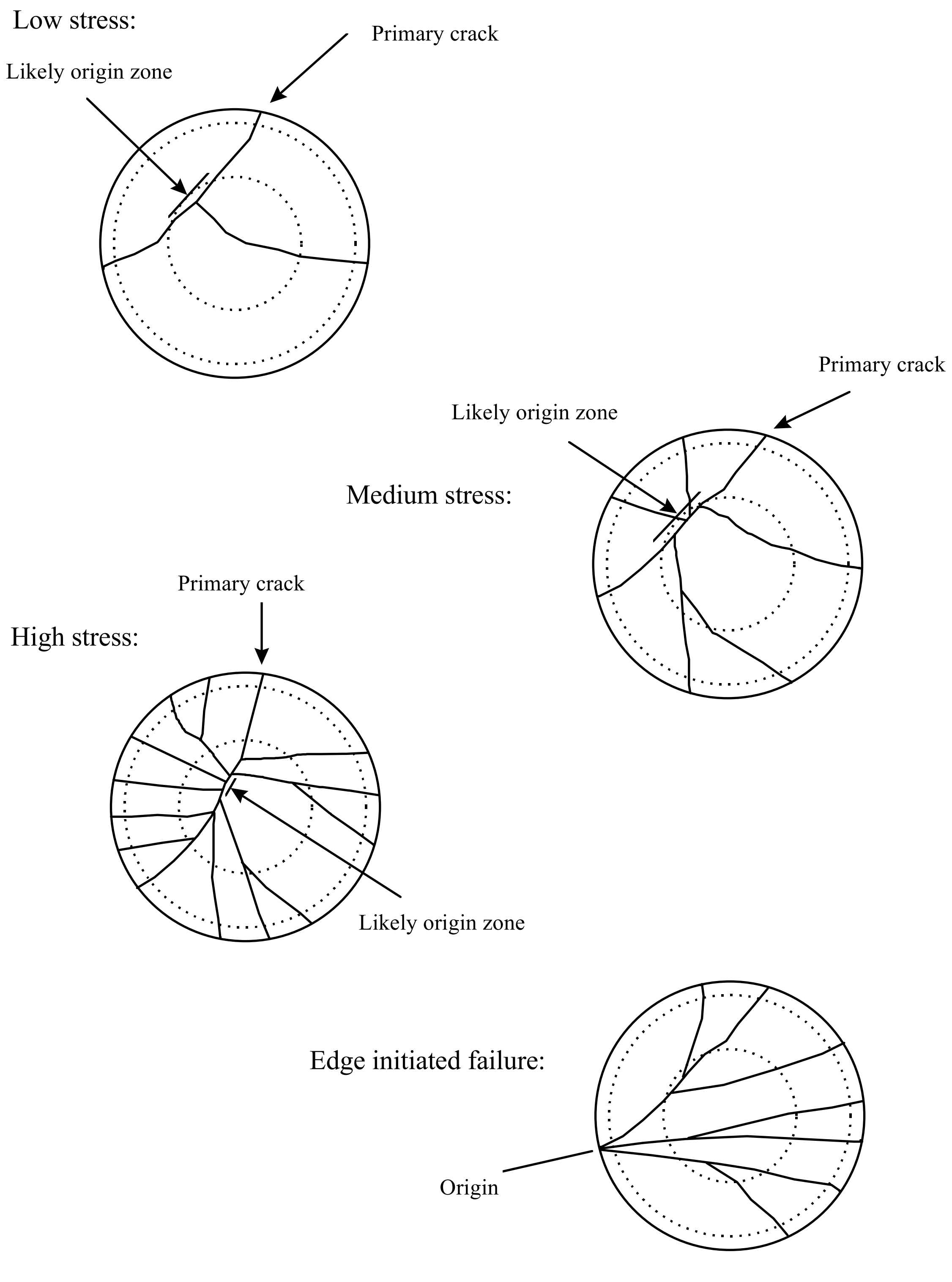

Figure 6 - Typical fracture patterns in ring-on-ring flexural testing of discs. The origin generally lies on a principal crack line, from which other cracks branch.

4.5.5 Longer range fracture markings

Close to the origin the hackle is essentially in the direction of crack propagation, and can be used as an indicator of this. Further away, other markings can result and be superimposed on the hackle. In particular, the fracture event can trigger sonic waves which can be initiated at the origin or any other discontinuity, and can be reflected back off surfaces. Wallner lines are one such example (Figure 7a). In addition, the stress field applied to the fracturing body will fluctuate as fracture progresses, through vibration or bifurcation, resulting in changes in direction (Figure 7b). Regular series of bands may occur under cyclic stressing, and such a technique has been used to `decorate' a deliberate fracture in order to determine its velocity.

Regions of compressive stress will slow down or halt cracks, or make them meander. For example, if a crack is propagating under flexural stress in a thin-walled article, crack growth is always impeded in the compressive zone (Figure 7c), and lags behind giving a semi-parabolic appearance to larger-scale marks. These can be used as an indicator of crack propagation direction.

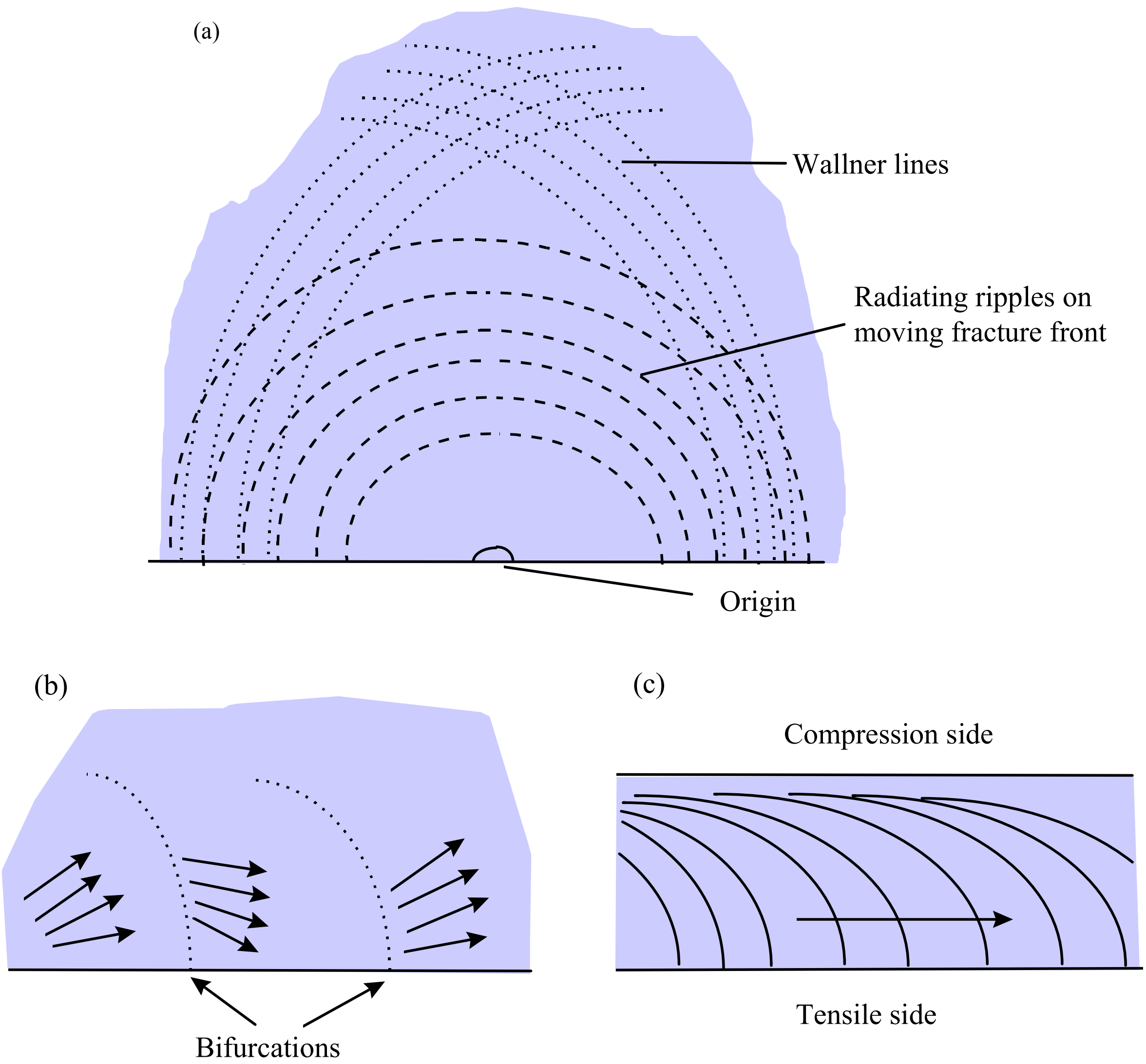

Figure 7 - Schematic representation of (a) Wallner lines, (b) bifurcation markings, and (c) compressive zone drag in flexural failure.

4.6 Fractal approaches

The apparent roughness of fracture surfaces varies somewhat dependent on distance from the fracture origin and the speed of crack propagation. The roughness and feature size are related to the microstructure of the material, notably the orientations of individual grains or grain boundaries, and to the fracture mode, whether predominantly transgranular or predominantly intergranular. However, the apparent roughness of the fracture surface depends also upon the scale on which it is observed. It has been proposed that an approach to evaluating roughness is through fractal analysis. The scientific literature on this topic is growing.

Fractal analysis is principally the determination of characteristic parameters which describe the non-planarity of the surface. One of the main difficulties with such an analysis is that the numerical parameters derived, particularly the fractal dimension, which is related to the apparent slope variance of the roughness, does not necessarily correlate with mechanical properties such as toughness. For example, although Mecholsky *et al.* (1988) found a clear relationship between fracture toughness and fracture surface characteristics expressed through the fractal dimension increment D^*, neither Baran *et al.* (1992) nor Wasén *et al.* (1998) find such correlations for dental porcelains and for alumina and various SiC whisker reinforced aluminas respectively. The universality of the approach remains unclear, particularly in regard to the role of microstructure.

One of the possible potential advantages of fractal analysis is that it permits an estimate of flaw size to be made from the mirror size when the mirror constant is not known. If the fractal dimension increment is determined by evaluating fracture surface remote from the origin, it can be used to estimate flaw size through its relationship with mirror size. However, the wider usability of the approach has yet to be demonstrated. Experimental evaluations tend to be restricted either to small areas of fracture surface, or to steadily propagated cracks, both with a limited scale of feature. Different methods have not yet been adequately compared on sufficiently wide scales, and material microstructures are found to play a dominant role which conflicts with the concept of continuous scalability. Its value to fractography thus cannot yet be properly assessed.

4.7 Concluding remarks

This section has described fracture features in the order in which they are typically produced by the process of fracture, commencing from a microstructural discontinuity, and creating a crack or cracks, and finally a number of fragments. However, the fractographer would normally have to work in the reverse direction, first identifying the fragments and how they match together, then locating the principal crack plane and the approximate position of the origin, and finally, using the fracture surface features to provide direction to the precise origin, which can then be categorised and the causes of fracture identified. There may also be some significant barriers to completing the task. For example, some of the fragments may be missing, or the fracture surfaces may have become corroded or contaminated and not readily cleanable. Sometimes the jigsaw of fragments is too complex to complete. Fractography always has to be conducted on a best-effort basis with the available evidence, and does not always yield a categorical result.

5. Fractography

5.1 Purpose

The above discussion of the appearance of fracture fragments and their surfaces clearly indicates that examination can yield useful clues as to why a component has failed:

1. The shapes of fragments and the directions in which cracks have propagated give clues to the orientation of the stress field applied at the instant of fracture, especially to the existence of stress concentrations, a common source of inadvertent fracture.

2. The sizes and shapes of fracture features, especially the mirror size, can be used to identify the magnitude of the stresses at the time of failure.

3. The pattern of fracture surface features can be used to identify the position of the origin, and the nature of the origin can then be identified by microscope examination at high magnification.

This section gives some suggestions on conducting an investigation in fractography.

5.2 Typical procedures

5.2.1 The fractographer's kit

5.2.1.1 Handling and storing fragments

Avoiding further contamination is the most important aspect, especially if there is an expectation of having to employ local chemical analysis at some point. Some important items are listed below.

- Storage containers: these should be such that individual fragments can be stored without coming into contact with each other, which might induce further damage, especially edge chipping. Multicompartment plastic trays with lids are ideal. Avoid paper or card, since fibres can be picked up.

- Gloves: surgeon's rubber gloves are useful to avoid finger grease contaminating surfaces. Fracture surfaces are extremely rough, and are difficult to clean, so it is best to avoid contaminating them, rather than trying to clean them later.

- Tweezers: in preference, use plastic-tipped tweezers for handling small fragments, rather than metal ones. Ceramics and hardmetals are hard and readily abrade metal. Plastic tweezers can also leave debris behind, but it tends not to adhere in the same way as metal abrasions. Ceramic-tipped tweezers, such as those used in the semiconductor industry, would be even better.

- Hand lens: up to 10 times magnification is useful for free-hand examination of fragments, especially for those with long sight. A system incorporating illumination is particularly useful.

5.2.1.2 Microscopes

By far the most useful tool for fractography is a low-magnification, long focal length microscope, often termed a ***macroscope***. Instruments are available with magnifications typically in the range 3x to 50x, with binocular eyepieces, and with steerable illumination. Such an instrument is of particular value for viewing fracture surfaces on fragments which can be hand held or mounted in a universal clamp for easy re-orientation. Photomicrographic facilities incorporated into the macroscope are useful for recording important features.

General illumination from conventional lamps or from ring-lamps around the objective are satisfactory for inspecting general shapes, but low-angle directional lighting produces a dramatic change in appearance of the fracture surface from one in which shadows are almost non-existent to one in which shadows are enhanced to reveal the fine-scale topography. For this purpose, a fibre-optic focusable light source is particularly useful, since it can be readily positioned and adjusted.

Conventional metallurgical microscopes have limited value for fractography because they tend to be designed for high magnification use on flat surfaces, while fracture surfaces are seldom flat, and are thus mostly out of focus. In addition, effective side illumination is usually impossible at magnifications much above 100x. Occasionally it may be desirable to check on a fracture origin at high optical magnification before attempting scanning electron microscopy, for example when the suspected origin is too small to see confidently with a macroscope. However, in the main, metallographic microscopes have limited application.

While much can be done with an optical macroscope, the ***scanning electron microscope*** (SEM) is the key tool for identifying and evaluating fracture origins, typically at magnifications between 200x and 5000x, the chief advantage being the depth of focus coupled with the possibility of local chemical analysis by characteristic X-ray analysis. SEMs have a disadvantage in tending to flatten out the appearance of rough surfaces with loss of subtle information visible under grazing incidence optical illumination. In addition, the appearance of the image may depend on the imaging conditions used. Figure 8 shows an example of a small deliberately introduced indentation crack as a fracture origin for fracture toughness measurement of a silicon nitride. At an accelerating voltage of 5 kV with the test-piece uncoated, the crack is virtually unidentifiable except to the skilled eye making out very subtle changes in fracture marking directions at the crack boundary, whereas with a gold/palladium sputtered coating and viewed at 30 kV, the outline of the semielliptical crack can be clearly seen.

5.2.2 Handling and storage of fragments

Fractured fragments should be treated as the unique evidence in the case, and should be handled with care. The following guidelines should be used.

- **Individual fragments should be uniquely identified**: use a pencilled number or other marking well away from the regions of fractographic interest, but it may be possible to avoid marking them at all if they can be described by shape.

- **Wear gloves** (see 5.2.1.1): not only does this keep the fragments clean, but it also reduces risk of being cut by sharp fragments.

- **Take care in cleaning fragments:** fragments may arrive dirty, or may have been subject to cutting processes involving glueing or clamping, plus the use of cutting fluids. Cleaning should be undertaken only with a soft brush and soapy water, followed by copious rinsing and final drying with ethyl alcohol. Take care not to lose fragments of friable materials or to induce edge chipping.

- **Try to avoid bringing fracture surfaces into contact:** abrasions may change surface appearances which could be misleading, and edge chipping can result in lost evidence; keep the fragments separate, or bring only external surface in contact with external surface (you are not trying to reconstruct the Portland Vase!).

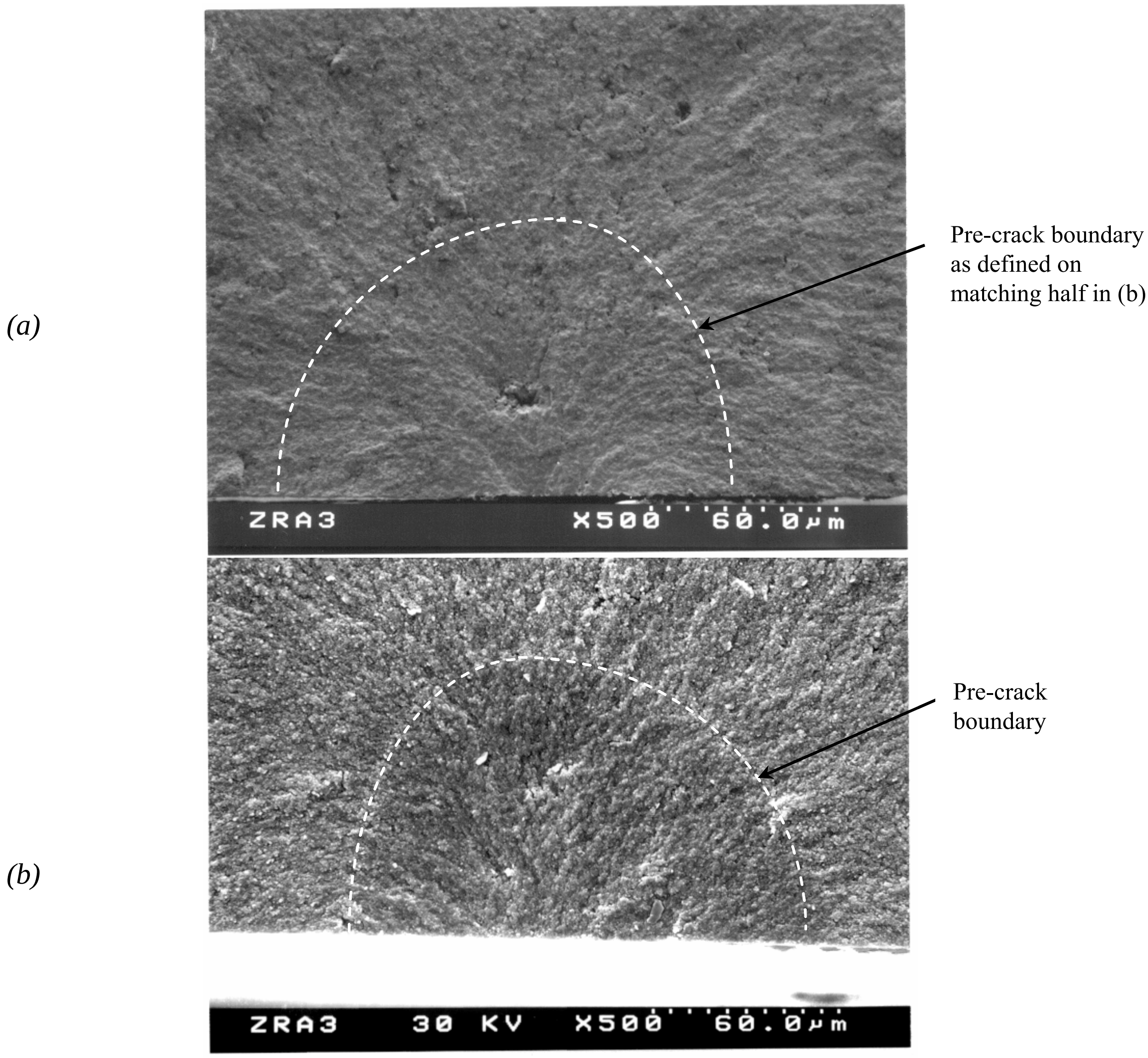

Figure 8 - Indentation induced pre-crack as a fracture origin viewed (a) uncoated at 5 kV and (b) coated at 30 kV.

- **Avoid contamination from mounting materials:** there is a great temptation to hold parts together with adhesive tape or modelling clay. These can become smeared over important surfaces even if the greatest of care is taken, and cannot be completely removed. Misleading SEM pictures could result. On the other hand, sometimes there is no practical alternative to using such materials, in which case use them well away from important areas and minimise subsequent handling.

- **Do not cut SEM test-pieces from larger fragments until you have made all macroscopic observations on them:** you cannot go back if you have forgotten something.

5.2.3 Photomicrography

Photomicrographs are the documentary evidence to support the interpretations being made. An optical macroscope fitted with a camera is ideal for low-magnification features, and an SEM is ideal for higher magnification pictures. Polaroid and conventional 35 mm film give excellent results provided that care is taken with exposure conditions. However, increasingly, digital images are being used, and these are particularly useful because they can be edited (overwritten) with information such as magnification, or arrows referring to particular features. Provided that the images comprised an adequate number of pixels and are printed on a high-quality printer, they can be as good as conventional photographs.

Knowing the correct image magnification is an important factor in fractography, and it is recommended that if measurements of features are to be made from micrographs, micrographs of a calibrated graticule at the same magnifications are made during the same photographic session.

Because fracture surfaces are not flat, it is important to optimise the depth of focus in the photomicrographic system. This is best done by using the smallest aperture available, commensurate with a sensible exposure time and without running into film reciprocity problems. Exposures of up to five minutes are not uncommonly required with side-illuminated fracture surfaces.

With SEM examination there is a strong temptation to examine the sample immediately at high magnification. This should be resisted. Instead it is wise to prepare micrographs at a series of magnifications (say, three levels, e.g. 50x, 200x and 1000x) in order to obtain general views of the fracture surface before homing in on the origin and photographing that.

5.3 Flow chart for fractography

To provide an overview of the entire process, Figure 9 shows a flow chart which lists the major steps in undertaking fractography. This figure contains all likely stages in an intensive investigation, but not all stages would be used in every case. For example, it may be sufficient to undertake only visual/optical evaluation, because sufficient evidence for the purpose in hand can be gleaned from such an evaluation. As another example, if local fracture damage caused by handling the component is seen by SEM examination as the likely origin, there is little point in undertaking local chemical analysis.

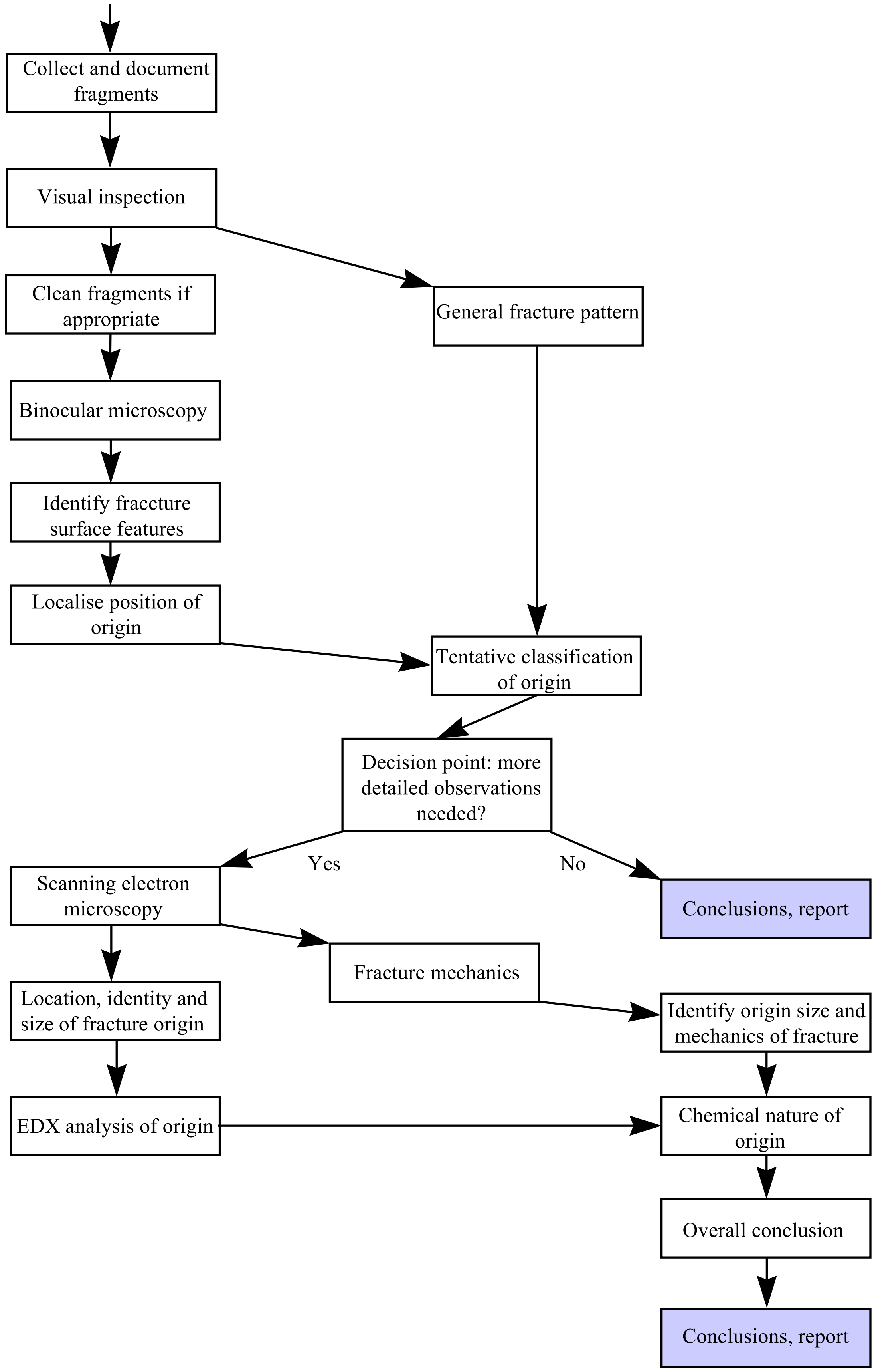

Figure 9 - Fractography action flow chart.

It is important to make appropriate interpretations at each stage, because the conclusions may influence the directions taken in the next stage. It is no use simply taking a series of photographs and expecting to interpret them later and come to the correct answer. The wrong areas may have been photographed. It is better to make the interpretation while using the microscope, and then to take the appropriate photomicrographs later.

5.4 Interpretation of fracture features

It is not possible to lay down a categorical procedure for identification of fracture surface features, because much depends on the geometry of the component or article under study, the material type, and the circumstances of fracture. However, perhaps the first step is the general evaluation of the pattern of cracks seen when the fragments are assembled. In order to track back to the fracture origin, the primary initiating fracture needs to be distinguished from secondary breaks, which are usually not continuous across the article. The latter often start or terminate at existing fractures. The pattern of crack directions can sometimes be identified from the features on the fracture surface, particularly the direction of the hackle marks at intersections with original surfaces. The advancing crack front propagating in a thin-walled component tends to be parabolic in shape, with the parabola nose in the direction of propagation (Figure 5c). Using this criterion, the pattern of crack directions can often be determined, from which the primary crack or cracks can be identified.

The next step is to examine the suspected primary fracture surfaces and, using the same type of criteria, to identify the position of the origin. The most reliable method is to follow radiating hackle markings back towards their focus. Sometimes the pattern is very distinct, making the task trivial, but in other cases these markings may be interrupted by other ridges and troughs caused by stress wave reflections from the surfaces of the component, so this interpretation is to be done with care. Further, it should always be borne in mind that the true origin may be lost as a result of it being in a missing fragment, or from chipping after the initial fracture. The perfection of matching of opposing surfaces is the best criterion to use. A useful technique for white ceramics that gets over the translucence problem is to hold the fracture surface up to a light source and to view the fracture surface at grazing incidence. The origin often appears much more shiny than the rest of the surface.

Finally, when the origin region has been identified, evaluation at high magnification can be used to seek the probable origin type. If the feature is large, such as a 100 mm pore, this can be done readily using a stereo macroscope, but in cases where magnifications above 100x are needed to give a positive identification it is necessary to use the scanning electron microscope. SEM images are much more categorical in nature, and the real nature of the origin is much more readily identified, than when using optical microscopy with limited resolution, possible optical translucency, possible false reflections, and misleading discolorations. Also, if necessary, the origin can be chemically analysed.

Origins from surface cracks are the most difficult to obtain clear identification. The possible shapes of surface flaws may be identifiable from changes in fracture direction (on a microscopic scale), from hackle or crack branching directions which focus outside the test-piece surface, or from scratches or pits on the external surface. It is always useful to employ fracture mechanical estimates of flaw size as a check on identification of such origin types.

5.5 Reporting a fractographic study

It is important to record findings in a clear and logical manner, particularly if the results are to be conveyed to another party. If the flow diagram, Figure 9, is followed, then details from each relevant stage need to be reported. A generalised reporting proforma might be rather large, so individual reports might need to be tailored according to the steps employed. As an example, ASTM C1322 provides a proforma for the primary purpose of fractographic evaluation of a batch of flexural strength test-pieces, and includes data on apparent origin and mirror sizes and their locations, together with computations of local stresses or expected origin size. Generally the items listed in Table 4 should be considered for inclusion in any report, and relevant ones selected.

Table 4 – Reporting fractographic information

Laboratory:	Fractographer:	Date of examination:
Item identification:	No. of fragments:	Condition of fragments:
Information supplied concerning conditions of fracture:		
Initial examination (observation conditions, fracture pattern, deductions):		
Cleaning procedure (if used):		
Optical examination(macroscope, photographs, fracture paths, modes, deductions):		
Sample preparation for SEM (sampling, cutting, coating):		
SEM Examination (conditions, chemical analysis by EDX, photographs, deductions):		
Fracture mechanical information:		
Mirror size/shape:	Origin type/size:	Estimated toughness:
Estimated stress at fracture:		
Overall conclusions:		
Signature of fractographer:	Approving signature:	Date of approval:

6. Limitations and problems

Fractography now has a strong technical background, and with some experience, can be used with confidence in many situations. However, there are many situations in which it cannot work effectively, for a number of reasons.

1. **Missing fragments:** all fragments, no matter how small, must be collected, because the vital one containing the origin is needed for finalising any conclusions.

2. **Dirty fragments:** fractured fragments readily pick up dirt which may be impossible to remove even with extensive cleaning. Although component failures in the field limit the options, try to keep fragments as clean as possible so that the key markings remain identifiable.

3. **Coarse-grained and porous materials:** when the local microstructure is varying over the dimensions of the fracture features, the features tend to be swamped, and clear origins often cannot be identified. For example, in a porous refractory with a glassy clay bond, each bond neck can often be studied and individually will show fracture features that can be identified, but one neck that was the original cause of failure is unlikely to be identified. In some alumina ceramics, the roughness of intergranular fracture in a 10 mm mean grain size material can obliterate crack branching marks, and result in no obvious origin being detectable. In such cases, the microscopic study of fracture markings on individual grain facets can sometimes give clues as to the general direction of fracture at that point, and when these markings are mapped they may be helpful.

4. **Multiple origins:** these can arise when several distinct breaks occur in a test-piece or component. For example, a component with a hole in it may break both sides of the hole, or a running crack may run into a hole, and be restarted from the opposite side. All possible origins need to be examined. The chances are that the one giving the larger mirror pattern, i.e. the larger size or origin with the lower strength will be the one initiating fracture, assuming the stress concentration around the hole is uniform. The fractographer needs to be alert to such possibilities.

7. Practical examples

The scientific and technical literature contains many practical examples of fractography of different materials fractured in different circumstances. The interested reader is recommended to consult such texts, many of which are conference proceedings, and which are listed in the second part of the Bibliography.

Some of the examples gathered as part of the study leading to this Guide are given in Annex A.

8. Bibliography

8.1 Specific references

Baran, G.R.; Roques-Carmes, C.; Wehbi, D.; Degrange, M. (1992), Fractal characteristics of fracture surfaces, *J. Amer. Ceram. Soc.* **75**(10) 2687-91.

Byrne, W.P.; Morrell, R. (1990), Biaxial strength tests on bioceramic materials, NPL report DMM (A) 18, December 1990.

Congleton, J.; Petch, N.J. (1967), Crack branching, *Phil. Mag.* **16**(142), 749-60.

Luyckx, S.B.; Sannino, S. (1988), Crack branching and fracture mirrors in cemented carbide, *J. Mater. Sci.* **23** 1243-7.

Mecholsky, J.J.; Rice, R.W.; Freiman, S.W. (1974), Prediction of fracture energy and flaw size in glasses from measurements of mirror size. *J. Amer. Ceram. Soc.* **57**(10), 440-3.

Rice, R.W. (1984), Ceramic fracture features, observations, mechanisms and uses, in *Fractography of ceramic and metal failures*, edited by Mecholsky, J.J.; Powell, S.R., ASTM STP 827, Philadelphia, USA, pp 5-103.

Rosenfield, A.R.; Duckworth, W.H. (1988), Comparison of methods for the analysis of fracture mirror boundaries, *Glass Technol.* **29**(5), 193-7.

Swab, J.J.; Quinn, G.D. (1995), Fractography of advanced structural ceramics: results from the VAMAS round robin exercise, VAMAS Technical Report No. 19, NIST, Gaithersburg, MD, USA; also published as US Army Research Laboratory Technical Report ARL-TR-656, 1994.

Wasén, J.; Heier, E.; Hansson, T. (1998), Fractal analysis of fracture surfaces in ceramic materials, *Scripta Mat.* **38**(6), 953-7.

8.2 General references on fractography

ASTM C1322-96a, Standard practice for fractography and characterization of fracture origins in advanced ceramics, ASTM, Conshohoken, Pa, 1996.

Bradt, R.C.; Tressler, R.E. (eds.), *Fractography of Glass*, Plenum Press, New York, 1994.

CEN EN 843-5, Fractographic analysis of advanced technical ceramics.

Fréchette, V.D. *Failure analysis of brittle materials*, published as *Advances in Ceramics* **24**, American Ceramic Society, Westerville Ohio, 1990.

Mecholsky, J.J.; Powell, S.R. (eds.), *Fractography of ceramic and metal failures*, ASTM STP 827, Philadephia, Pa, 1984.

Swab, J.J.; Quinn, G.D., *Fractography of advanced technical ceramics: results from the VAMAS round robin exercise*, Army Research laboratory Report ARL-TR-656, 1994, 141 pp.

Varner, J.R.; Fréchette, V.D. (eds.), *Fractography of ceramics and glasses*, published as *Advances in Ceramics* **22**, American Ceramic Society, Westerville, Ohio, 1988.

Varner, J.R.; Fréchette, V.D.; Quinn, G.D. (eds.), *Fractography of ceramics and glasses III*, Proc. Third Alfred Conference, Alfred, NY, July 9-12, 1995, published as *Ceramic Transactions* **64**, American Ceramic Society, Westerville, Ohio, 1996.

Annex A - Practical examples of fractography

A.1 Introduction

This Annex contains some practical examples of fractographic investigations on both flexural strength test-pieces, where fracture is deliberate and the fracture stress is generally known, and components which have failed in the field.

A.2 Uniaxial flexural strength test-pieces

Mostly, these pose few problems for effective fractography because they are small, and the two halves are readily assembled side by side for viewing to provide increased guidance on interpretation. In particular, if there is damage to the fracture origins, it can be seen very clearly. The origins are usually easy to find.

Twelve examples (A.2.1 to A.2.12) are given for various materials. Mostly, optical microscopy is a sufficient tool, although scanning electron microscopy has been used to gain a clearer picture of the origin detail. Example A.2.12 shows a variety of fracture origins typical of those found in hardmetals, while Example A.2.13 shows misleading effects due to lack of cleanliness in preparation of fracture surfaces for microscopy.

Example A.2.1 - silicon carbide

The two matching halves of a standard flexural test-piece of an experimental grade of sintered silicon carbide are shown placed tensile faces together in (a) under normal general illumination using a stereo optical microscope. The matching fracture patterns are quite clear because of the relatively metallic appearance and behaviour of the fracture surfaces, but are made even clearer when viewed with grazing incidence illumination from the top (b). The appearance is classical for a flexural strength test-piece. The fracture marks radiate from a point at the centre of the original tensile surface of the test-piece, and become rougher the further away from the origin. About 0.5 mm to each side of the origin, crack branching is clearly seen as the dramatic increase in roughness. Inside this region is the mirror zone, which has a radius of about 0.3 mm. Because of the stress gradient through the thickness of the test-piece at the instant of fracture, roughening and crack branching do not occur to the same extent away from the tensile face, leaving the mirror zone definitely non-circular. Note that determining mirror zone radii is somewhat subjective. On the compression side of the test-piece, the crack no longer runs in the same plane. This is the compression side "curl" as the crack slows down under axial compressive stress and becomes subject to shear stresses. This feature is useful in unambiguous identification of the compression side of unmarked test-pieces. At higher magnification, still under grazing incidence illumination (c), the radial markings are even clearer, and emanate from a highly localised origin which appears to contain some irregularity at or close to the surface. Finally, changing to a conventional metallurgical microscope at even higher magnification (d) details of the origin become clear as a small grouping of pores and inclusions. The radial fracture markings are still visible, mainly in the lower fragment surface, and come from the most right-hand of the features. The depth of focus is quite limited, so such images are difficult to capture, needing patient and careful vertical and lateral positioning of the two fragments. By use of focus control, it is possible to identify whether the features are holes or pulled-out inclusions; in the present case the most right-hand of the features is clearly an inclusion.

Identification of the nature of the inclusion cannot be achieved by optical microscopy, and would need much better resolution and depth of focus offered by SEM. However, this example serves to show how far optical microscopy can be taken.

(a) (b)

(c) (d)

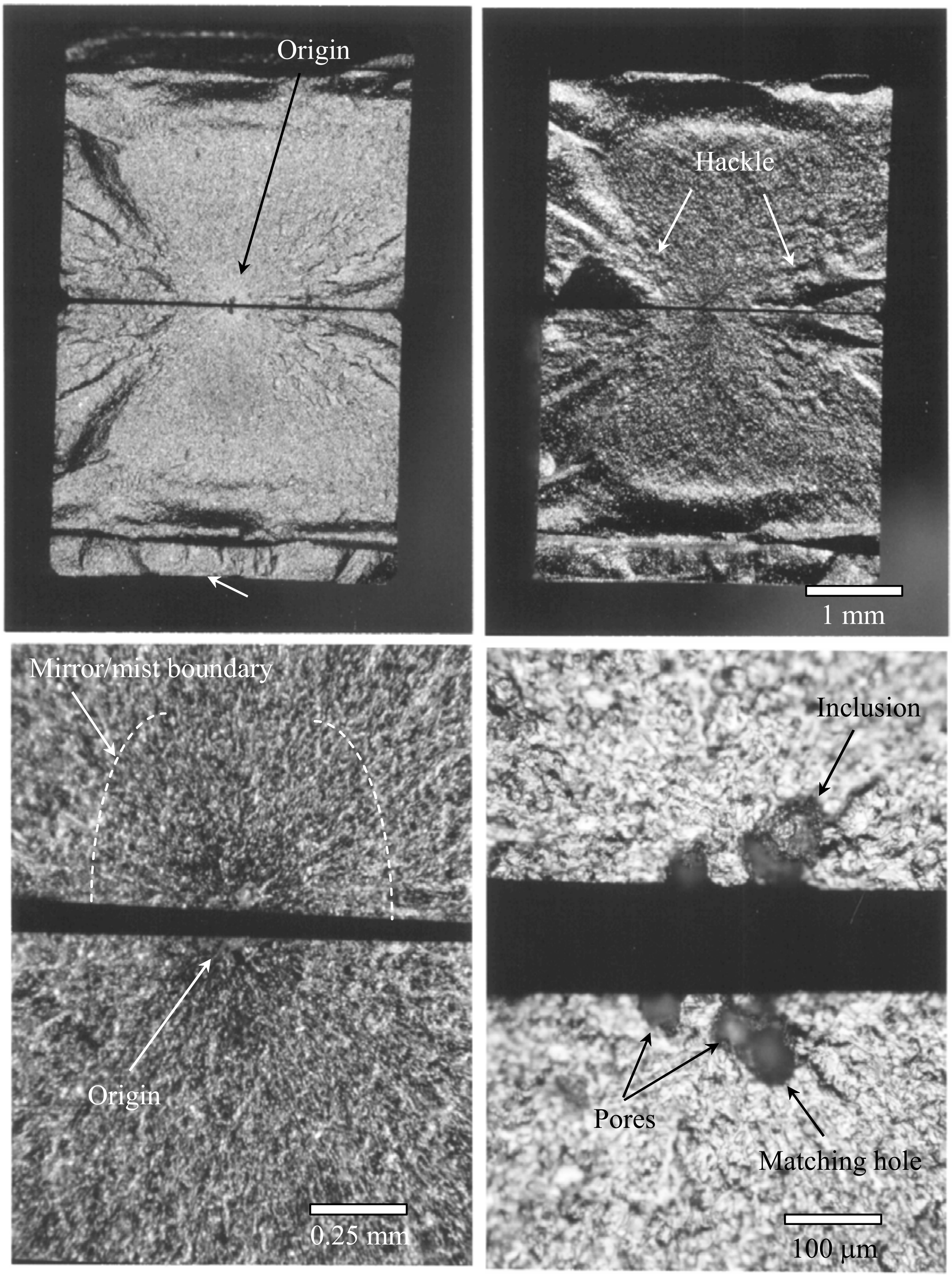

Figure A.2.1 - Fracture surfaces of a silicon carbide test-piece showing classical behaviour (a) in normal incidence illumination, (b) in grazing incidence illumination, (c) the origin region, and (d) details of the inhomogeneities acting as the fracture origin.

Example A.2.2 - silicon carbide

In contrast with the previous one, this example is of a second type of experimental silicon carbide which has suffered some exaggerated grain growth. In (a) matching faces of the primary fracture of the flexural test-piece are shown tensile faces together. The surfaces are very rough, but the compression curl near the outer surfaces is clear and indicates which faces are which. In the rest of the surface, the markings are irregular and not as clear as in the previous example. To the right there is a series of large grains appearing white or black. Locally, fracture markings appear to radiate from this region, whereas elsewhere in the tensile zone of the test-piece directions are not clear at this magnification. At higher magnification (b), so-called "river marks" appear in the facets of two large grains, emanating from an indistinct feature between them, and at still higher magnification (c), the presence in the lower half specimen of a near spherical inclusion becomes more obvious, from which all fracture lines originate.

This is interesting, because while the large grains might well have be the origin of fracture in such a material, particularly if they were close to the tensile surface, in fact a different type of processing defect appears to control the strength of the material.

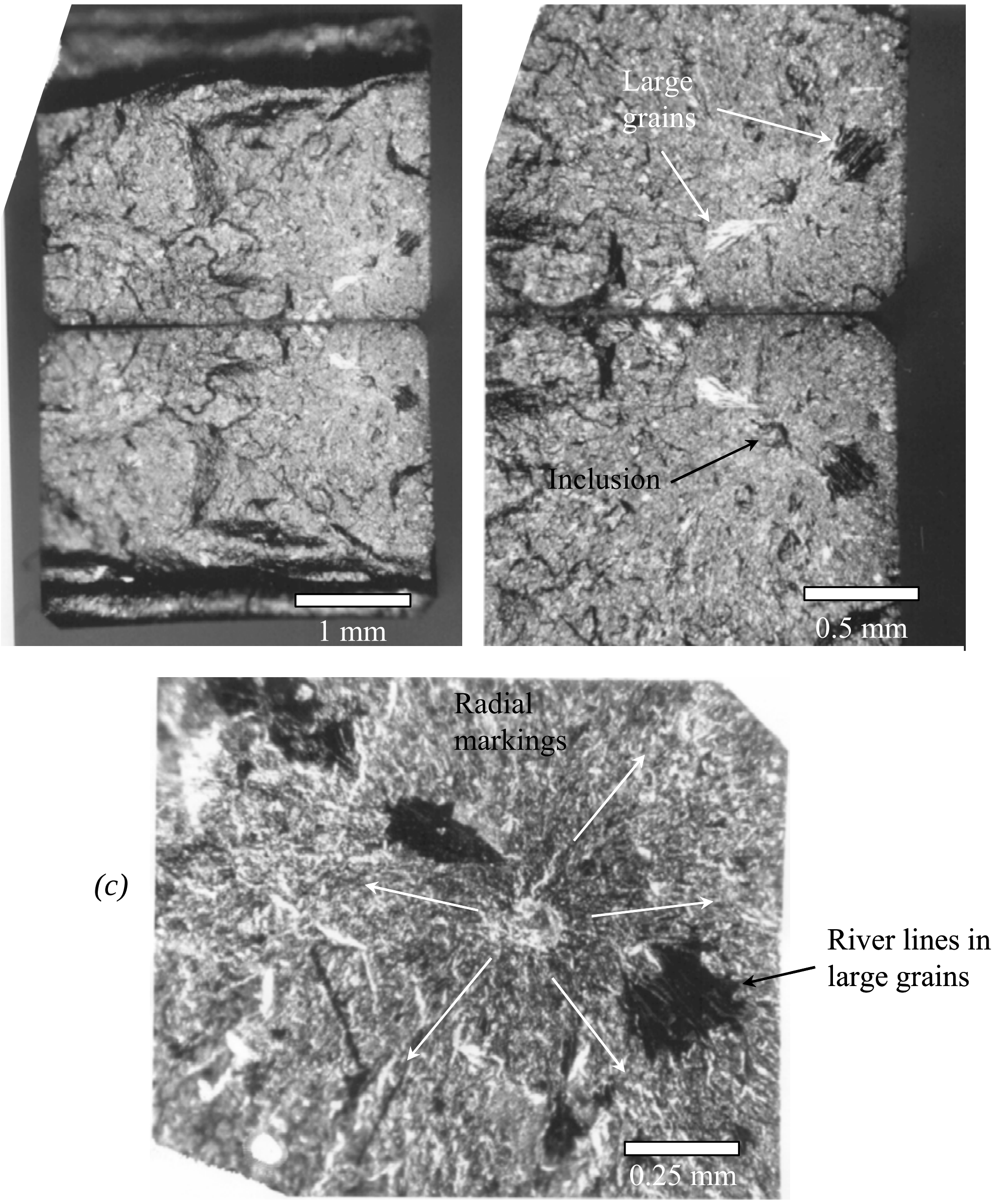

Figure A.2.2 - Fracture surface of a coarse-grained silicon carbide test-piece showing (a) very rough features, (b) approximately radial fracture markings from a subsurface position, and (c) the fracture origin, which is an inclusion between two large grains.

Example A.2.3 - silicon carbide

This example is of a third type of sintered silicon carbide. A comparison of the pair of fracture surfaces (a) shows that they do not match over their entire area, but there is similarity over the right-hand area with a clear fracture mirror. If the reassembled tensile face of the test-piece is examined (b), it is immediately clear that crack branching occurred soon after fracture, and a large wedge of material is in fact missing. Returning to image (a), the boundary of the unbranched area becomes clearer, and in fact lies just outside the mirror region, which accords with a high-energy, high-strength failure.

At higher magnification (c), the origin is seen to lie on the surface, but is highly localised, and has a slightly different texture to the surrounding material, suggesting an inclusion or agglomerate. Again, as in Example 1, without recourse to scanning electron microscopy it is not possible to identify the real nature of the origin. However, such a feature is clearly an intrinsic origin intersected during preparation of the test-piece, rather than an extrinsic origin caused by machining.

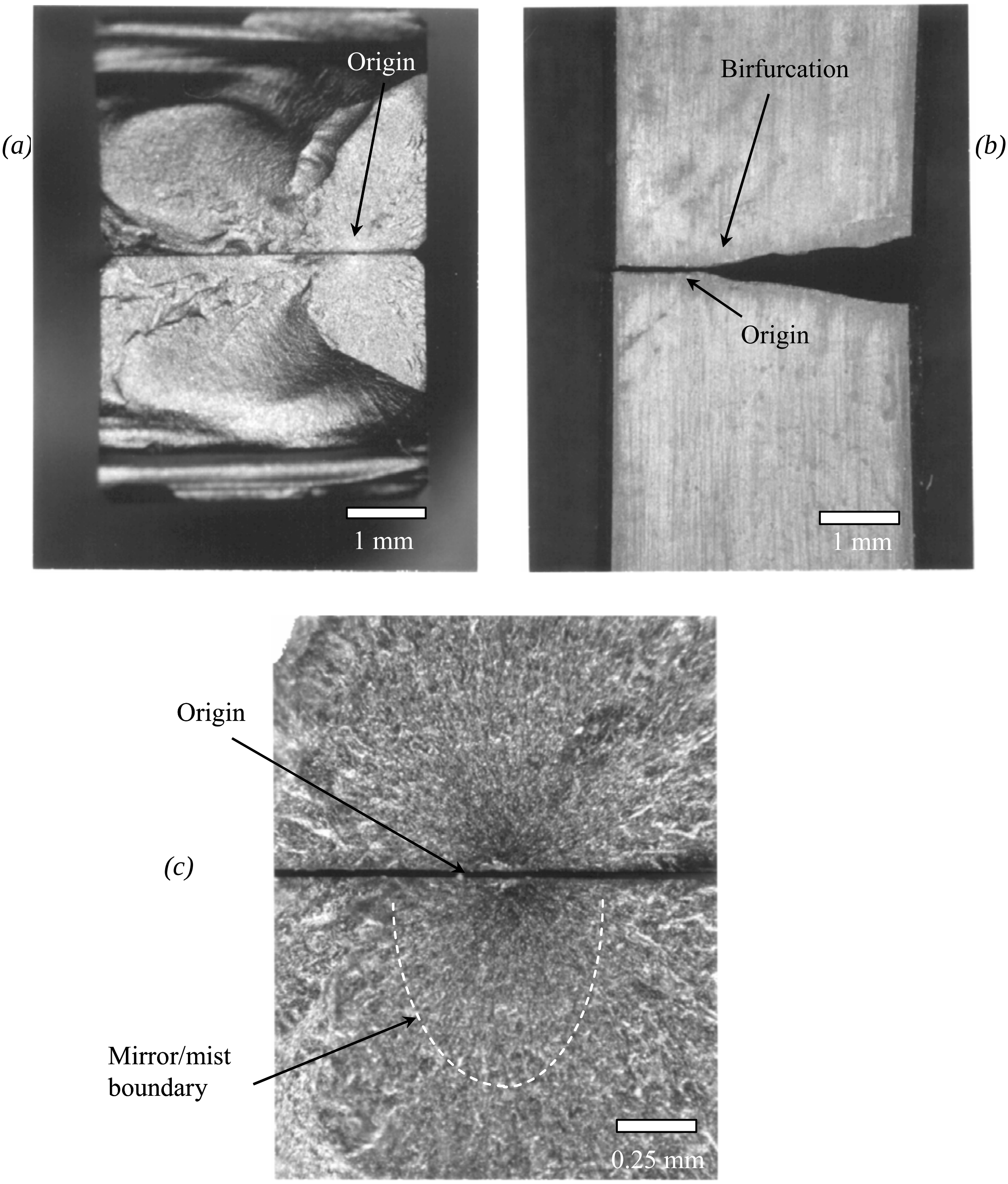

Figure A.2.3 - (a) Matched fracture surfaces of a silicon carbide test-piece in grazing incidence illumination showing only partial matching, (b) clear evidence for crack branching causing a flake to form, and (c) an image of the origin, which appears to be an inclusion intersected by machining the surface.

Example A.2.4 - high-strength, high-purity alumina

One of the main problems with many white oxide ceramics is translucence. Light penetrates typically a millimetre or so into the material, and produces a glare which makes fractography much more difficult. Despite the use of grazing incidence illumination, (a) shows very poor contrast in matched fracture surfaces of a high-purity alumina test-piece failing from a surface connected defect. The crack branching region is just visible on either side of the central origin. Contrast can be improved using grazing incidence illumination by preventing the sides of the test-piece from being illuminated, but a better solution is to apply a thin metal coating. Evaporated gold has been used in (b), with a dramatic improvement in the detail of fracture markings. The overall appearance and consequent interpretation are very similar to that of Example A.2.1, being for a high-strength failure in a fine-grained material.

Coating is an irreversible procedure, and should be done only if the original evidence does not need to be retained in the as-fractured state.

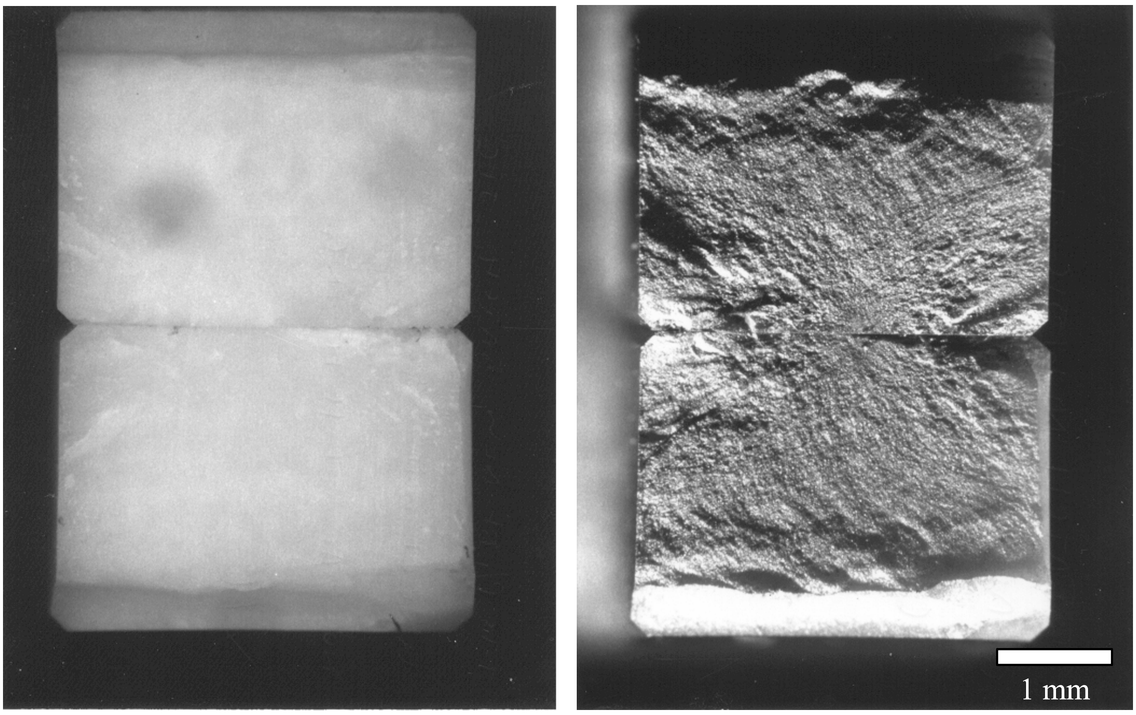

(a) *(b)*

Figure A.2.4 - Matched fracture surfaces of a high-strength, high-purity alumina (a) under grazing incidence illumination with very poor contrast, and (b) after gold coating to improve reflectivity.

Example A.2.5 - high-strength alumina/zirconia

A similar pattern to the previous example is seen when the uncoated fracture surfaces are matched and viewed in grazing incidence illumination from the top (a). The hackle is most marked to the left and right of the origin which is discrete and subsurface. At higher magnification, (b), the mirror/mist and mist/hackle boundaries are clearly visible. At still higher magnification, the radial markings appear to emanate on the tensile surface side of what is clearly an ellipsoidal pore. The crack presumably initiated in the narrow ligament between the machined surface and the pore, ran round the pore in both directions, and then radiated out in all directions. The small tail to the feature indicates that the two parts of the initiating fracture were not quite coplanar when they meet around the pore, leaving a gap between the two levels to join up later.

Despite the limitations of not coating the test-piece, in this case there is sufficient contrast and resolution to clearly identify the origin, even though it does not photograph particularly well. As with example A.2.4, minimising stray light illuminating the sides of the test-piece helps greatly.

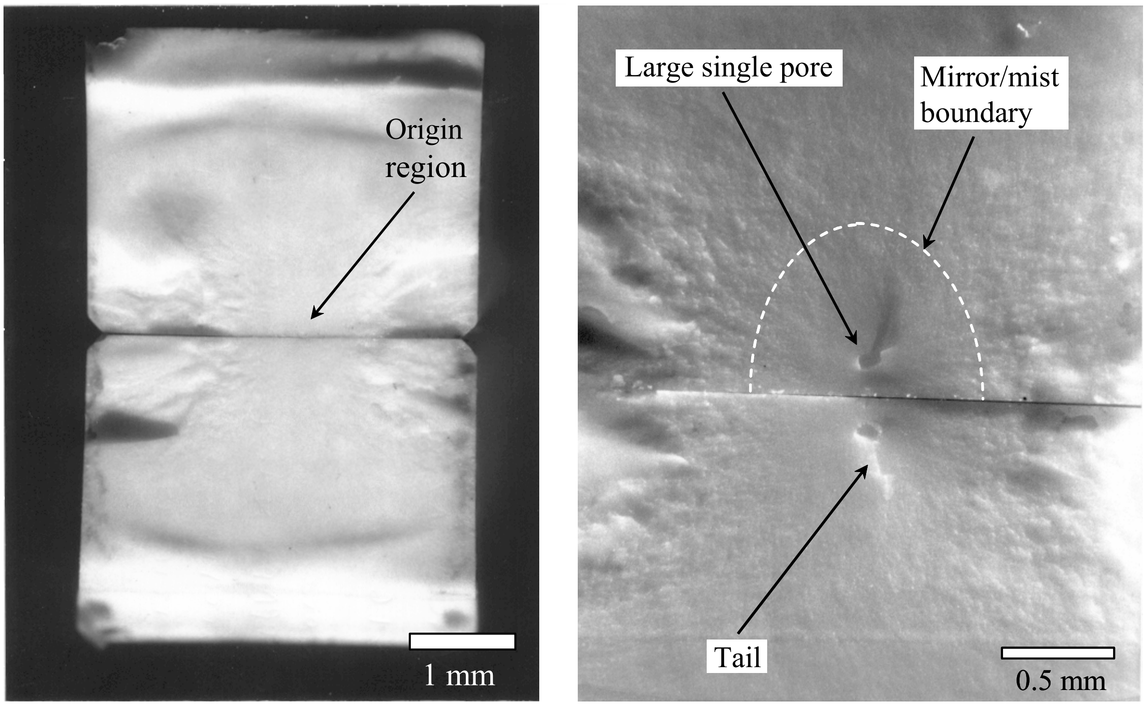

(a) (b)

Figure A.2.5 - Matched fracture surfaces of an alumina/zirconia material showing (a) a classical mirror/hackle pattern, and (b) at higher magnification that the origin is a large subsurface pore.

Example A.2.6 - medium-strength, refractory mullite porcelain

Materials such as these can be very difficult subjects for fractography. Not only do are they somewhat translucent, but cracks tend to bifurcate readily, leaving the fracture surfaces covered in raised flakes which scatter light differently from unflaked regions (a). Under grazing incidence illumination (b), these flakes are less obvious and the pairs of fracture faces match quite well, the compression side faces being distinguished by the compression curl. Fracture markings appear to radiate from near the left hand side of the adjacent tensile faces. At higher magnification (c, d with different lighting orientations), however, the mirror markings are rather weak, and the origin is indistinct. The only possible feature at the origin is a small agglomerate very close to the tensile surface seen as a raised lump on one face and a depression on the other. Scanning electron microscopy is needed to improve identification of detail at the origin.

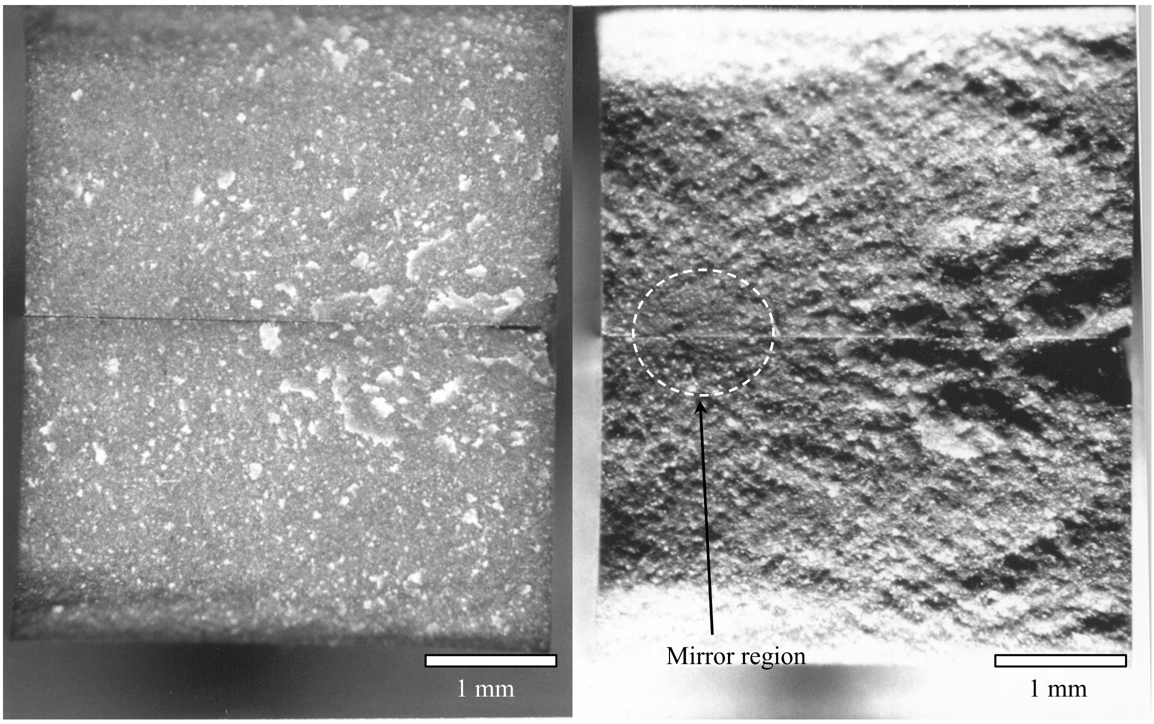

(a) *(b)*

Figure A.2.6 - Matched fracture surfaces of a refractory mullite porcelain, (a) with normal incidence illumination, (b) with grazing incidence illumination identifying the smooth mirror zone.

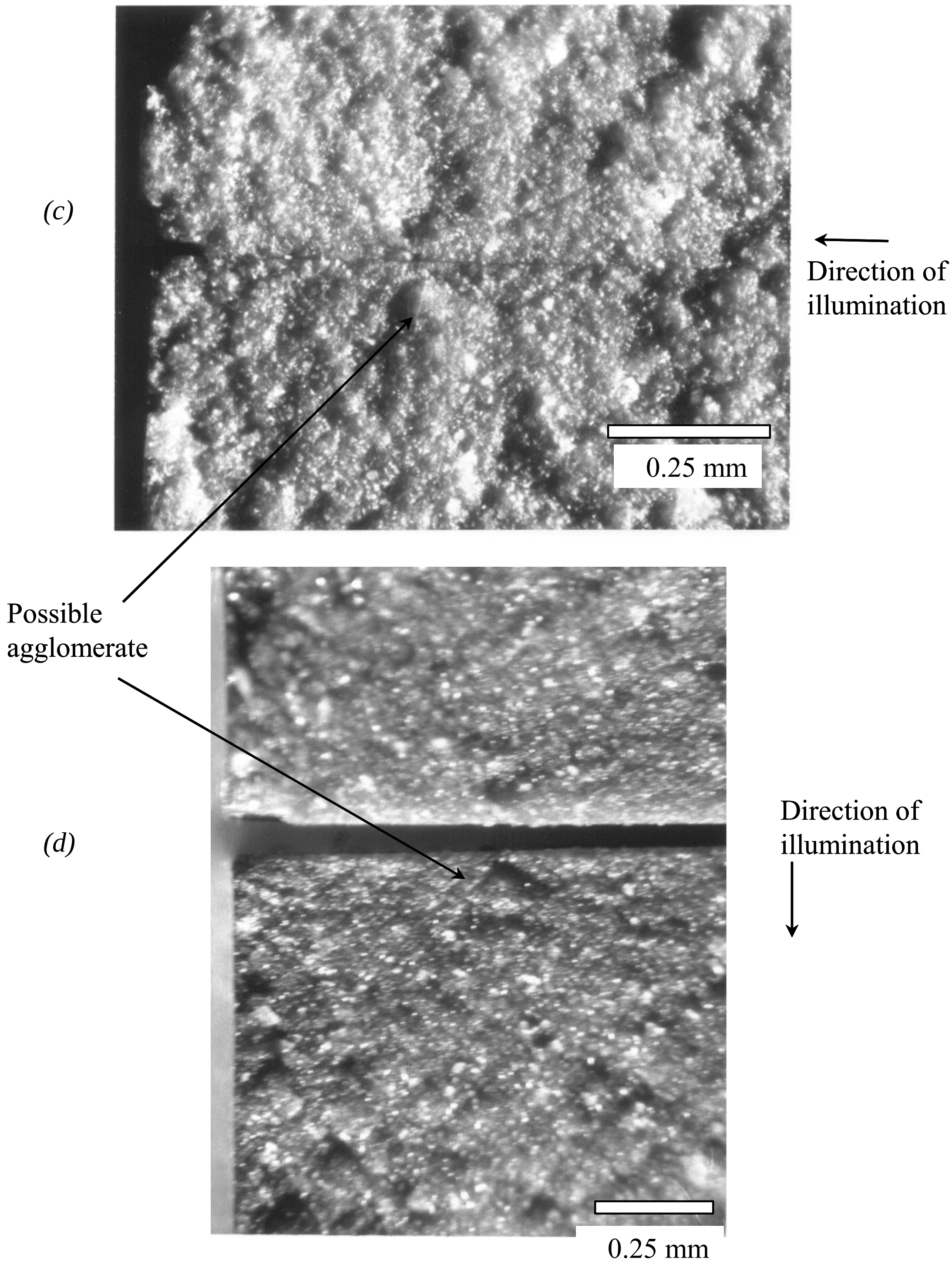

Figure A.2.6 - (c) and (d), as (b), but at higher magnification and illuminated in two different directions, revealing a possible agglomerate as the origin.

Example A.2.7 - sintered silicon nitride

This example is one of deliberately induced damage, but could equally well be representative of harsh adventitious damage. A Vickers indentation has been made in the centre of the test-bar surface with the intention of performing a so-called indentation fracture toughness test. The indentation has caused a pair of orthogonal half-penny cracks to be introduced into the surface, the one lying perpendicular to the direction of stressing in the test-piece having acted as the fracture origin. Under optical evaluation (a), the origin is clearly in the centre of the tensile faces, but fracture markings are not strong. There is no crack branching, and the compression curl (not shown in (a)) is weak. This is generally indicative of a low-stress failure, where the mirror limits would effectively lie outside the size of the test-piece.

The true nature of the deliberately introduced origin is readily visible in the scanning electron micrograph (b), where the local surface damage left by the indentation is clear, as is the half-penny crack intersected by the one acting as the origin. The limits of the original half-penny crack forming the fracture origin can just be made out as the approximately semicircular boundary between the heavily striated region and the more irregularly fractured region. This is typical of the evidence needed to support the identification of pre-existing cracks or machining damage as the origin. There is often a change in direction of striations, or a change in the intergranular/transgranular nature of the fracture surface between the original crack and the final fracture surface.

(a)

(b)

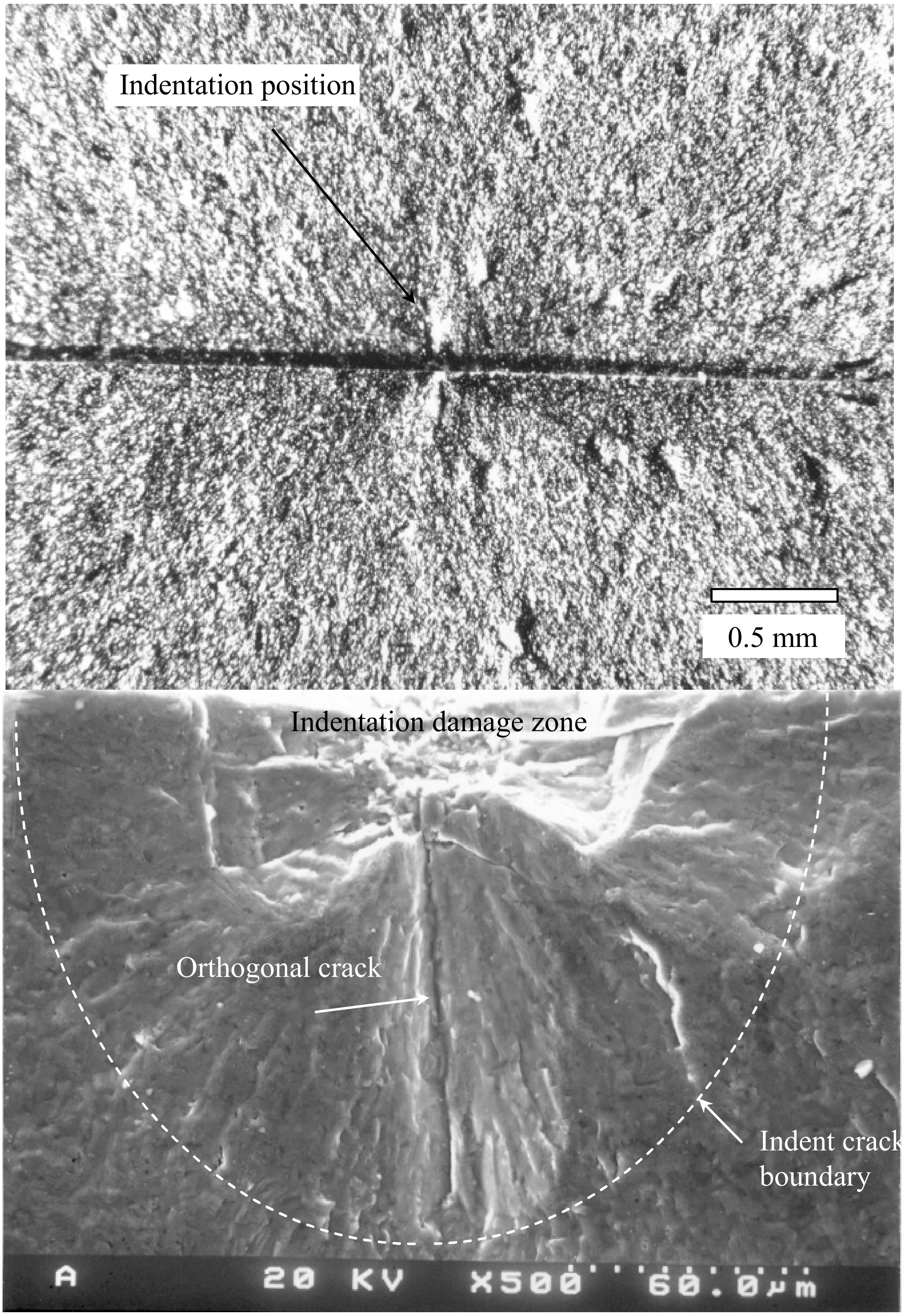

Figure A.2.7 - (a) Matched fracture surfaces of a deliberately indented test-piece of sintered silicon nitride, and (b) an SEM micrograph of the indentation site, showing the boundary of the indentation crack.

Example A.2.8 - sintered silicon nitride

In this experimental high-strength material, very clear fracture markings are produced radiating from a distinct origin visible as a raised feature in grazing incidence optical microscopy (a). There is strong compression curl, and very marked crack branching resulting in the production of a wedge of material matching to the left-hand side of the pair of faces. At higher magnification (b), the pattern of fracture marks around the origin becomes clearer. The small ridge running away from the origin into the material is indicative of the crack running in both directions around the origin from the side closer to the tensile test-piece faces, being slightly out of plane when meeting and leaving a step which eventually disappears as the crack propagates across the test-piece. Because of the fine grain size, the mirror/mist and mist/hackle boundaries are very clear, which would permit a good fracture mechanical assessment of the fracture process.

Using the SEM, the origin can be clearly seen in (d), the raised feature, as a poorly sintered region associated with much residual porosity, visible in (c), the matching depressed feature. It can thus be identified as an abnormal, presumably unintentional, processing defect.

(a)

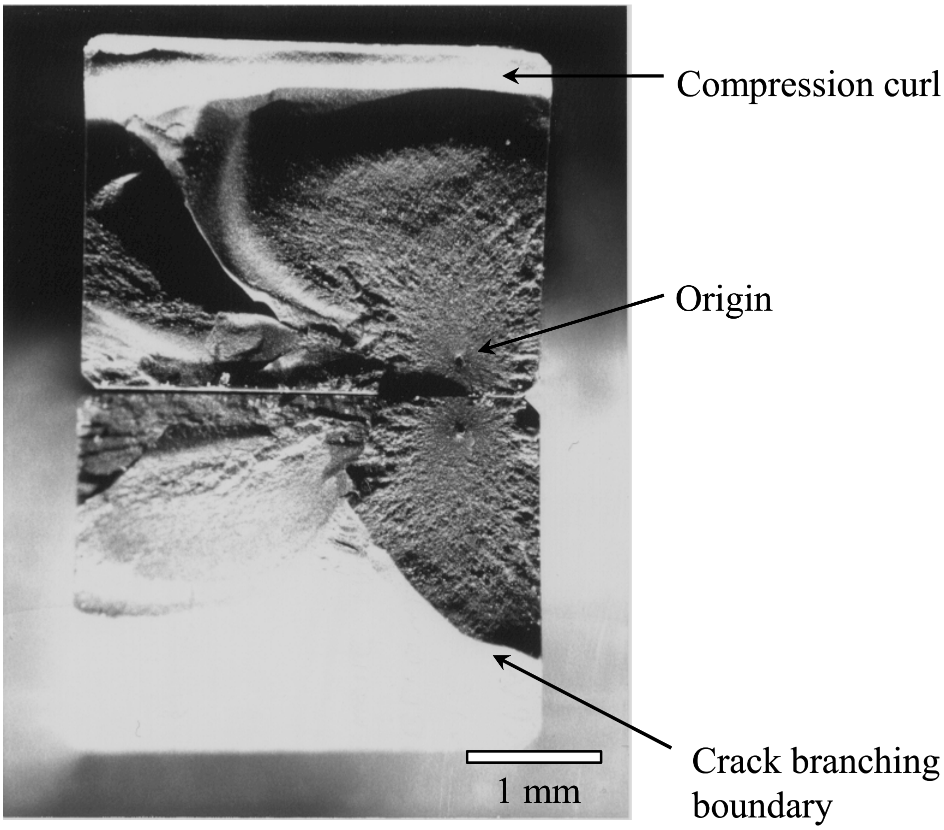

Figure A.2.8 - Matched fracture surfaces of a sintered silicon nitride test-piece failing at high stress from an internal defect. Only parts of the fracture surface match.

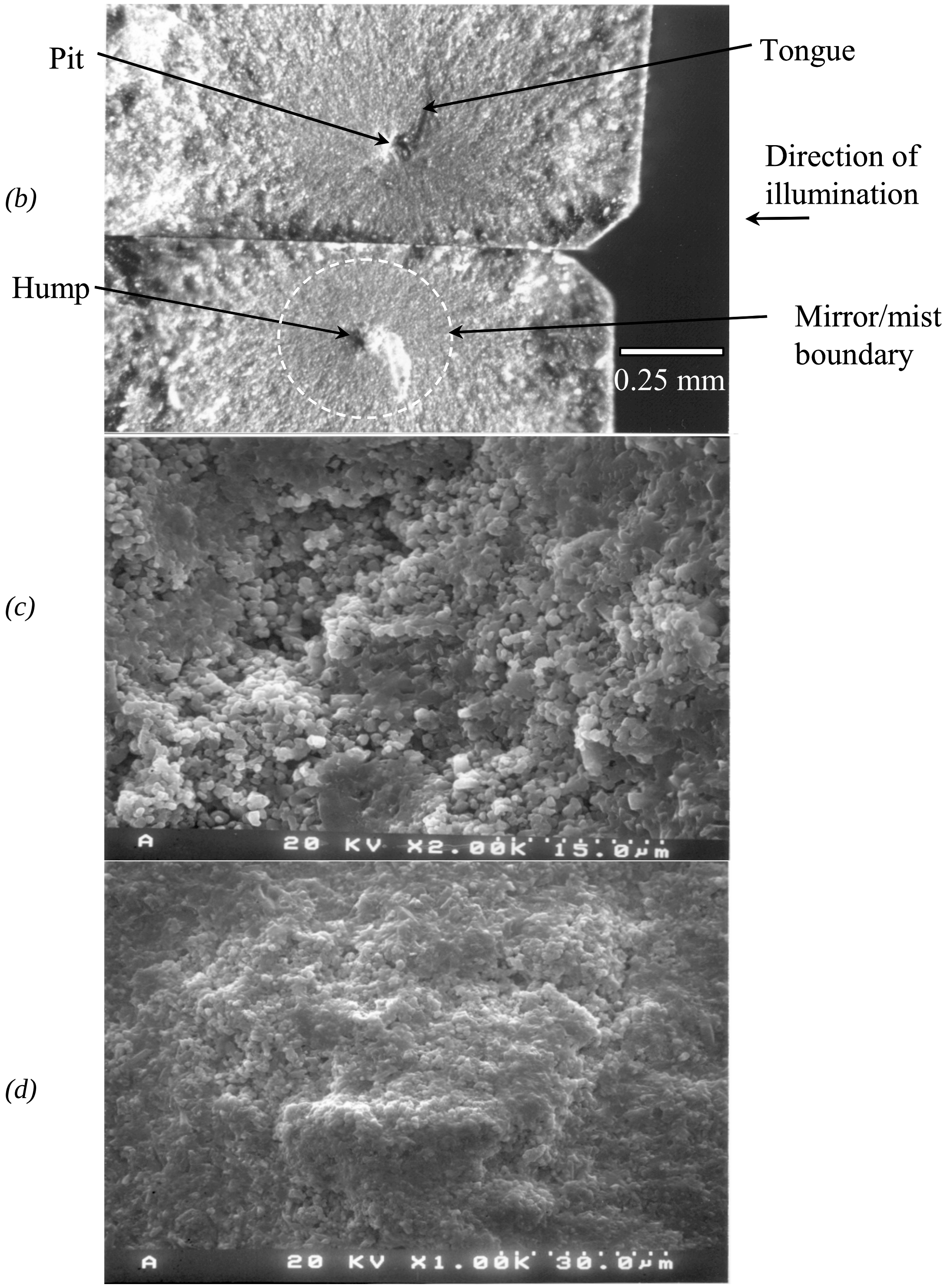

Figure A2.8 (cont.) - (b) Close-up of fracture origin showing the clear mirror/mist boundary; and SEM photographs of (c) the pit in one surface and (d) the raised hump in the other, identifiable as being a hard agglomerate with associated porosity.

Example A.2.9 - sintered alumina-based hard particulate composite

In (a), we see a test-piece which has an abnormal appearance. There are many small chips and flakes removed from the tensile edge. This is caused by damage subsequent to the main fracture. In this case, the test-piece impacted with the test-jig sufficiently severely that most of the original fracture surface has been lost. The only small area that might be original fracture is to the left side, where radial fracture marks can be seen. In (b) we see a second test-piece that has also received secondary damage obliterating a near edge origin which was presumably close to the centre of the test-piece. This was a high strength failure which resulted in severe and early branching removing a wedge-shape to the left-hand side of the centre and leaving a distinct ridge down the test-piece centre. These two examples show how the fractographer's task can be hampered by subsequent damage. In the third example (c), life is much easier. This test-piece failed at lower stress, and we see a distinct mirror/mist/hackle region surrounding a discrete origin away from the original tensile surface. Crack branching has occurred, but has not caused confusion. In (d), use of the SEM reveals the nature of the origin to be a coarse-grained inclusion which has produced a small halo around it with some pores. This is likely to result from lack of cleanliness in processing the original powder.

(a)

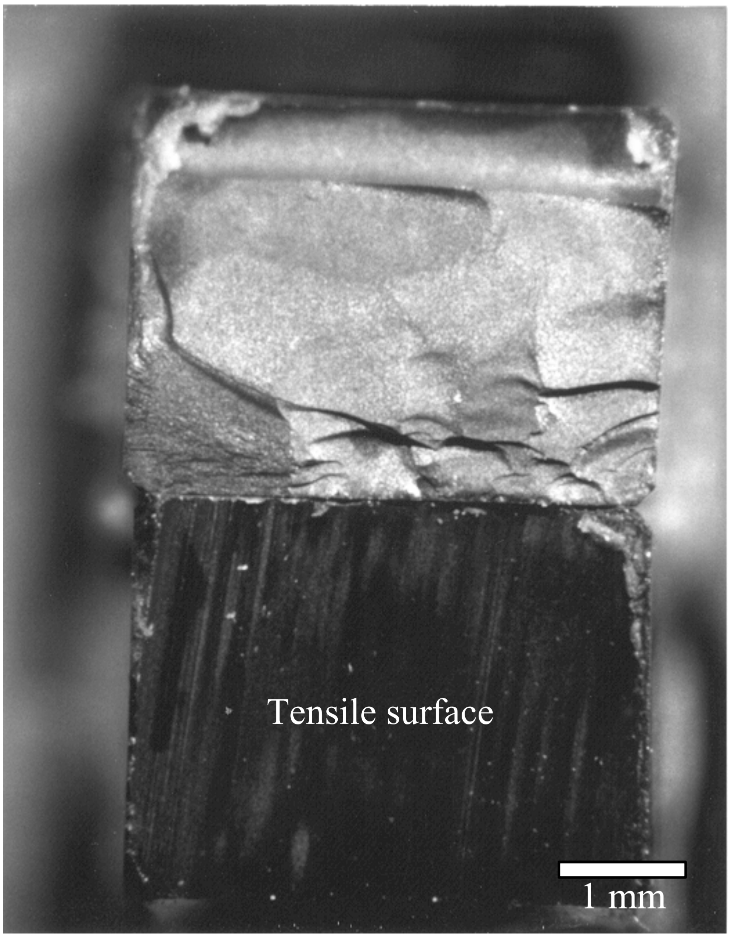

Figure A.2.9 - (a) Fracture surface of an alumina composite test-piece suffering from impact with the test jig during fracture, the chipping eliminating the original surface features.

(a)

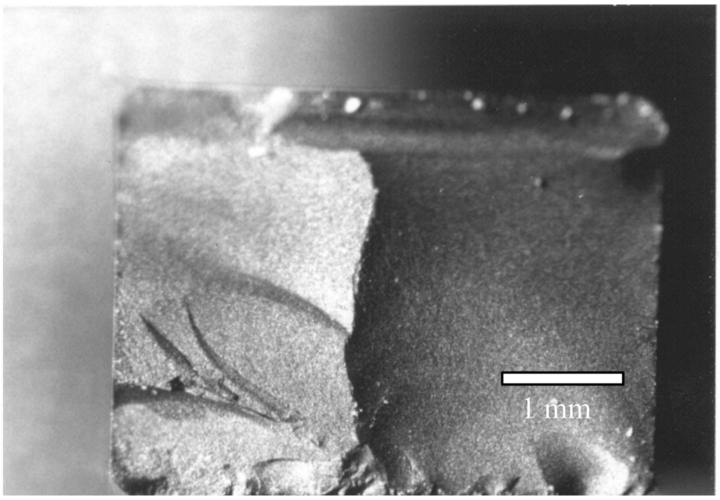

(c)

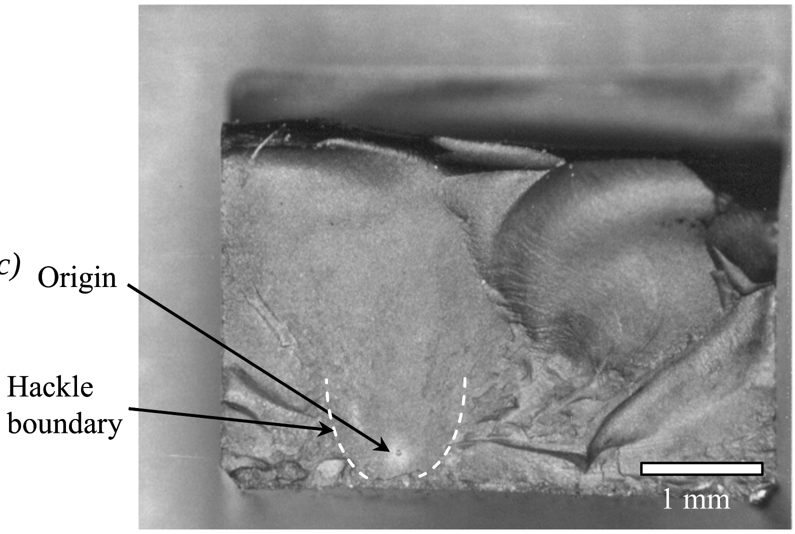

(d)

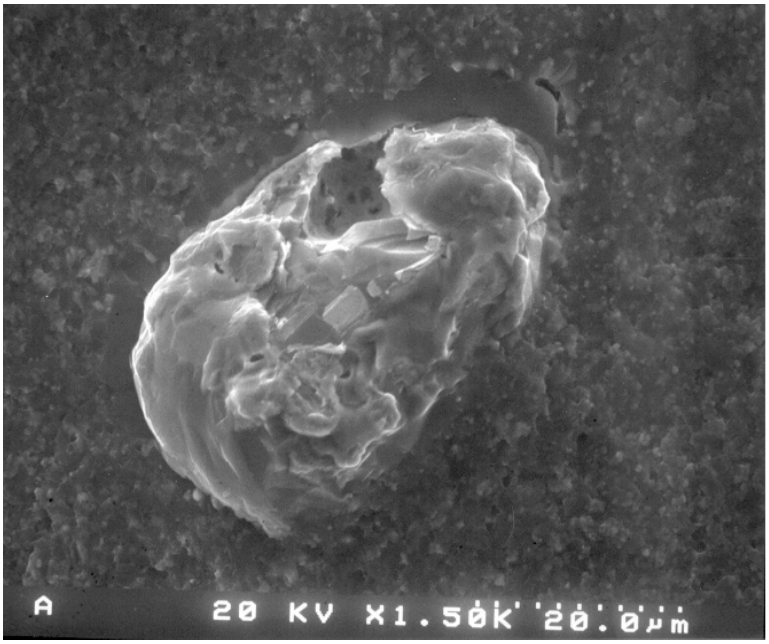

Figure A2.9 (cont.) - (b) as (a), but second specimen with large flakes resulting in loss of original surface; (c) third specimen with distinct origin, which is a clear inclusion in (d).

Example A.2.10 - partially stabilized zirconia

This relatively coarse-grained material is particularly difficult. The test-piece failed prematurely during a cyclic loading test to determine Young's modulus, but after the fracture it was unclear which side of the test-piece had been stressed in tension and might contain the fracture origin (the tensile face had not been thus marked). The pair of fracture surfaces (a) viewed with general illumination contains no compression curl, so it is not even certain whether the tensile faces are placed together. The surfaces are covered in light-scattering flakes from multiple cracking, but the pattern of these leaves no clue as to directions of fracture. Examination of the tension and compression faces of the test-piece shows that the line of fracture is more irregular on one than the other. In particular, there is a discrete meander which could represent the rough position of the origin. In grazing incidence illumination (b) (arranged as in as in (a)) there is still no clear pattern of fracture marks, the undulations in the fracture surface probably reflecting more the microstructural inhomogeneity than classical markings. Viewing the possible origin region with at an oblique angle (c) reveals no additional information.

If SEM evaluation had been attempted, it would have proved very difficult to localise on a potential origin with a material of this type.

This example illustrates where fractography cannot easily provide definitive answers, but has to clutch at straws in seeking an explanation. In this case a possible explanation is that a combination of grinding damage and a particularly large grain or pore region interacted to cause the failure, but the scale of the microstructural irregularities obliterates all the classic markings that the fractographer relies upon..

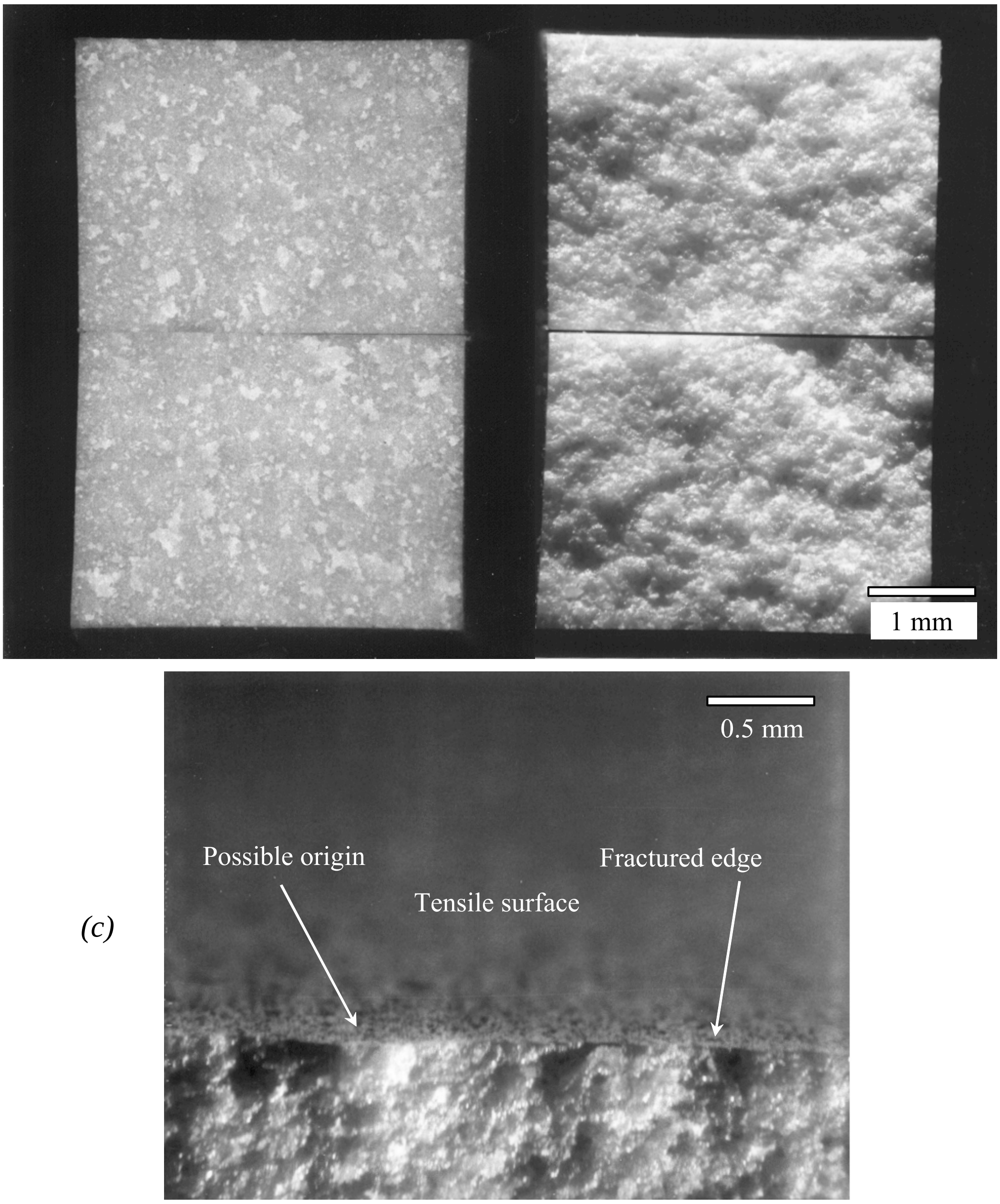

Figure A.2.10 - Matched fracture surfaces of a partially stabilised zirconia test-piece (a) under normal illumination, (b) under grazing incidence illumination showing difficulty in fracture pattern identification; (c) the uneven edge of the test-piece with a possible agglomerate as the origin.

Example A.2.11 - Y-TZP machining flaws

This example is classical of machining flaws. Machining can leave a surface with a network of semi-elliptical cracks, mostly quite shallow. This example is of a low-strength yttria partially stabilised zirconia (Y-TZP) test-piece fractured from the edge chamfer, the fracture lines clearly radiating from the left-hand angled corner in (a). (Note that the chamfer is rather large, much greater than normal in flexural testing. Also, the contrast is poor because the material is translucent.) There is no hackle or crack branching normally seen in high-strength test-pieces, suggesting that a large origin should be sought. At higher magnification in (b), the fracture lines (arrowed) do not have a common focus inside the test-piece. At still higher magnification (c) (using grazing incidence illumination in a conventional metallographic microscope resulting in limited depth of focus, and hence a poor quality image), the elongated nature of the origin along the chamfer becomes apparent, with a chip missing at the lower corner. The suspected flaw shape is marked, and is essentially delineated by a subtle change in roughness.

(a)

(b)

(c)

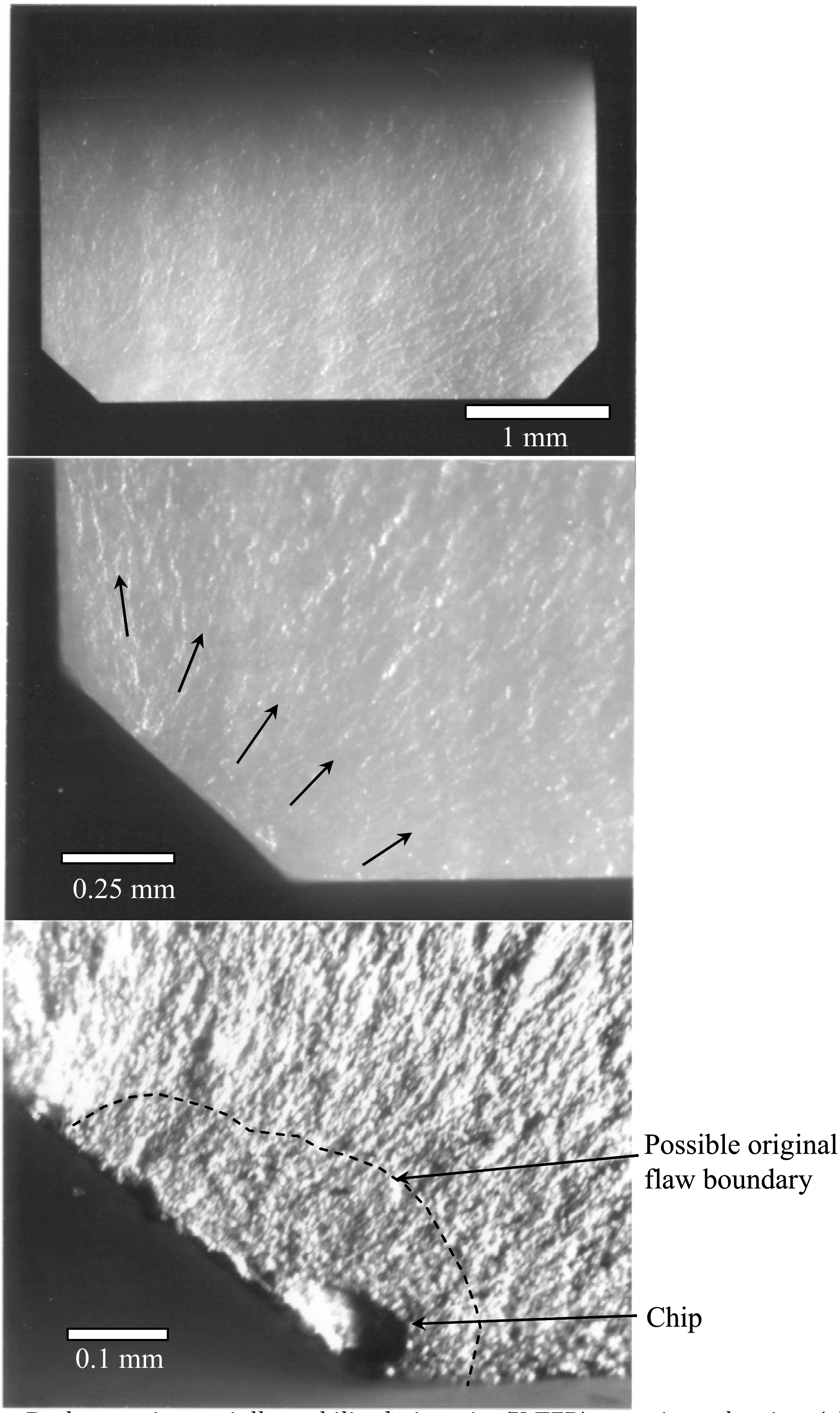

Figure A.2.11 - Broken yttria partially stabilised zirconia (Y-TZP) test-piece showing (a) failure from a large corner chamfer, (b) fracture marks radiating from an extended origin, and (c) possible demarked flaw as boundary between smoother and rougher regions.

Example A.2.12 - hardmetal fracture origins

The overall appearance of fracture origins in hardmetals tends to be very similar to those encountered in high strength ceramics, and usually show the same types of features and origins are found. Even though fracture stresses tend to be in excess of 1 GPa, up to 3 GPa, depending on material quality, test-piece dimensions and machining practice, the higher toughness levels mean that fracture origins tend to be of similar size to those encountered in ceramics. Example (a) shows a discrete near-surface pore with radiating fracture markings and a clear mirror, while example (b) shows the origin to be an elongated porous seam resulting from inadequate compaction and incomplete closure during sintering. Example (c1) shows a pore as the fracture origin, the surface of which contains islands of cobalt binder phase (c2) showing characteristic terracing (c3). Example (d) is of a large pore which shows a number of spherical features inside, which can be identified as original granules which have been inadequately compacted together in the unfired state. Fracture has occurred at the nearest point to the external surface and has propagated round the pore in both directions. Examples (e) show a large carbide grains at the surface of the test-pieces, one of which (e3) has been readily damaged by machining leaving a clearly marked semicircular pre-crack inside the large grain.

The most difficult types of origin to distinguish conclusively are those with no apparent discrete origin. An example of initiation at the surface is shown in (f1) and at higher magnification in (f2). Although not distinct, this may be caused by machining damage because fracture lines do not radiate from a point within or at the surface, but from outside it. The machining direction is parallel to the crack face, and could have generated shallow semielliptical cracks. A second example is shown in (g1) to (g3). The clearly radiating fracture markings in (g1) when viewed as (g2) do not originate from the surface, but some distance below it, but there is no significant abnormality in this region, even when viewed at higher magnification still (g3).

(*a1*)

(*a2*)

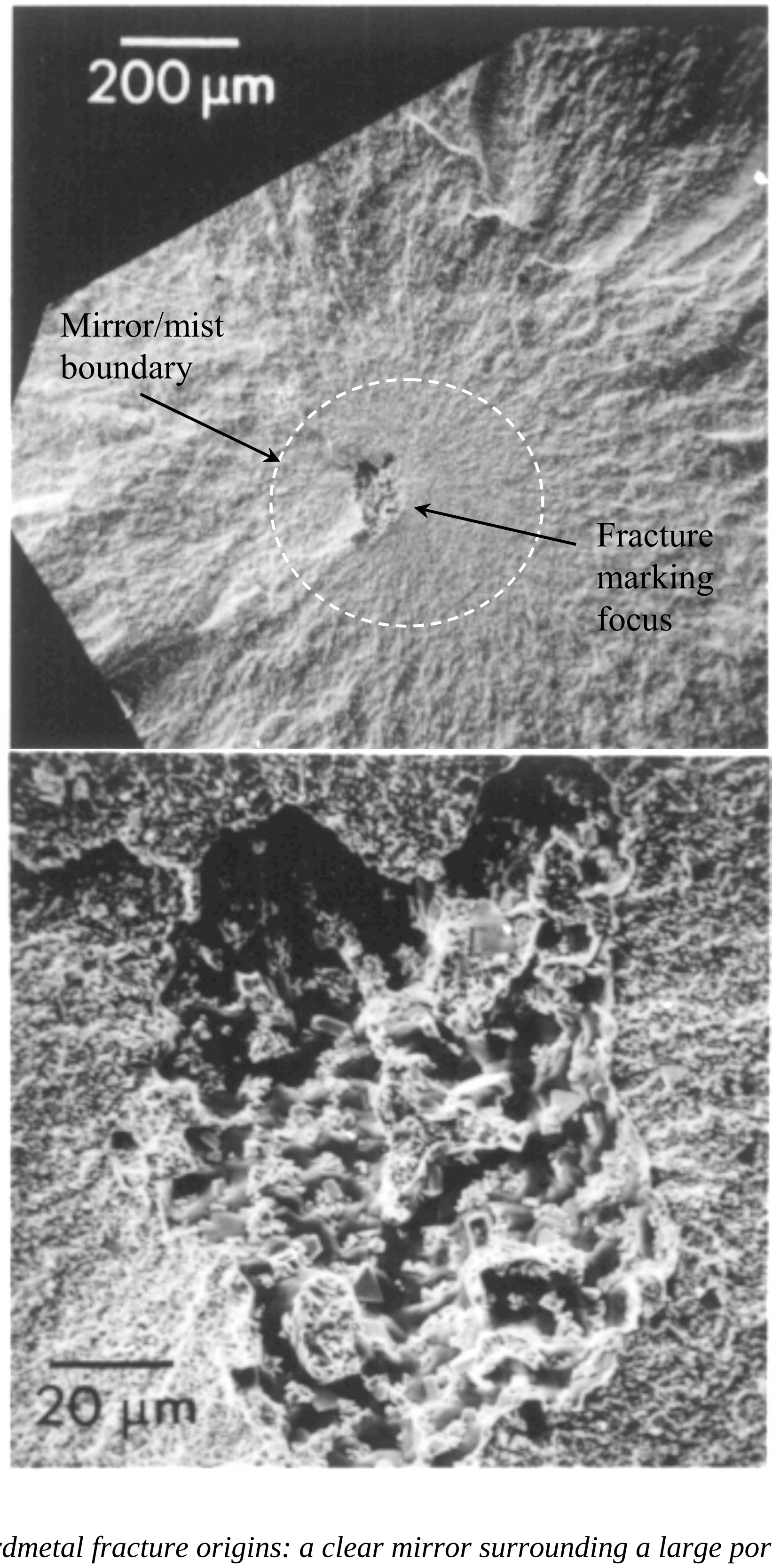

Figure A2.12 - Hardmetal fracture origins: a clear mirror surrounding a large porous region (a1), and at higher magnification (a2) showing the morphology of the defect.

(*b1*)

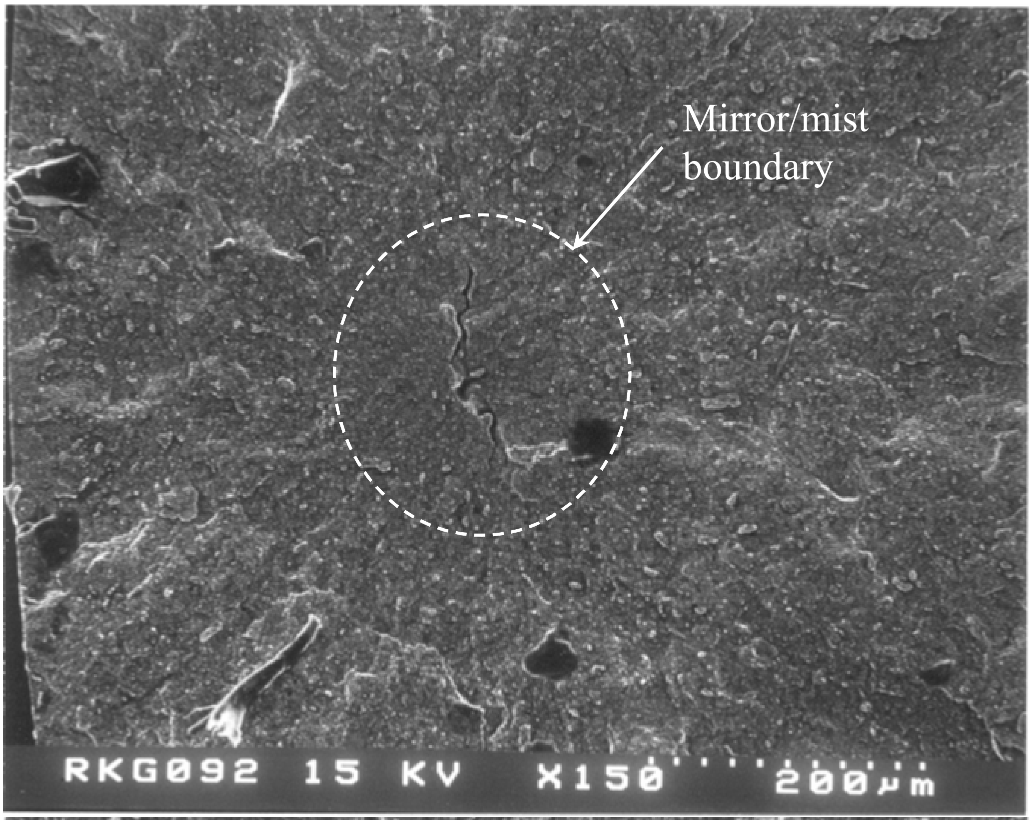

(*b2*)

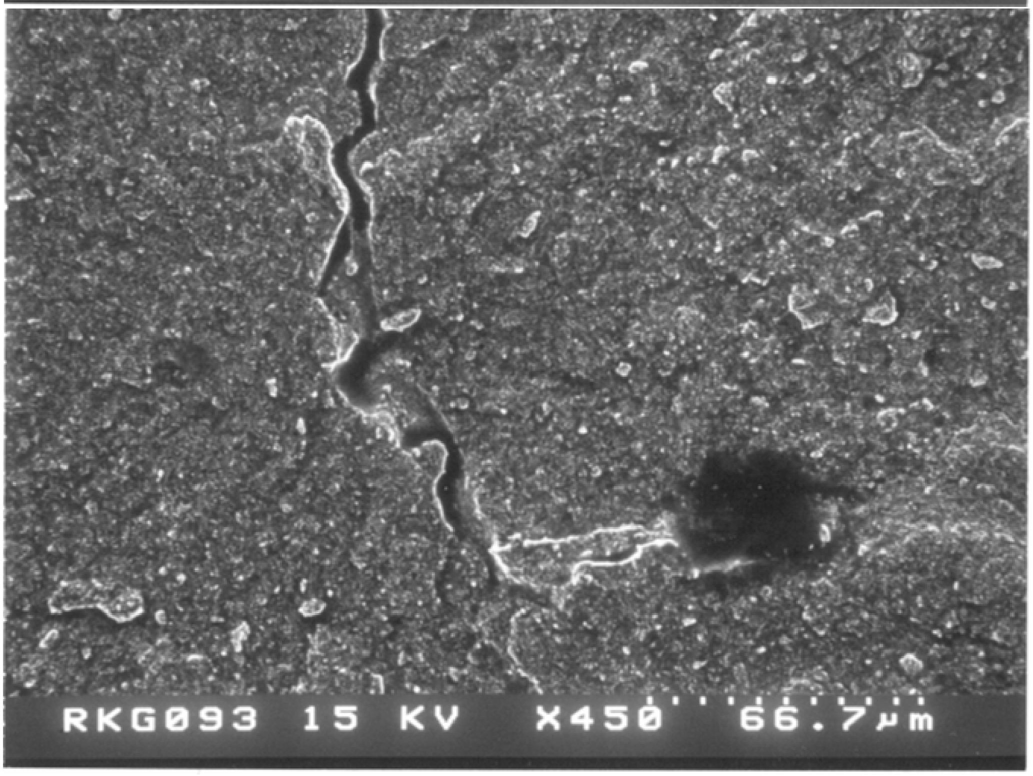

Figure A2.12 (cont.) - Hardmetal fracture origins (cont.): (b1) showing fracture from a discrete delamination with fracture mirror marked, and (b2) at higher magnification.

(*c1*)

(*c2*)

(*c3*)

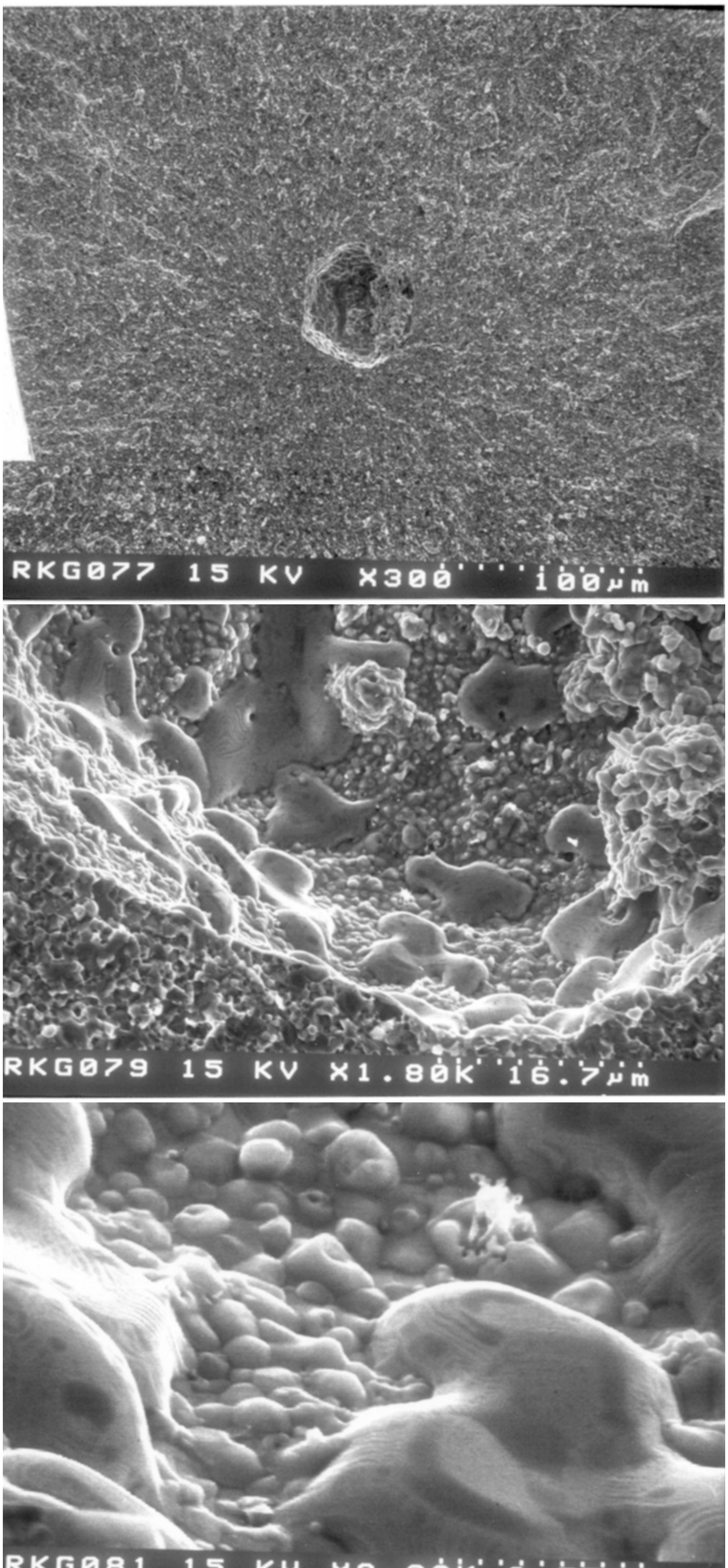

Figure A.2.12 (cont.) - Hardmetal fracture origins: (c1) fracture from a large pore with radial markings, (c2) the pore surface showing a cobalt concentration with characteristic steps (c3).

(*d1*)

(*d2*)

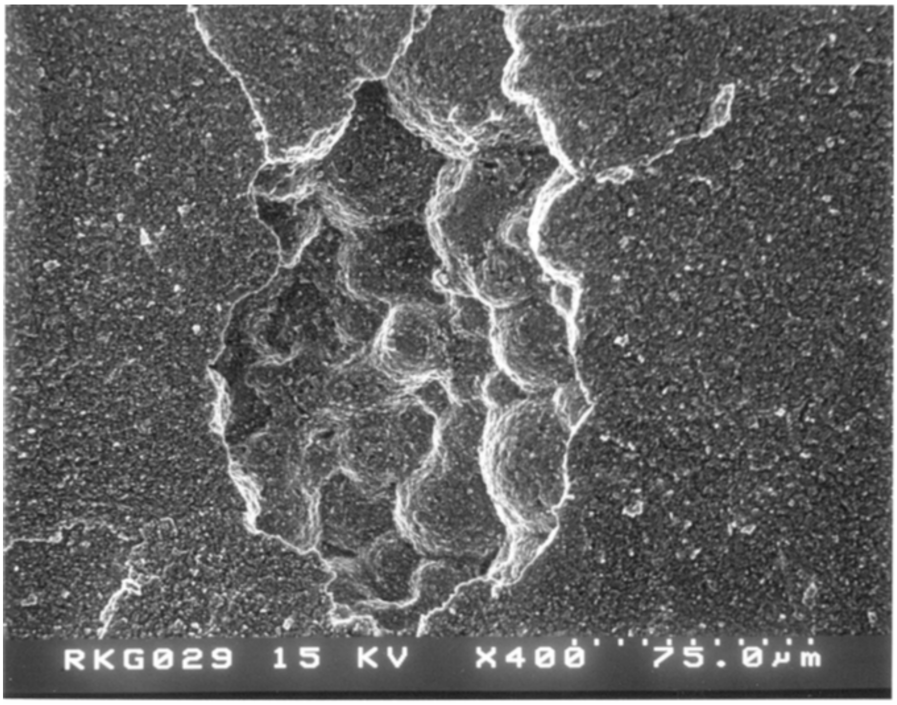

Figure A.2.12 (cont.) - Hardmetal fracture origins: (d1, d2) two examples of voids associated with original granulates which have not compacted adequately in pressing.

(*e1*)

(*e2*)

(*e3*)

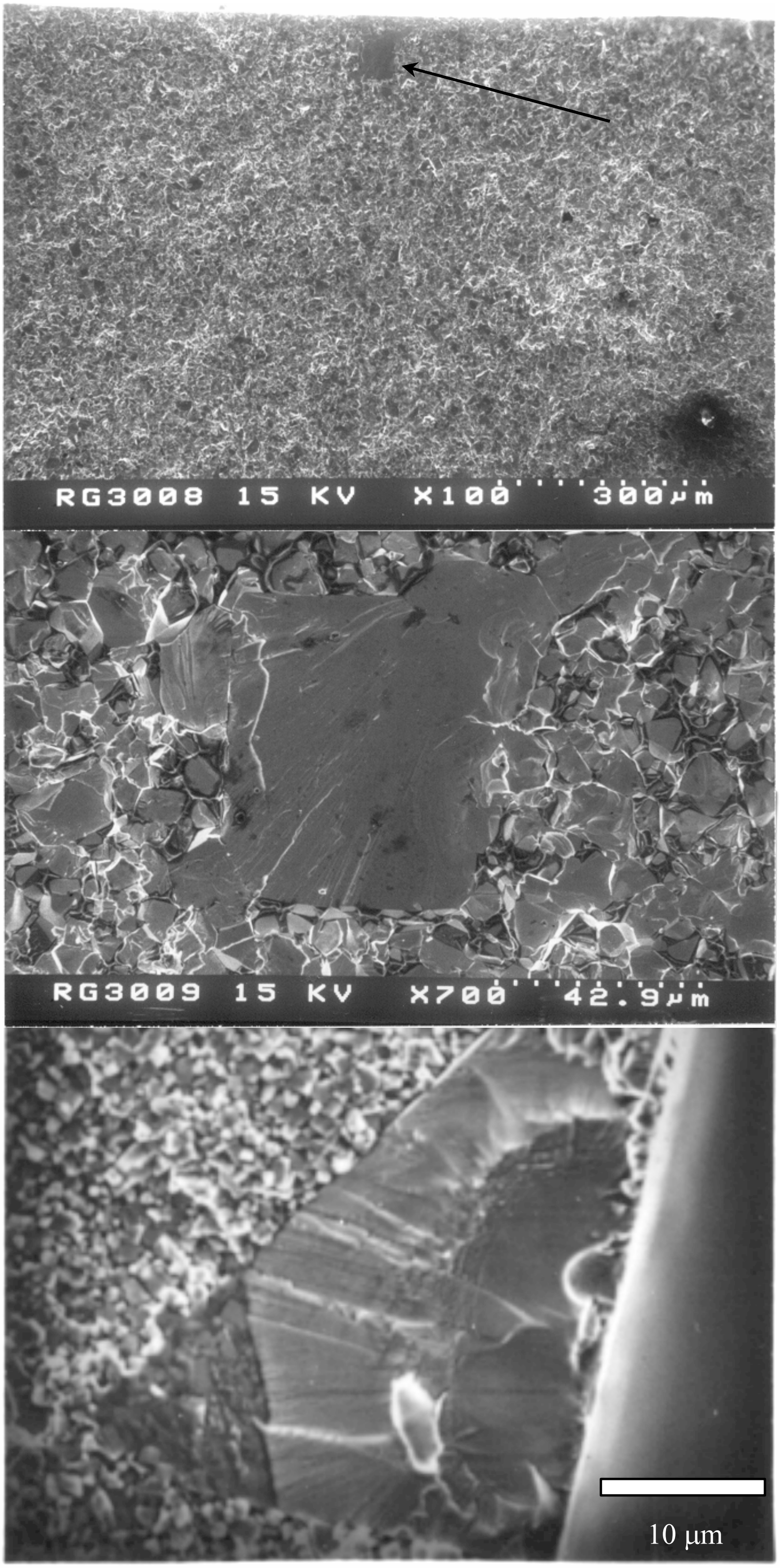

Figure A.2.12 (cont.) - Hardmetal fracture origins: (e1, e2) a large near-surface grain, and (e3) a large grain intersected by machining showing a large elliptical precursor machining flaw inside the grain.

(*f1*)

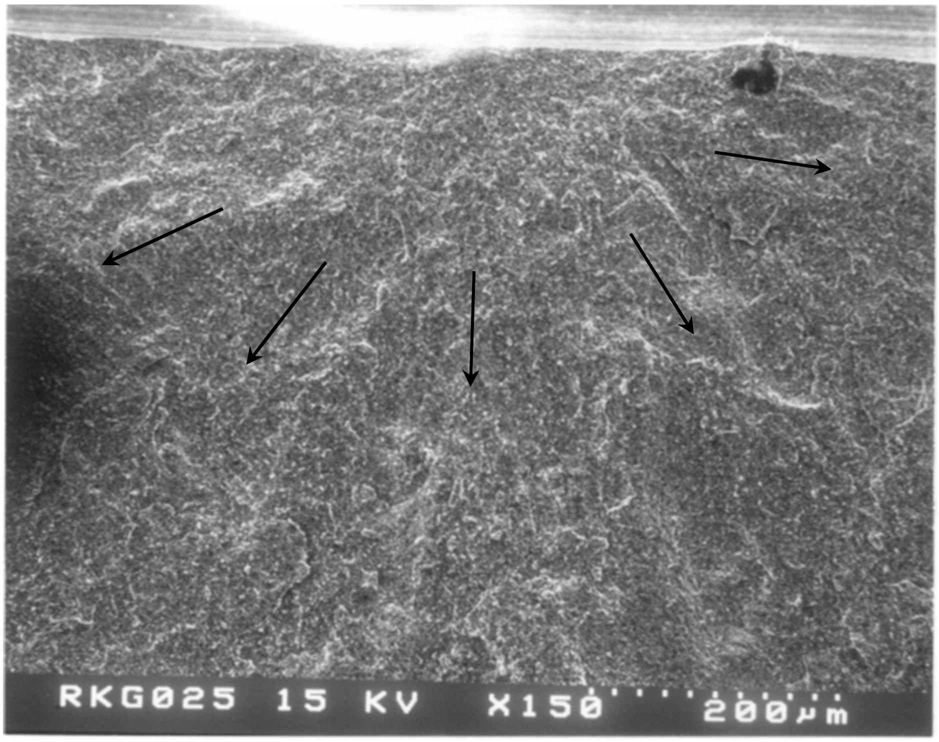

(*f2*)

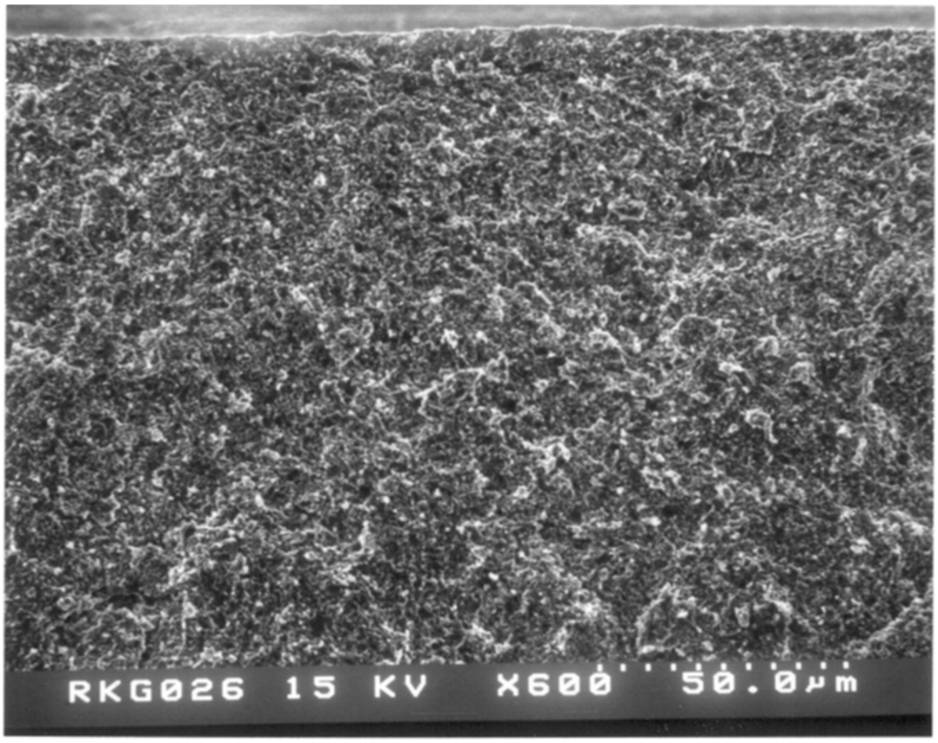

Figure A.2.12 (cont.) - Hardmetal fracture origins: an example of possible machining damage acting as the origin. Fracture markings are clear at low magnification (f1), but no obvious flaw demarcation can be identified at higher magnification (f2).

(g1)

(g2)

(g3)

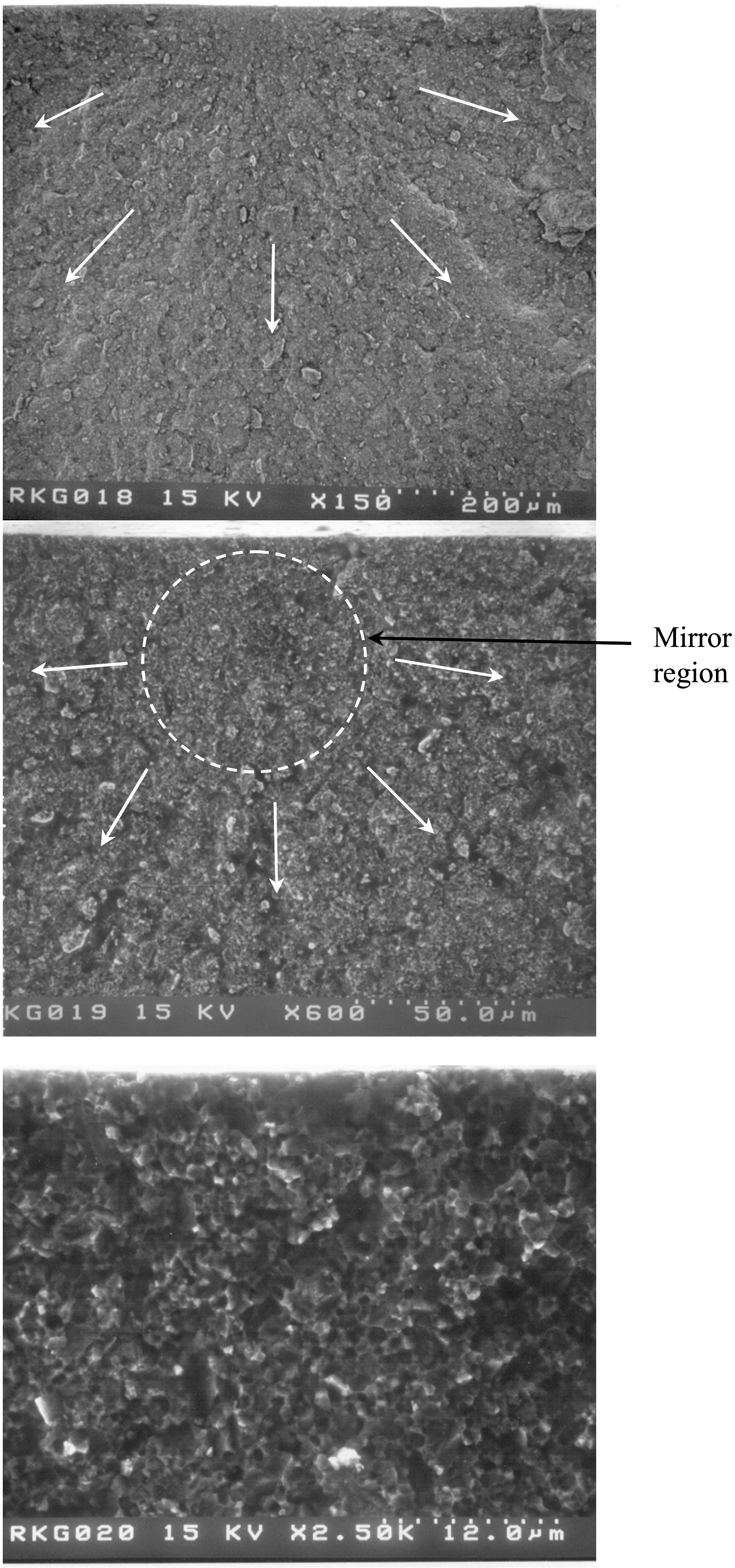

Figure A.2.12 (cont.) - Hardmetal fracture origins: (g1 - g3) an example of possible normal microstructural failure. Fracture markings suggest a subsurface origin, but (g3) no obvious defect in the origin region can be seen.

Example A.2.13 - misleading effects

Adherent dust particles, fracture debris, finger grease, skin fragments, metal marks, plastic mounting medium, etc, can usually be quickly seen and dismissed when examining fracture surfaces at low magnification. Rinsing with alcohol and blowing dust off is all that is often necessary to provide reasonable quality pictures. However, at higher magnification, particularly in the scanning electron microscope, even small amounts of remaining contamination can spoil photographs, or produce misleading effects. Example (a) is of what are probably skin fragments trapped in a pore intersected at the surface of a hardmetal test-piece. The radiating appearance of the fracture marks clearly indicates that this is the position of the origin. Example (b) shows a featureless dark patch situated over the origin. This is probably a grease spot which reduces the secondary electron intensity emitted by the surface, rather than a significant microstructural feature. Example (c) shows adherent lumps of material which appear to shadow the underlying material. Unfortunately, the decoration of the edge completely obscures the fracture origin. Example (d) is of a skin fragment trapped over the fracture origin, which appears to be a pore near the surface, but might be misconstrued as an inclusion.

The solution to these problems is cleanliness. The risk of contact with other materials should be minimised, and surfaces should be cleaned in an ultrasonic solvent bath and air dried before examining with the SEM, especially if they are ceramic test-pieces which require coating with a conductive layer before examination.

(a) (b)

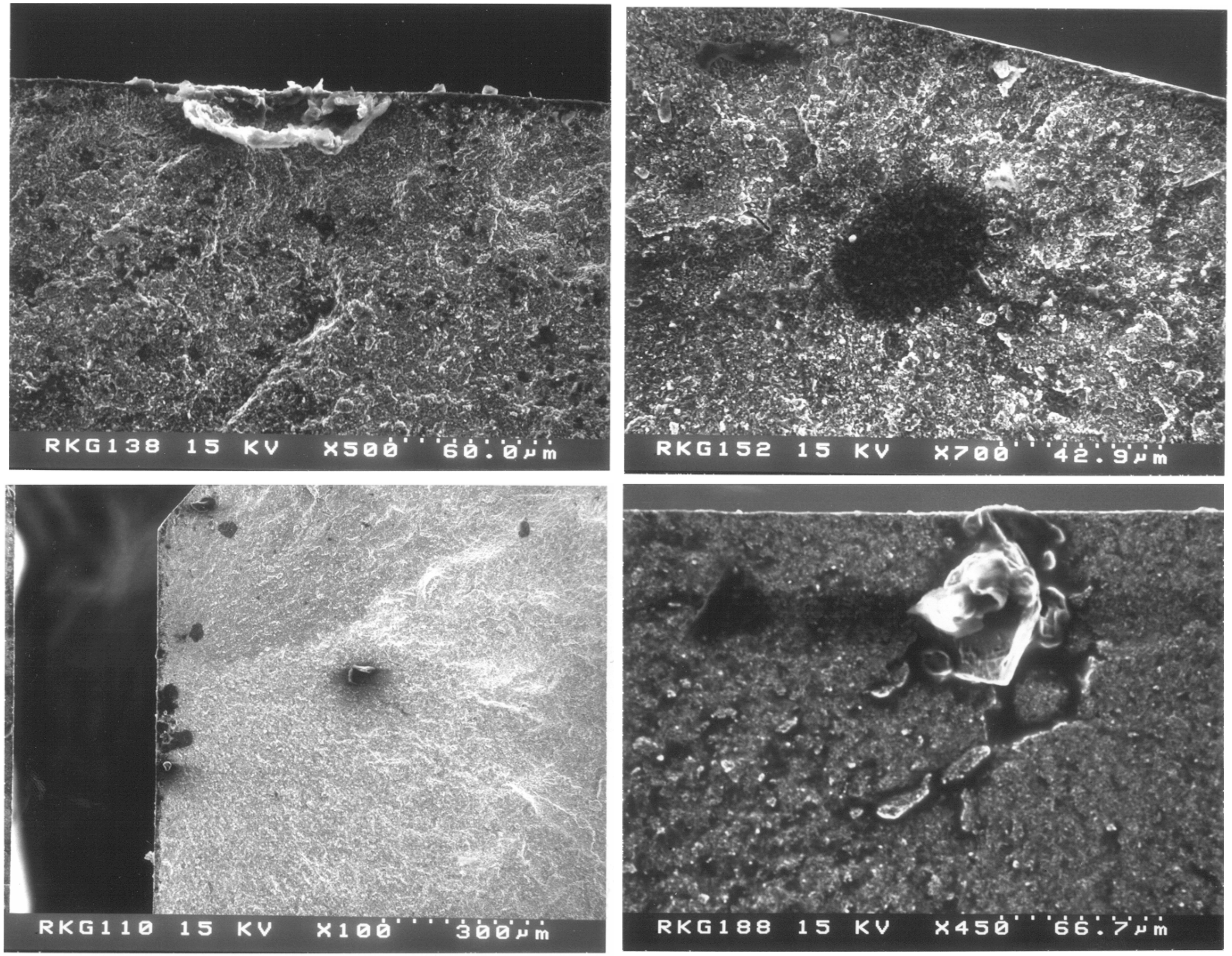

(c) (d)

Figure A.2.13 Misleading effects in fractography, (a) skin fragments in a surface pore, (b) grease spot, (c) adherent debris, and (d) skin over a fracture origin

A.3 Biaxial disc flexural strength test-pieces

These tend to pose greater problems for analysis owing to the larger number of fragments produced and the greater area of fracture surface to examine. It is often helpful to prevent the fragments flying apart during the test by placing a piece of adhesive tape on the compression side. This does not influence the fracture stress, but keeps all but the smallest fragments in relative position. Care needs to be taken that the fracture surfaces do not fret, and that the adhesive on the tape does not spread across the fracture surfaces. However, generally this is outweighed by the advantages of being able to fold the fragment mass along the line of suspected primary fracture to reveal possible origins.

The principal steps are as follows. Firstly assemble the fragments and examine the pattern of failure. Then examine the fracture direction on each fragment to get a systematic picture of the sequence of events. There will be a primary fracture, which may fork several times, and there may also be secondary fractures where the larger fragments break again from different origins. The pattern is related to the material toughness and the stored energy at fracture. Finally, identify the likely position of the origin and examine the matched fracture surfaces close to this point.

Two examples (A.3.1 and A.3.2) are given.

Example A.3.1 - microwave dielectric ceramic (1)

Microwave components are often in simple shapes such as cylinders or discs. In this case, ring-on-ring disc biaxial flexure tests were performed to determine fracture strength. This particular disc showed relatively high strength (150 MPa) for this type of material with low toughness, and ten fragments were produced on fracture, (a), viewed from the tensile side. There is good "tree-like" symmetry to the pattern, and all the fragments appear to have been produced by forking of the fracture path, a fact determined from the apparent directions of propagation revealed by the fracture surfaces, (b). The symmetry and forking pattern suggest that the origin should be in the fracture region corresponding to the trunk of the tree. Pairing up the fracture surfaces of this region reveals the origin (c) with radiating fracture marks, and higher magnification (d) shows that the origin is a small discrete defect, possibly an inclusion or agglomerate, intersected by the lapped surface of the component. In this case, the position of the origin was found to be outside the most highly stressed region of the test-piece defined by the inner of the concentric loading rings used to stress the test-piece.

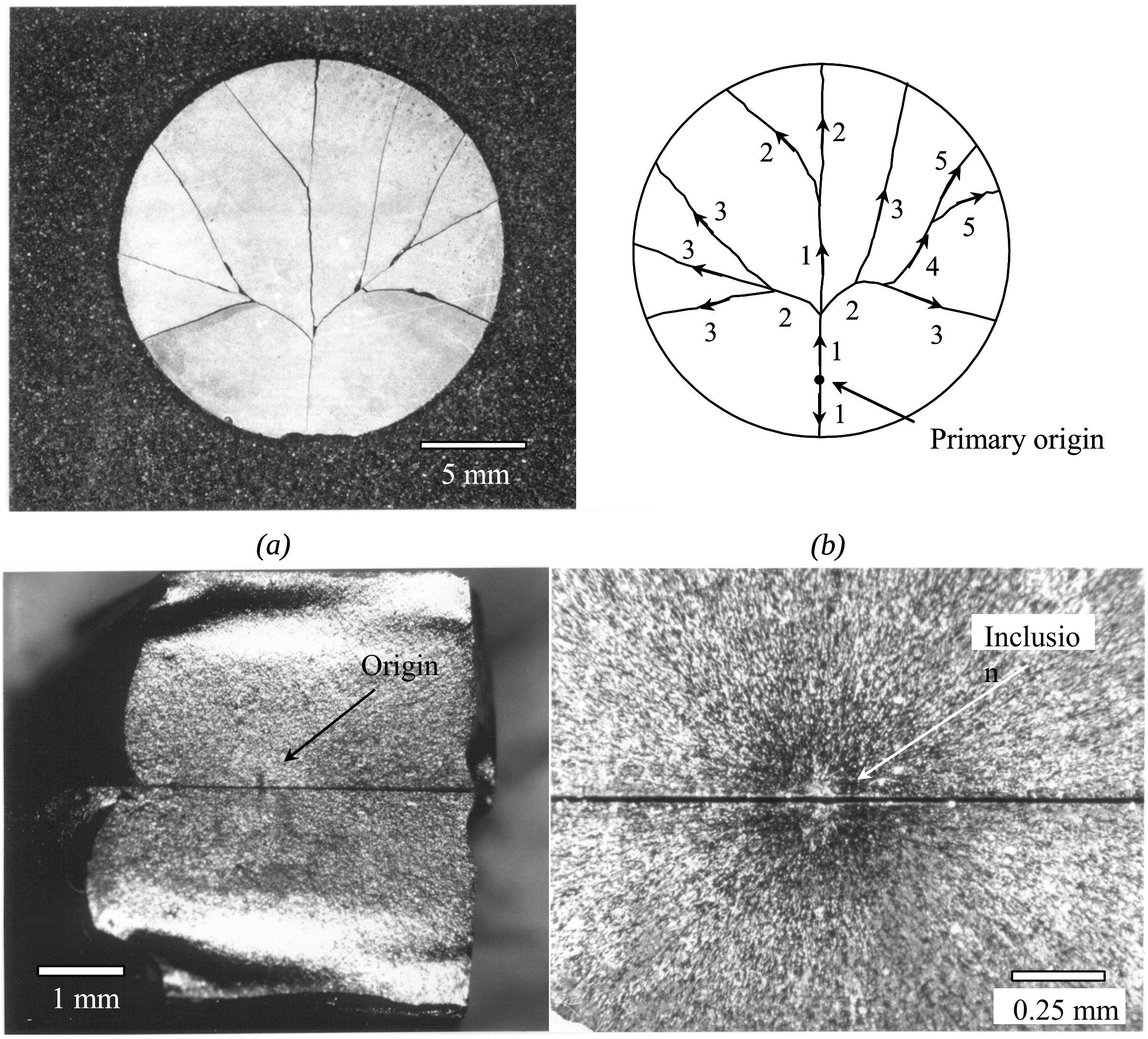

(c) *(d)*

Figure A.3.1 - Microwave dielectric ceramic disc tested in ring-on-ring geometry with failure initiating between the loading rings, showing (a) assembled fragments viewed from the tensile side, (b) crack propagation directions determined by observing the fracture surfaces, numbers referring to the sequence of branching, (c) matched fracture surfaces showing the origin with no crack branching typical of a low toughness material, and (d) the origin as a surface intersected inclusion.

Example A.3.2 - microwave dielectric ceramic (2)

This example shows that a similar material to the previous example subjected to the same mode of loading can behave in a totally different way. In this case, the test-pieces have been unidirectionally diamond ground rather than lapped. The assembled fragments are seen from the tensile side in (a), which indicates that the tree-like appearance is absent. Evaluation of the fracture surfaces shows two possible origins, A and B, and a set of fracture directions in which only some fragments are produced by forking (b). However, consideration of the fracture directions suggests that the strength-limiting origin is A, which broke first producing forking to give fractures 1 and 2. The large remaining area, still under the influence of the testing machine force but with a loss of stiffness compared with symmetrical disc geometry, then broke from B, producing forked fractures 3. When the fracture surfaces are paired (c), the fracture lines from origin A can clearly be seen to focus from outside the test-piece surface, which suggests a semielliptical machining flaw, which is clearer at higher magnification (d). In fact, reference back to the assembled fragment pattern in (a) shows that the origin orientation lines up with the grinding marks on the surface, providing confidence in this explanation. In contrast, the secondary origin B (e) shows a rather different pattern of fracture markings, possibly from a weak ligament between the test-piece surface and a pore or inclusion. The crack then ran around the pore, rather than propagating uniformly, giving the swirl appearance. Scanning electron microscopy would be needed to identify the real nature of the origin.

Examination of other test-pieces from the batch showed similar types of origin. In the case shown in (f), the origin is seen to be aligned with machining marks, but quickly changes direction as the crack starts to run, leaving a marked local undulation in the crack line. There is also a small flake removed from the tensile surface at this point. These features are consistent with machining damage limiting the strength of the component.

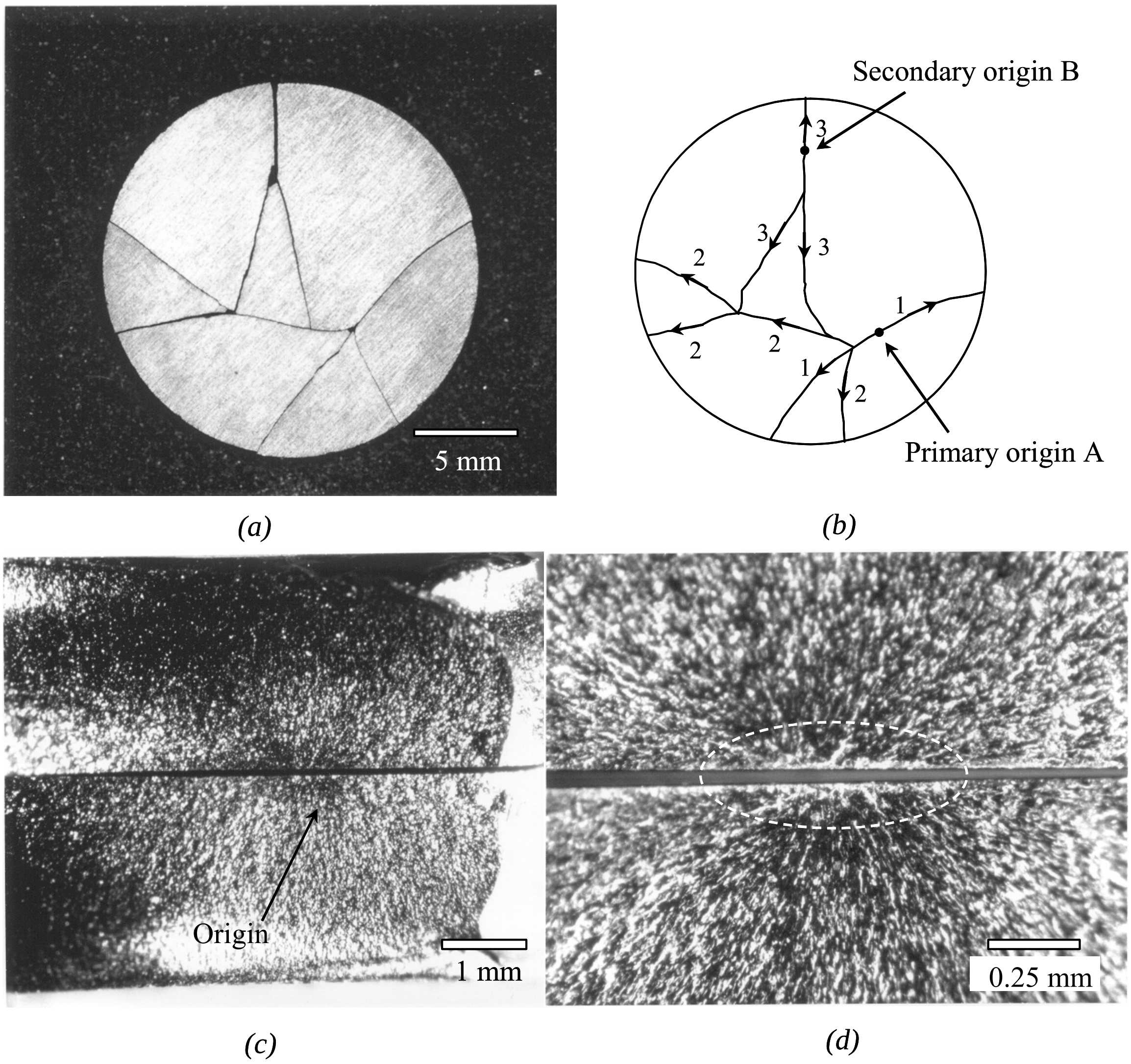

Figure A.3.2 - Microwave dielectric ceramic disc tested in ring-on-ring geometry with failure initiating inside the inner loading rings, showing (a) assembled fragments viewed from the tensile side; (b) crack propagation directions determined by observing the fracture surfaces, numbers referring to the sequence of branching; (c) matched fracture surfaces showing the origin with no crack branching typical of a low toughness material; (d) the origin as a probable machining flaw of extended width as marked by the dotted line.

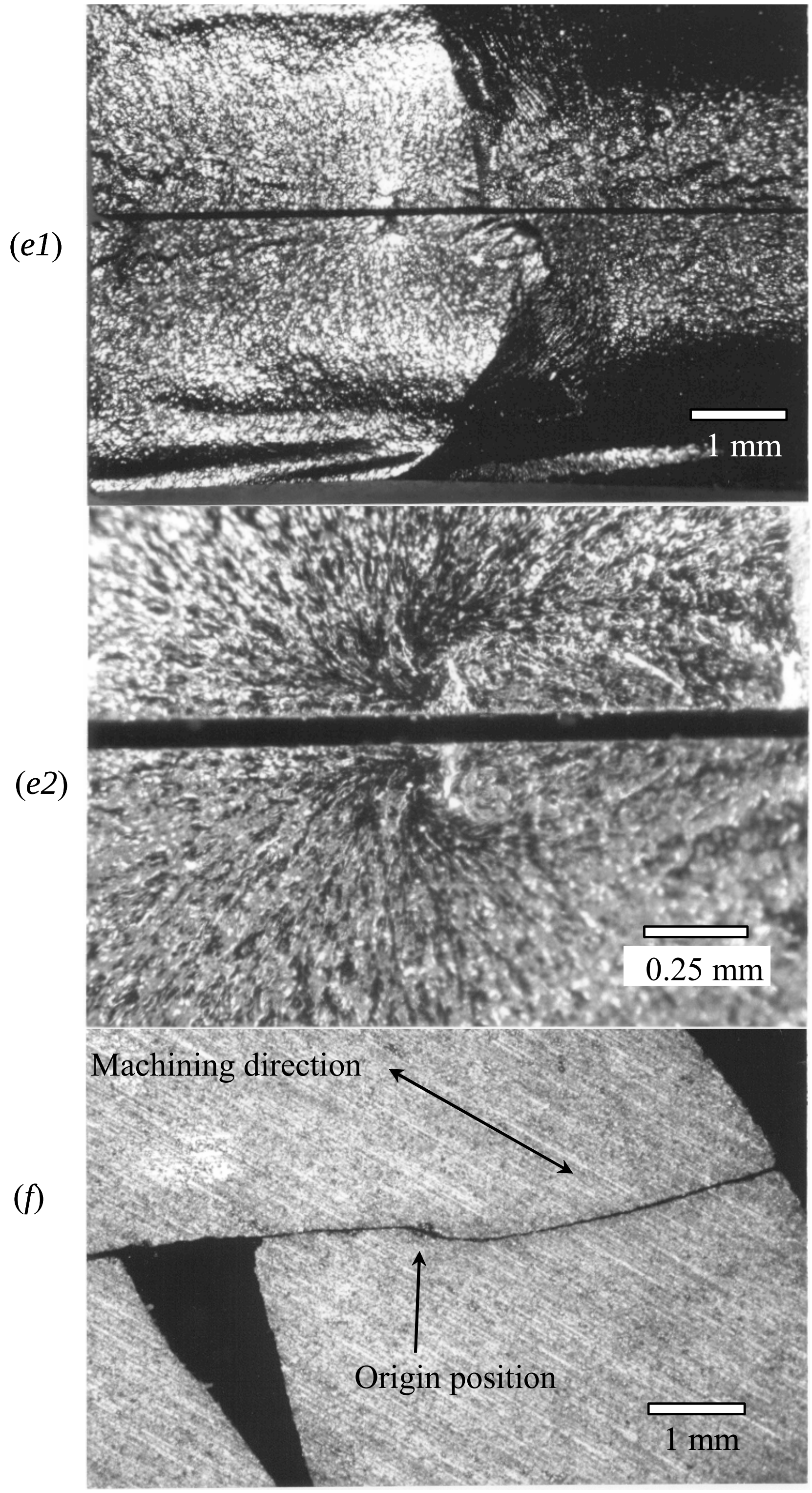

Figure A3.2 (cont.) - (e1) Matched fracture surfaces at secondary origin B, (e2) the origin at higher magnification showing fracture commencing leftwards and the tracking round to the right, and (f) the origin in another test-piece with the flaw aligned with machining marks.

A.4 Fractures in ceramic components

Piecing the story together relies on first documenting all the available fragments, and then solving the jigsaw puzzle. In order to identify the sequence of fracturing, the general pattern of cracks and the possible directions of cracking have to be determined to produce a map, from which the possible origin site or sites can be identified. The more information that can be gathered on the type of material, how it is normally assembled into a device, how the device is used, and what events might have led up to fracture, the easier this makes the task of analysing the fractures and coming to self-consistent conclusions.

Some of the key features to bear in mind are the design of the component and the processes of manufacturing and/or machining to produce it in relation to the forces applied to it. Details such as notches, grooves, sharp internal corners, sharp edges, localised gripping, localised impact, all act as stress concentrators, and can be placed high on the list of possible causes of failure. Four examples are given (A.4.1 to A.4.4) from different fields of use[3].

Example A.4.1 - ceramic machine base

This is an example of poor design philosophy identified by fractography. The electrically insulating ceramic base-plate of a small mechanical testing machine had broken in three parts at lower than the maximum predicted machine performance. The plate was subject to bending in use, and had broken in two places, apparently associated with machined gaps in a side ridge (top in (a)), but in one case running through some tapped holes (A) aligned with the side one of these gaps. Examination of the fracture surfaces near A revealed a slight compression lip on the underside of plate, as exemplified in (b) which shows matching sides of the fracture passing through the two tapped holes, but the markings on the surface were weak compared with general roughness of this low-strength, medium grain size material. The only unusual feature was near the plain bolt-hole B in the right-hand machined gap there was a lip in the fracture surfaces, the respective appearances being seen in (c). Using dye penetrant, closer examination of the machined surface in the region of the hole revealed a ring mark around the hole (d), and at higher magnification, a tangential crack can be seen emanating from this ring (e). Further examination of other bolt-holes revealed these also to have similar ring marking and associated cracking.

It can be concluded that a combination of the bending of the plate, the square-cornered gap in the side ridge and the development of cracks around bolt holes due to the use of hard, non-load-spreading washers on a soft but brittle ceramic material all contributed to poor performance.

The premature failure can probably be assigned to the pre-existence of the bolt-hole cracking, but the final paths of fracture were associated with the highest stress concentration in the gap

[3] The opportunity to study a series of component failures was made by R Wallis of John Crane UK Ltd, to whom grateful thanks are expressed for permission to use the findings as Example A.4.4 in this guide.

in the side ridge. The second fracture associated with the tapped bolt-holes can probably be considered to result from the unloading shock, and needed to originate at three sites to create the three separate parts. As seen in (b), this may have initiated at the sharp corner adjacent to the bolt-hole.

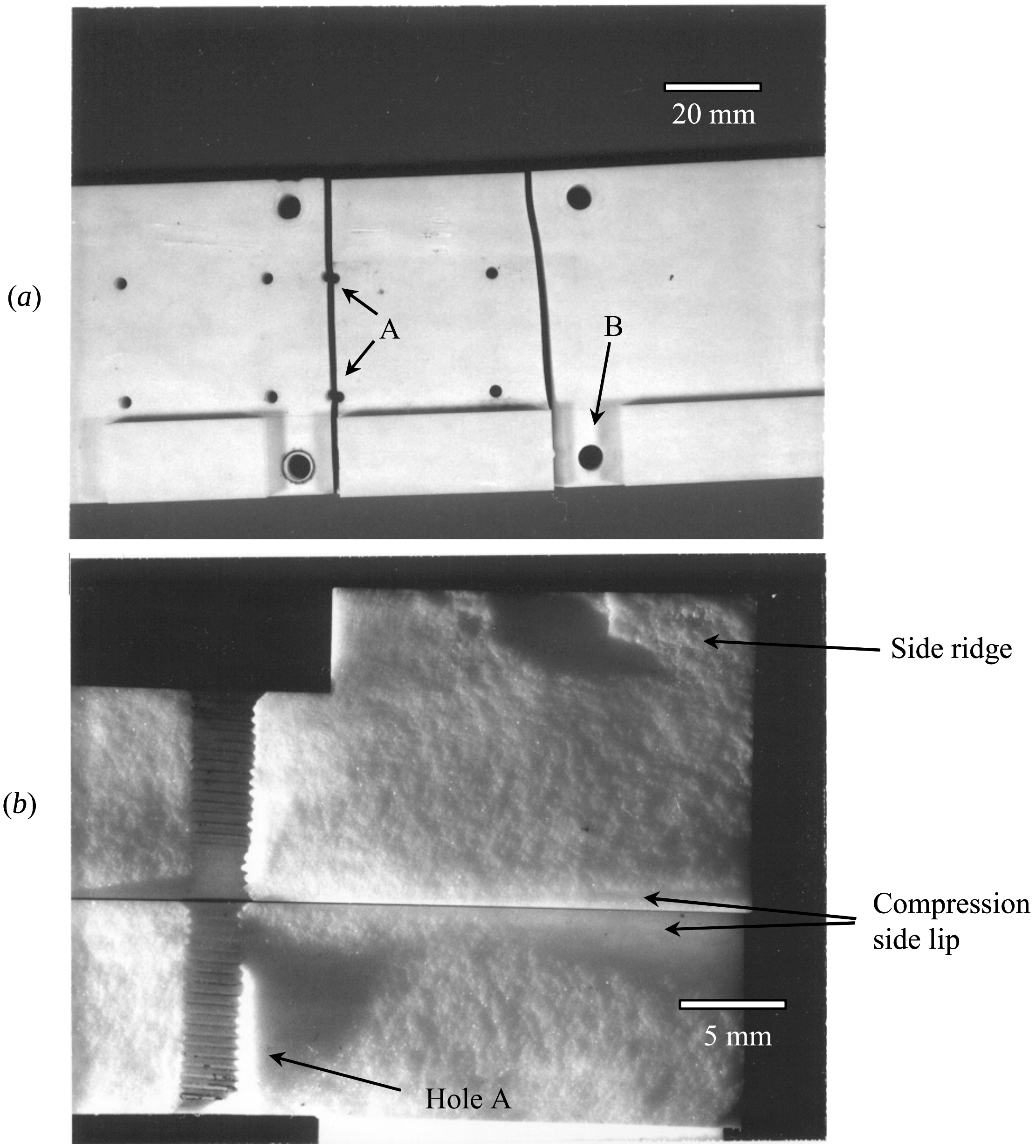

Figure A.4.1 - Fractured ceramic machine base showing (a) two main cracks with two identified holes A and B, and (b) the paired fracture surfaces adjacent to threaded hole A.

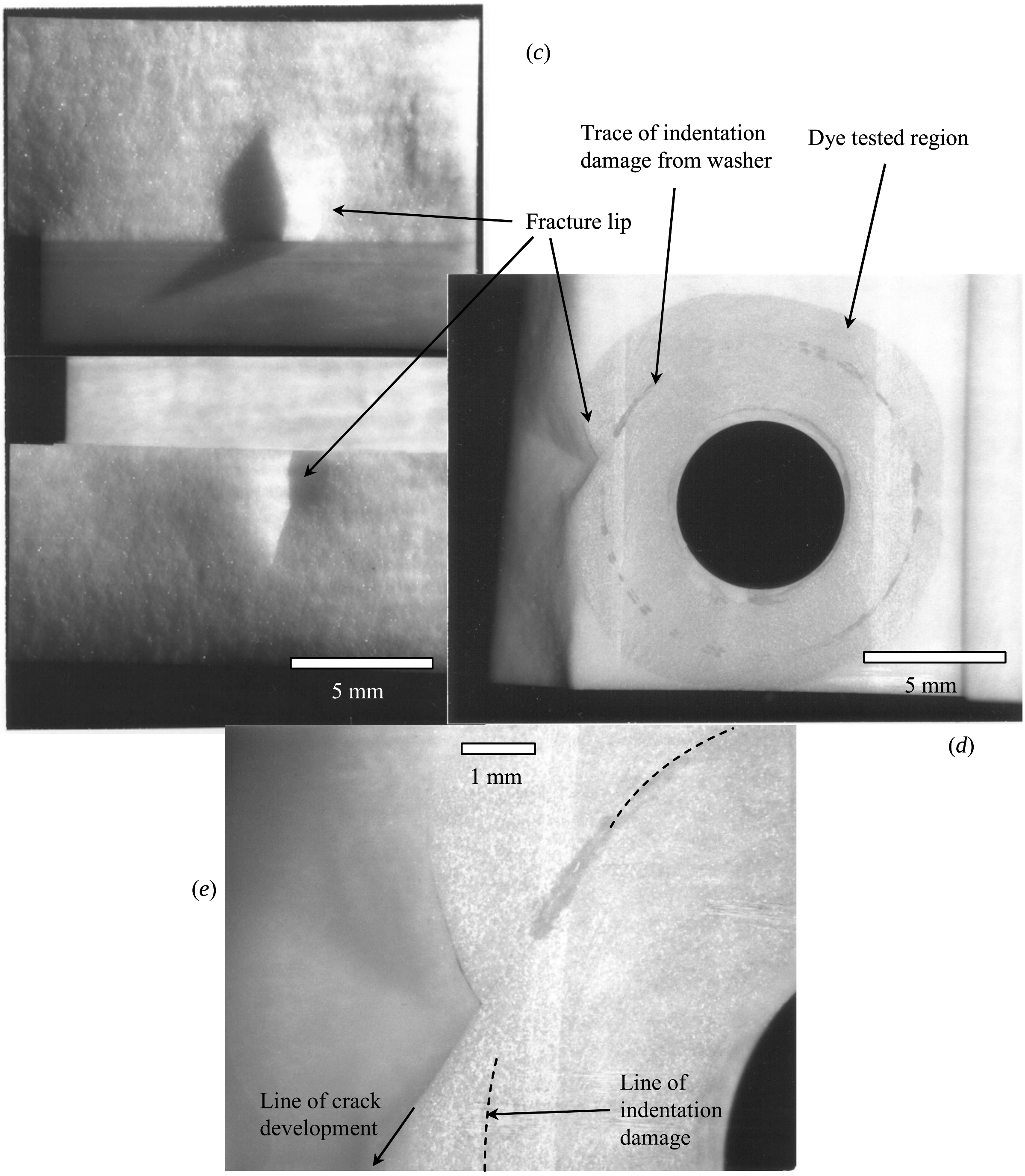

Figure A.4.1 (cont.) Ceramic machine base showing (c) matched fracture surfaces adjacent to hole B, with matching raised and depressed features, (d) plan view of hole B showing area subjected to dye penetration testing which reveals indentation damage due to the sharp edge on a washer, and (e) detail from (d) showing the development of a tangential crack from the line of indentation damage, forming the feature seen in (c).

Example A.4.2 - ceramic ball valve

A large (150 mm diameter) ball valve from a chemical plant unexpectedly split in two. It was unclear whether the ball split when attempting to turn it via a metal insert in the large slot in the upper end, or when the pipeline it was in was left filled with water in freezing conditions. The ball split into two more-or-less symmetrical halves across the slot (a). There are therefore three parts to the fracture surface, each of which must have its own origin, raising the question of which region broke first. Examination of each of the fracture surfaces shows that one (top left in (a)) was relatively smooth compared with the other two, suggesting that this was the lowest energy failure, and therefore the one likely to have the largest origin size. Fracture markings on this surface suggest that fracture initiated from the main cylindrical bore surface about two-thirds of the length along from the outside edge (b), rather than from the slot surface. The upper right surface (c) shows a higher energy fracture with some crack branching, probably initiating from the corner of the slotted hole, while the lower surface (d) has a classical high-energy flexural fracture appearance with a distinct mirror, crack branching predominantly to the sides, and a surface or near-surface origin (e).

The overall diagnosis is therefore that the ball split under internal pressure, first at the upper left side, then at the upper right side, and finally at the lower side, rather than as a result of torque being applied via the slot, which would probably have resulted in a more complicated set of fragments with fracture initiation from near the ends of the slot. It can therefore be concluded that this was an operational error rather than a material problem. However, the design can in any case be considered to have limitations. In particular, the inner edge of the slotted hole is not chamfered, and this can act as a stress raiser under any operational condition. While difficult to access with a suitable grinding tool, means should be found to chamfer this edge, possibly by as much as 1 to 2 mm, which would improve reliability.

(*a*)

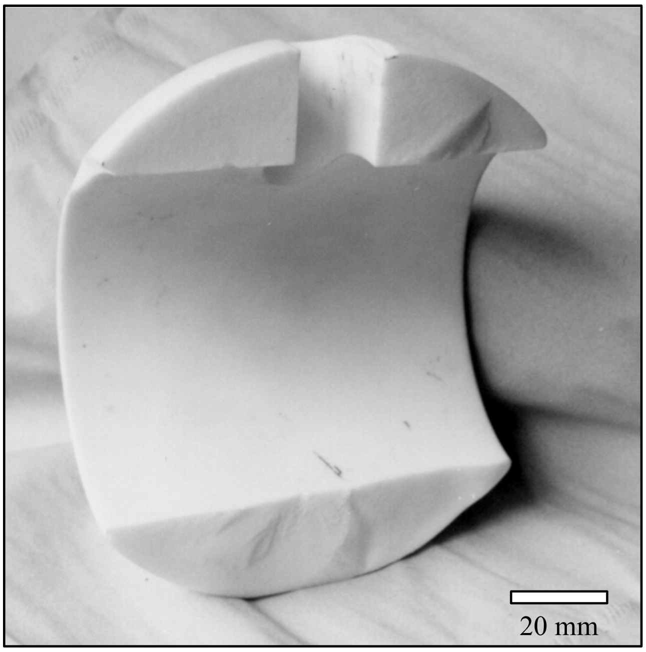

Figure A.4.2 - One half of a fractured ceramic ball valve exhibiting (a) a clean diametral break and three distinct fracture surfaces.

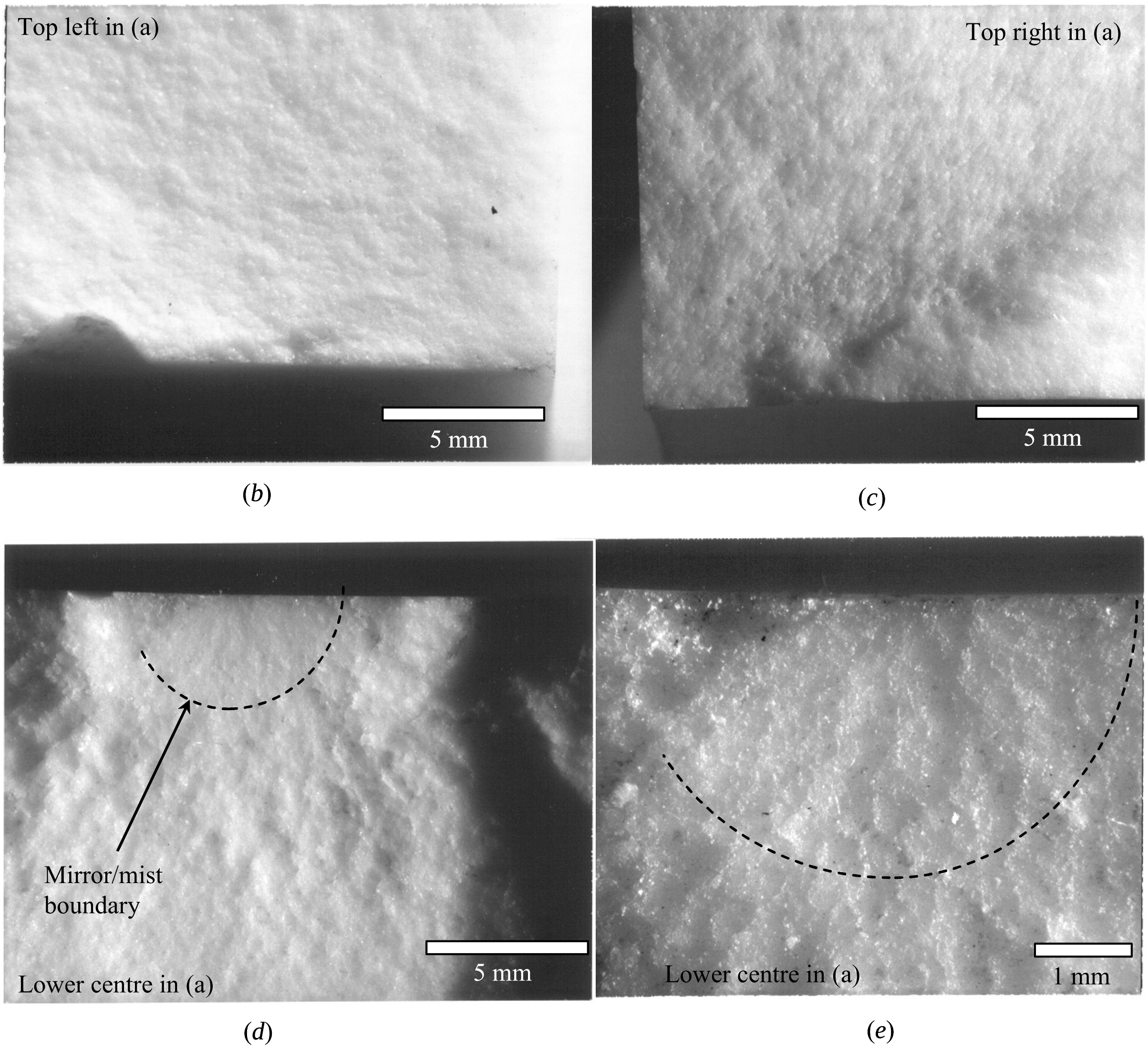

Figure A.4.2 (cont) - Ceramic ball valve fracture surfaces under grazing incidence illumination showing (b) region to top left in (a) with a smooth fracture surface but an unclear failure origin, (c) region to top right in (a) with failure from the corner, (d) the lower centre region in (a) with a clear high-strength fracture pattern with a distinct mirror, and (e) as (d) but at higher magnification.

Example A.4.3 - gas valve plate

A small gas valve plate containing small holes, one of a mating pair, had broken across the holes, (a). The material was a dark-coloured, fine-grained alumina. Examination of the matched pair of fracture faces revealed some missing fragments, but some evidence from radiating fracture markings that the fracture initiated from one of the holes when viewed under grazing incidence illumination (b). The lower side of the hole was more likely to be the initiating site than the upper side because the markings are weaker, indicating a lower energy fracture. At higher magnification (c), the translucence of the material precluded observing any specific origin, although it was clear that the unchamfered exit to the hole might act as a source of machining damage when the faces were lapped. When observed in the scanning electron microscope, a number of features were found near the suspected origin, although none were strictly abnormal for the material. In (d), a large grain is seen on the hole surface immediately below the corner, while close by in (e) is a cusped pore, a residual feature of the incomplete collapse of spray-dried granules during pressing. This latter type of feature was widespread and rendered the fracture surface quite rough, and although classical fracture markings could be seen at low magnification, they disappeared at high magnification in the SEM. In view of the failure occurring in an otherwise low-stress application, where there should be little or no bending force applied to the component, it has to be concluded that an unfortunate combination of possible lapping damage at a hole edge, coupled with the local microstructure, and some abnormal assembly or use condition, resulted in the failure.

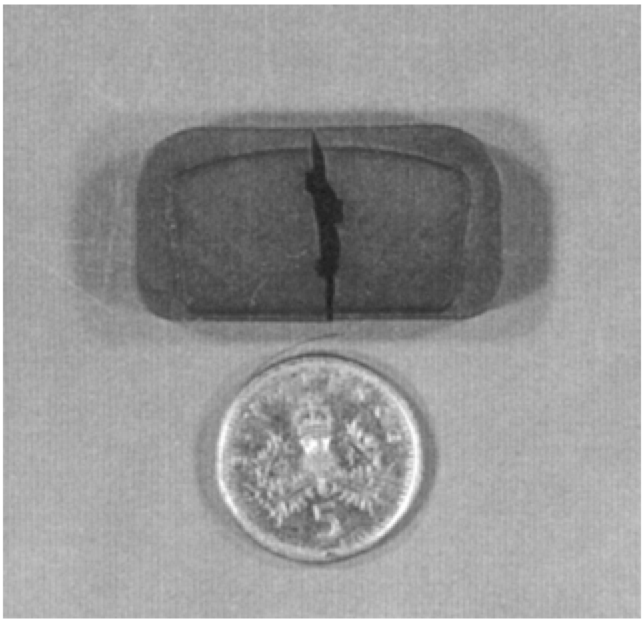

Figure A.4.3 - Gas valve plate (a) which has fractured into two pieces across the series of gas passage holes, with evidence of missing fragments.

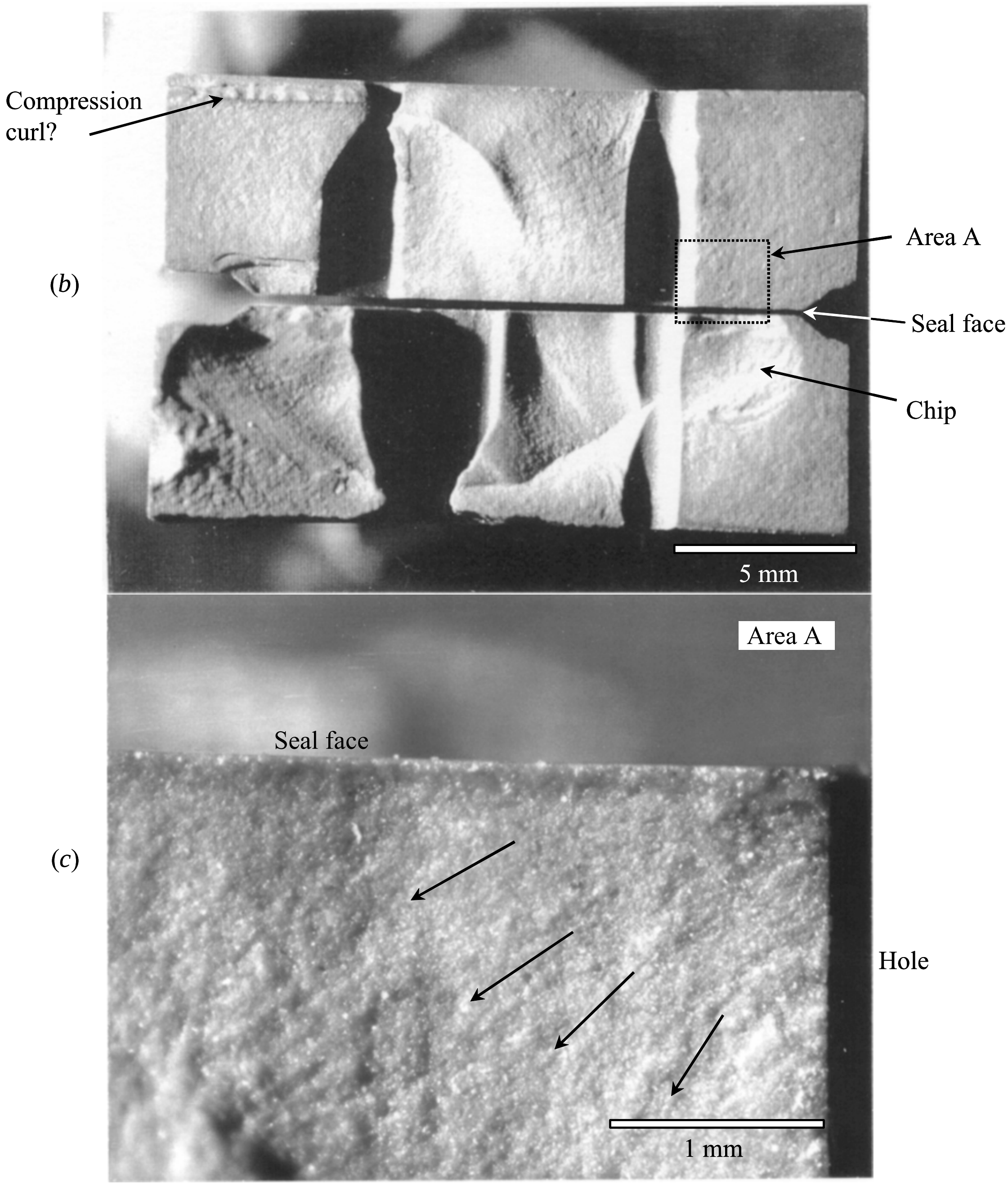

Figure A.4.3 (cont.) - Gas valve plate fracture showing (b) matched fracture surfaces indicating missing fragments but with the suspected tensile faces together, and (c) region adjacent to the unchamfered exit hole which might conceivably have been a low-stress fracture origin.

(*d*)

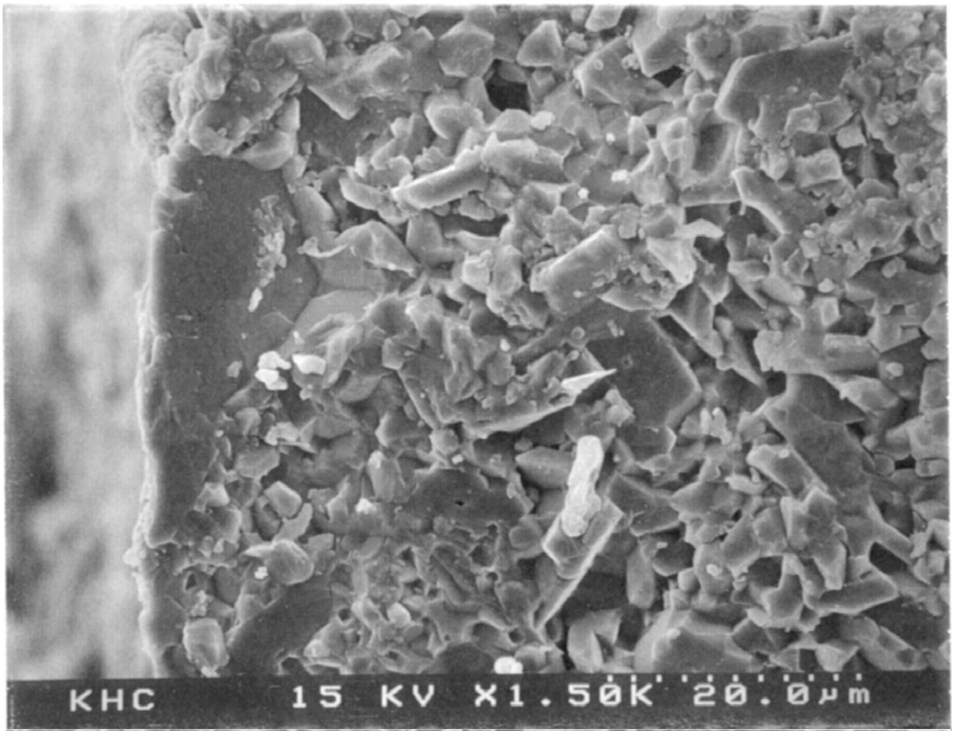

(*e*)

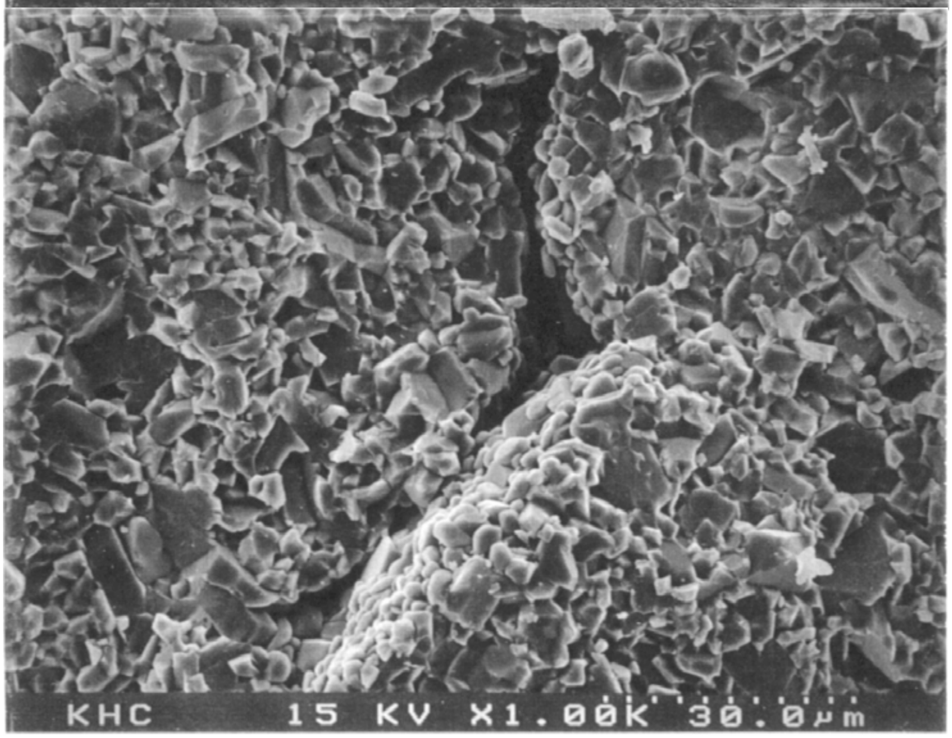

Figure A.4.3 (cont.) Gas valve plate fracture surfaces showing (d) a large grain adjacent to the exit of one of the holes, and (e) a cavity resulting from incomplete compaction of spray dried granules, either of which could be the origin of failure.

(Intentionally blank)

Example A.4.4 - mechanical gas seal rings

A number of failures had occurred in silicon carbide ceramic mechanical seal rings, which in service rotate at high speed. A problem was fragmentation, and the need to collect and reassemble a large number of fragments, but having done this, a number of different types of failure could be identified.

Case 1: failure from the outside edge. Reassembly of the fragments produced the pattern shown in (1a). There are five main areas of fragmentation, three of which give the impression of having started from the inside surface, forking towards the outside, while one was a straight-through break and one was straight but discontinuous. Examination of fracture directions showed that only the straight fractures ran inwards, while the rest ran outwards. Examination of the single straight-through, bifurcating crack (at the right) showed that it was associated with extensive chipping damage on the outside surface (1b), resulting in loss of the immediate origin (1c, 1d), but the propagating crack shows fracture markings radiating from the chamfered edge, which after a distance of about 8 mm became strongly hackled. Assuming this site is the initial origin, the remaining fractures can readily be explained by the bending forces that can be applied to the ring once it is split, opening it up like a C-shape. ***Conclusion: localised external impact damage***.

Case 1:

(*a*)

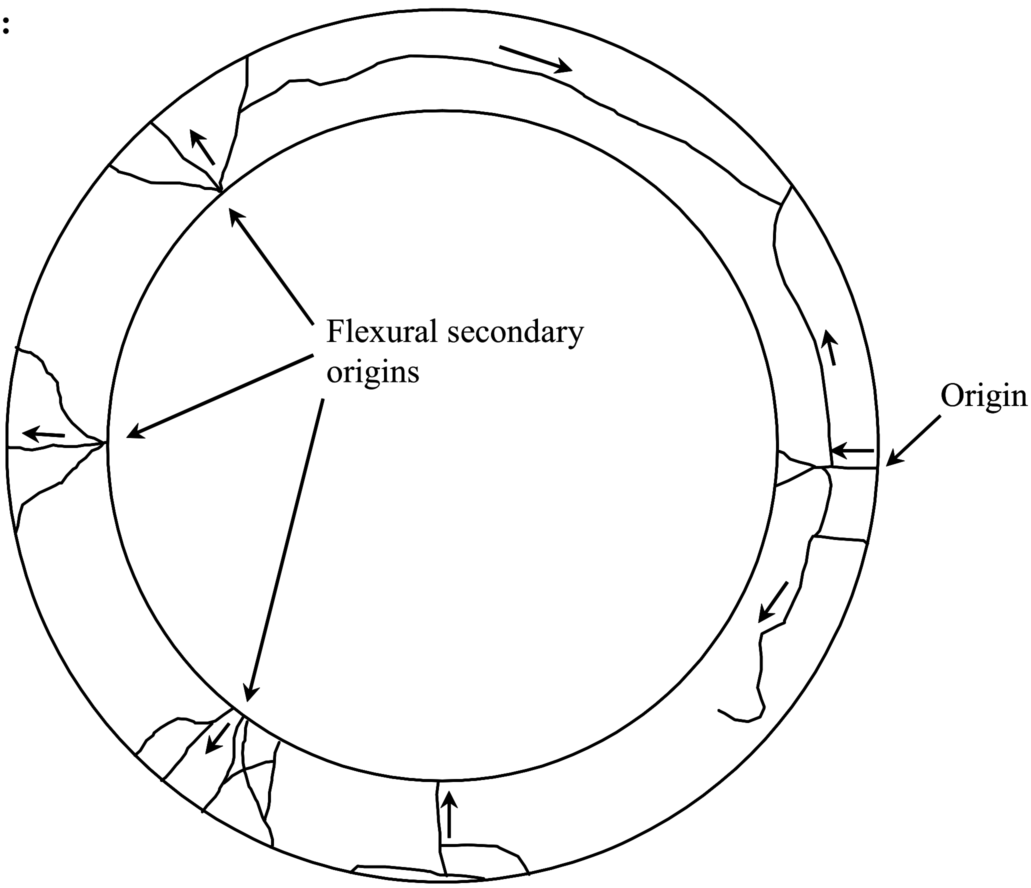

Figure A.4.4.1 – Large mechanical seal ring showing (a) a schematic representation of re-assembly of fragments with fracture directions marked

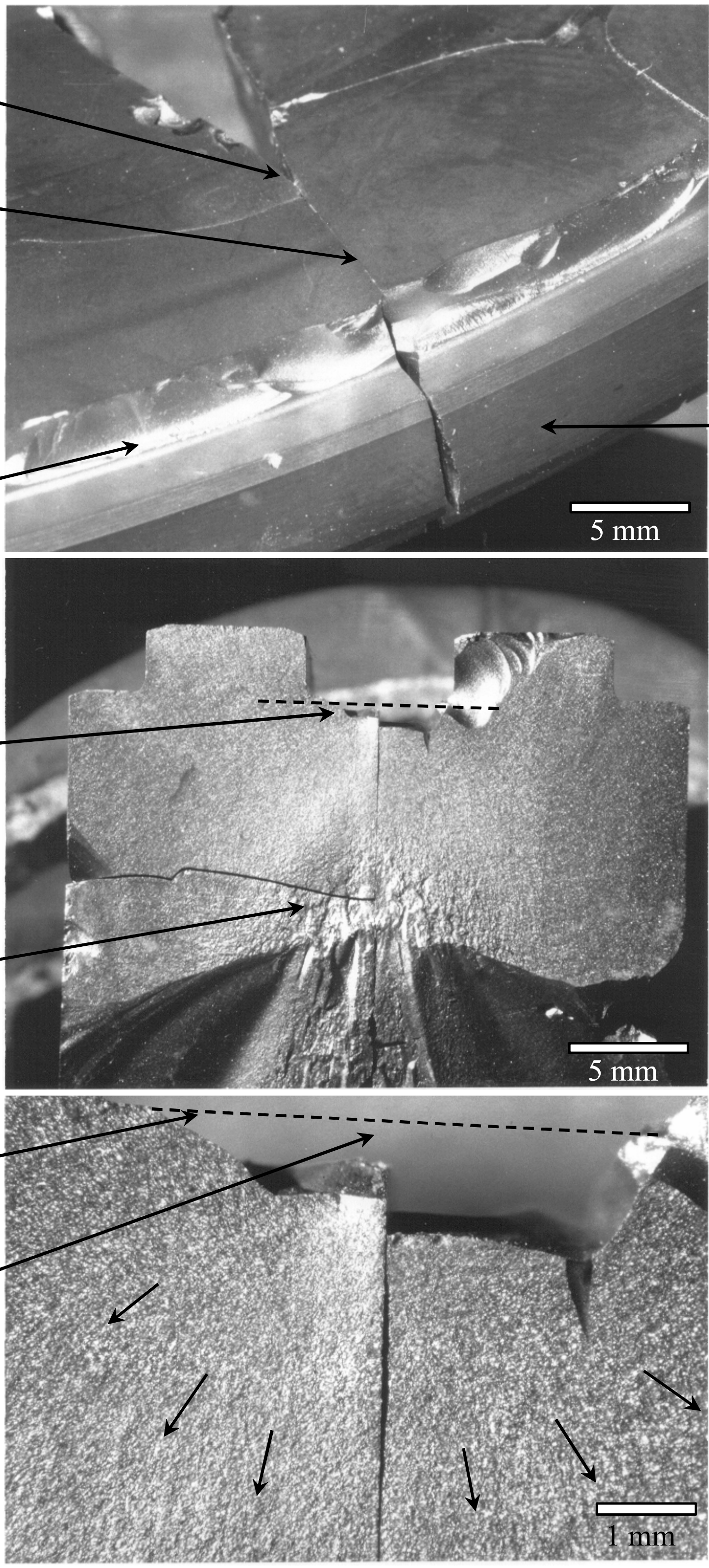

Figure A.4.4.1 (cont.) - Mechanical seal fracture showing (b) extensive chipping inside an external edge flange associated with the suspected primary origin, (c) matched fracture surfaces containing the suspected origin, with the fracture pattern suggesting that the actual origin is missing through chipping, and (d) as (c) at higher magnification with fracture marking directions indicated.

Case 2: failure from a back face: This example showed a fairly simple crack pattern with two large, near-semicircular and two small fragments (2a). The fracture between the two large fragments was found to be kinked on the lower surface near the inside of the ring, while the second forked fracture appeared like those in the previous example. Examination of the kinked region demonstrated (2b) that a pre-existing crack was the most likely fracture origin, growth initiating at its deepest extent and running both inwards and outwards (2c). The second, forked fracture occurred at an unusual just sub-surface defect (2d), a near circular disc-shaped pore at a steep angle to the average fracture surface.
Conclusion: pre-existing crack.

Case 2:

(*a*)

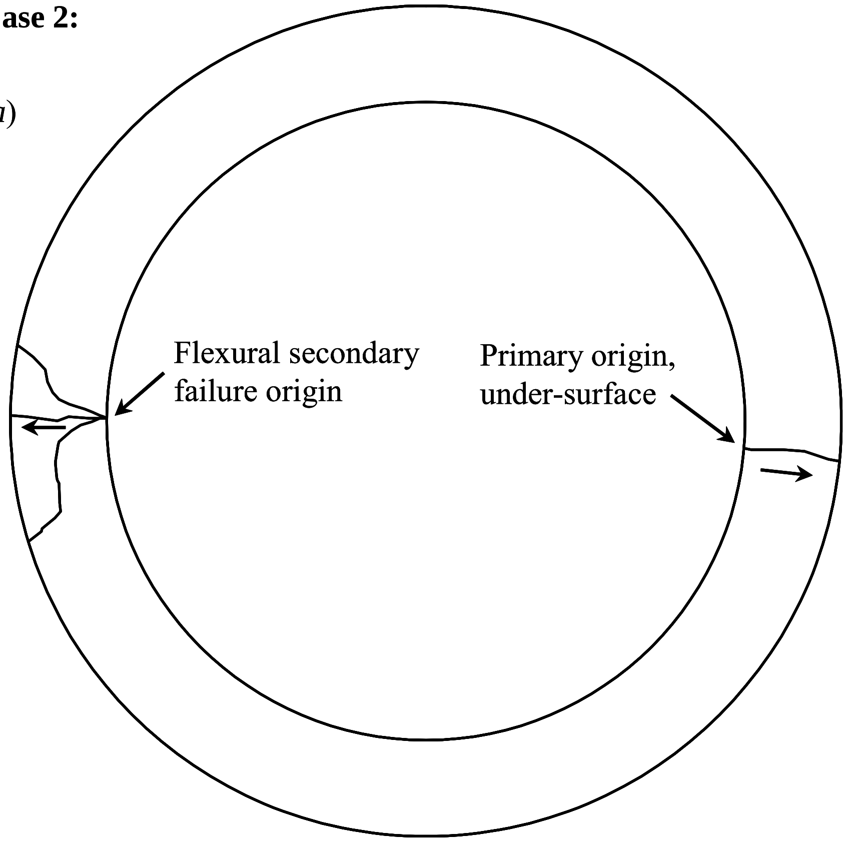

Figure A.4.4.2 – Large mechanical seal ring showing (a) a schematic representation of re-assembly of fragments with the fracture directions marked.

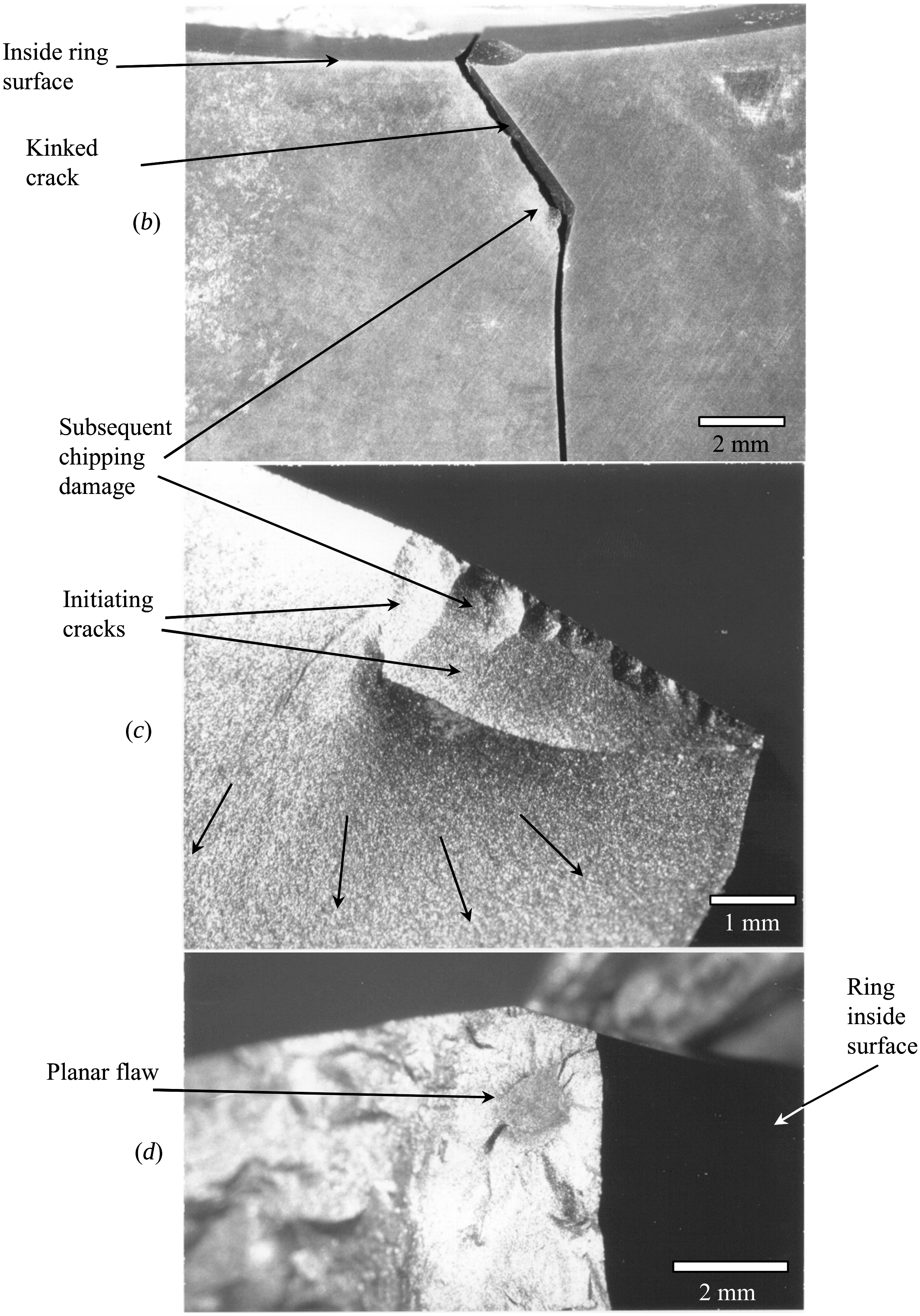

Figure A.4.4.2 (cont.) - Mechanical seal ring showing (b) a kinked fracture line on the under surface of (a) thought to be the primary origin, (c) detail of one side of the kink, showing a probable pre-existing crack from local damage, and (d) unusual planar feature, possibly a delamination, as the high-stress secondary origin.

Case 3: failure from drive notches: The gas seals have a number of notches around the periphery which are used to drive them. The notches are machined out using a diamond grinding wheel. The failure clearly originated from the corner of one of these grooves shown in plan view in (3a). Examination of the fracture surfaces (3b) shows a clear elliptical shape mirror region with hackle beyond, but the origin is not discrete. The fracture lines appear to emanate from outside the surface, which is indicative of an extended semi-elliptical machining flaw, possibly as delineated in (3c), acting as the origin.
Conclusion: machining marks.

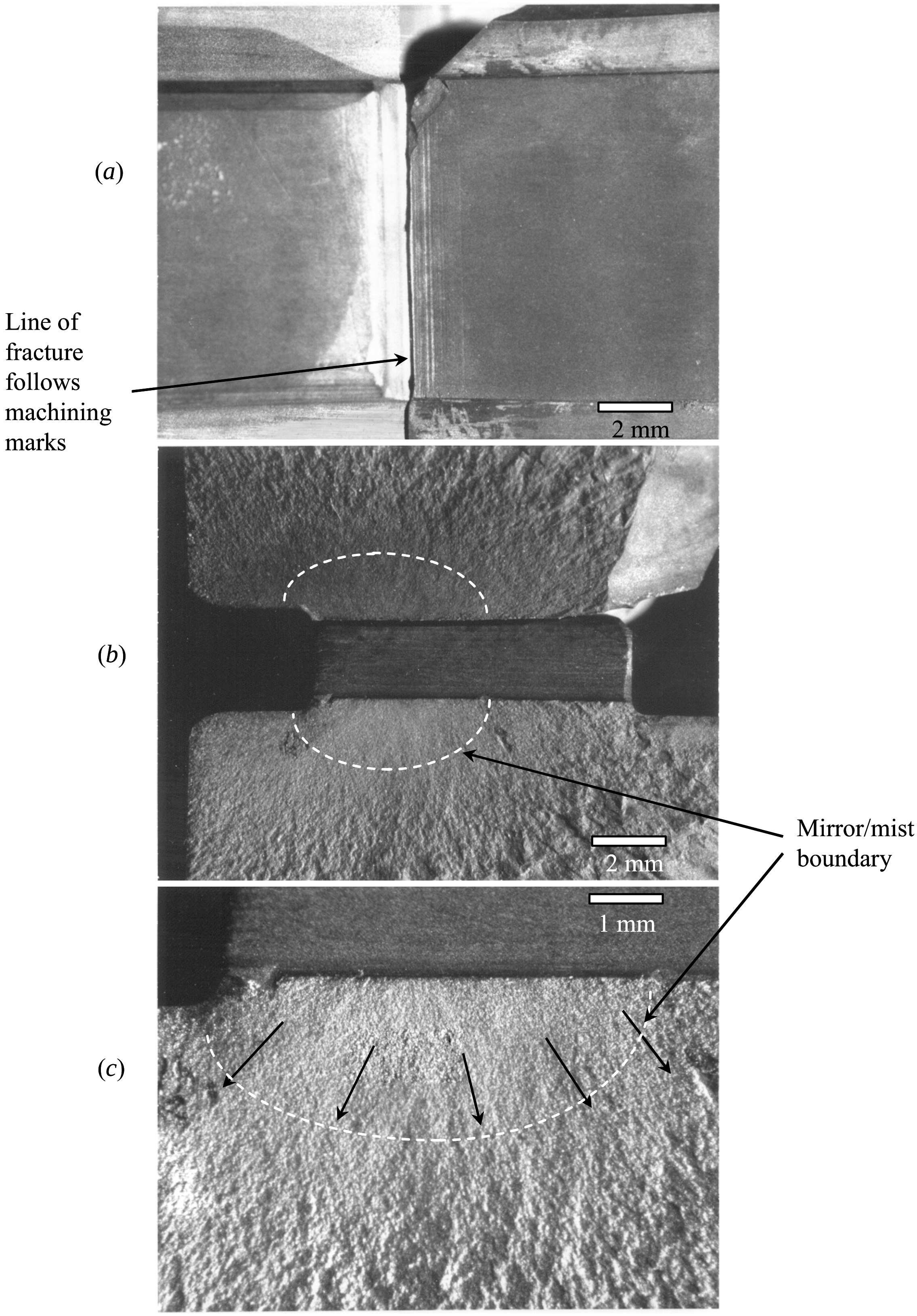

Figure A.4.4.3 - Mechanical seal fracture showing (a) coincidence of the primary fracture with machining marks, (b) matched fracture surfaces showing a large elliptical mirror zone, and (c) fracture markings with directions originating from outside the surface suggesting an extended origin from a machining flaw.

Case 4: hoop failure: This example has an unusual fracture pattern, the dominant feature being a hoop crack (4a). This initiated from the outside surface and propagated in both directions, one running out on the opposite side, and the other halting in the wall. There were some subsequent straight breaks in the inner ring. The logical explanation is that the formation of the hoop crack was the main cause of failure. Once initiated, the crack bifurcated and ran around in a hoop-wise fashion driven by the radial tensile component of the stress generated by rotation. Examination of the starting region of this crack (4b) revealed a strongly bifurcated crack pattern which showed clear evidence of a localised origin (4c), possibly a small chip or crack on the main seal face very close to the edge chamfer (4d).
Conclusion: localised external damage

Case 4:

(*a*)

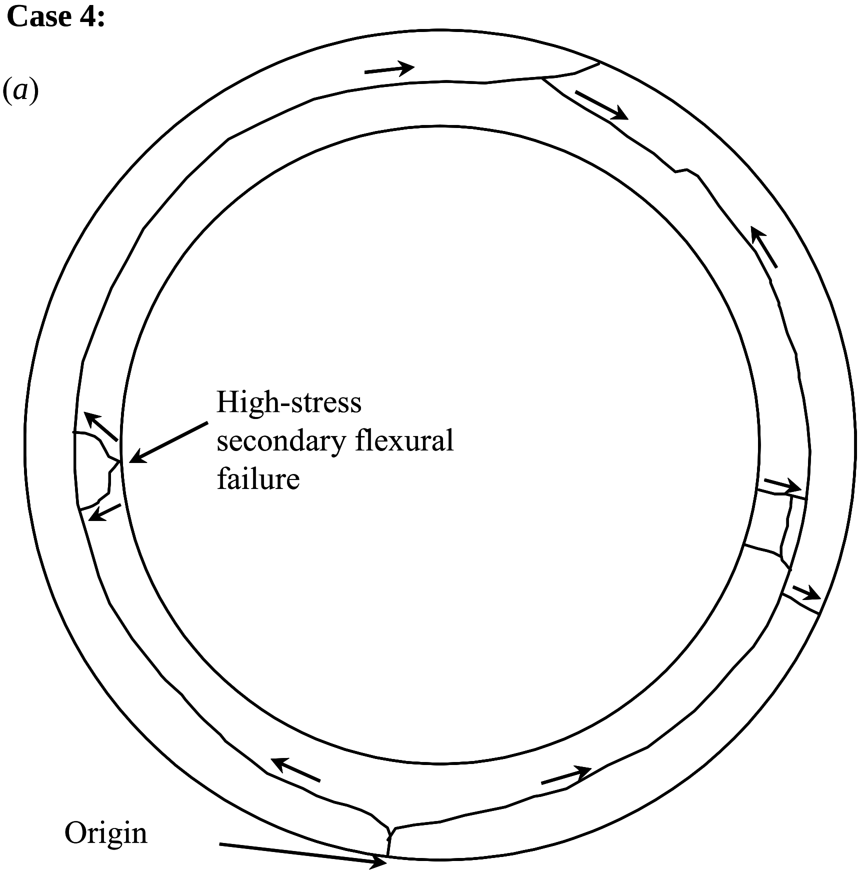

Figure A.4.4.4 – Large mechanical seal ring showing (a) a schematic representation of re-assembly of fragments with the fracture directions marked.

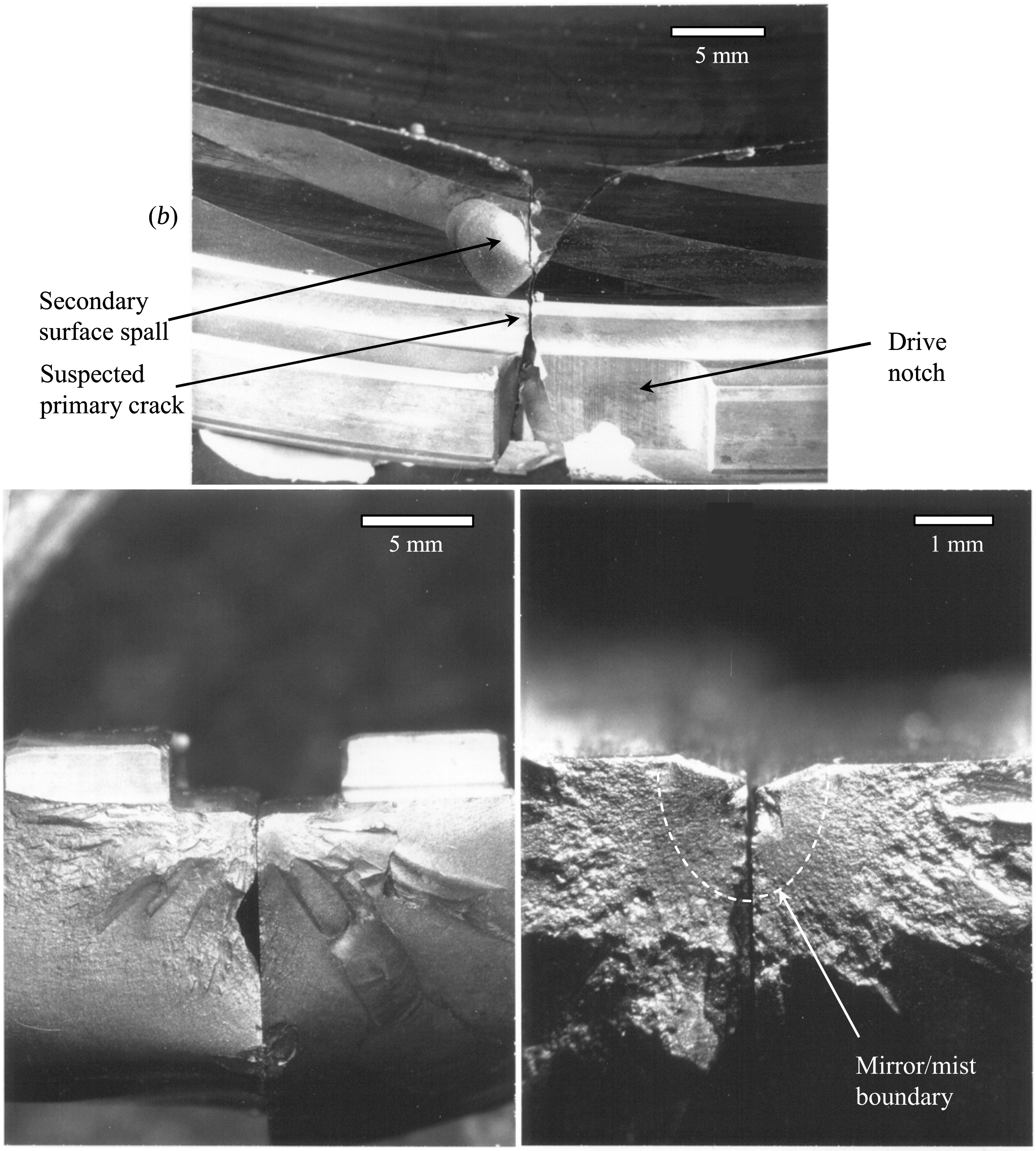

(*c*) (*d*)

Figure A.4.4.4 (cont.) - Mechanical seal fracture from drive notch, (b) showing secondary chipping, (c) fracture origin with a small mirror, strong hackle and bifurcation, suggesting high stress failure, and (d) detail of the origin with localised chipping damage and fracture lines suggesting initiation at the chamfer.

Case 5: complete fragmentation: Once the jigsaw puzzle has been correctly assembled (5a), the similarities between this and the previous case become clear. Again there is a hoop fracture, which from its appearance and directions of fracture must have originated from the inside of the ring, not the outside. The inner part of the ring showed some forked fractures suggestive of ring expansion after initial fracture, as in Cases 1 and 2, but also some planar breaks which ran some distance before bifurcating and turning in hoop direction. In two cases, evidence of Hertzian ring crack formation was found as the possible origin, both sites being near the inner ring edge on the non-working face. Either could have been the origin, but the more spectacular one (5b, 5c) produced the more distinct cone shape, and was probably the larger pre-crack, but the other also showed signs of ring-crack formation and surface contact damage (5d). It is suspected that such defects arise in handling the product, either in gripping for machining, or in assembly, and points to the need for changed procedures.

Conclusion: handling damage

Case 5:

(*a*)

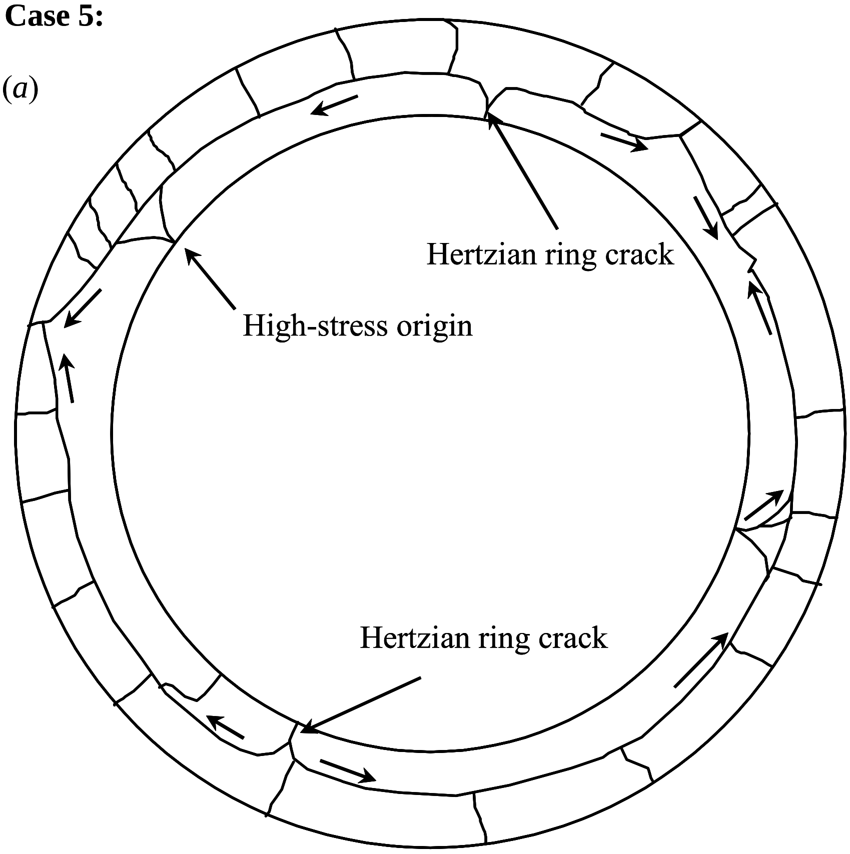

Figure A.4.4.5 – Large mechanical seal ring showing (a) a schematic representation of re-assembly of fragments with the fracture directions marked.

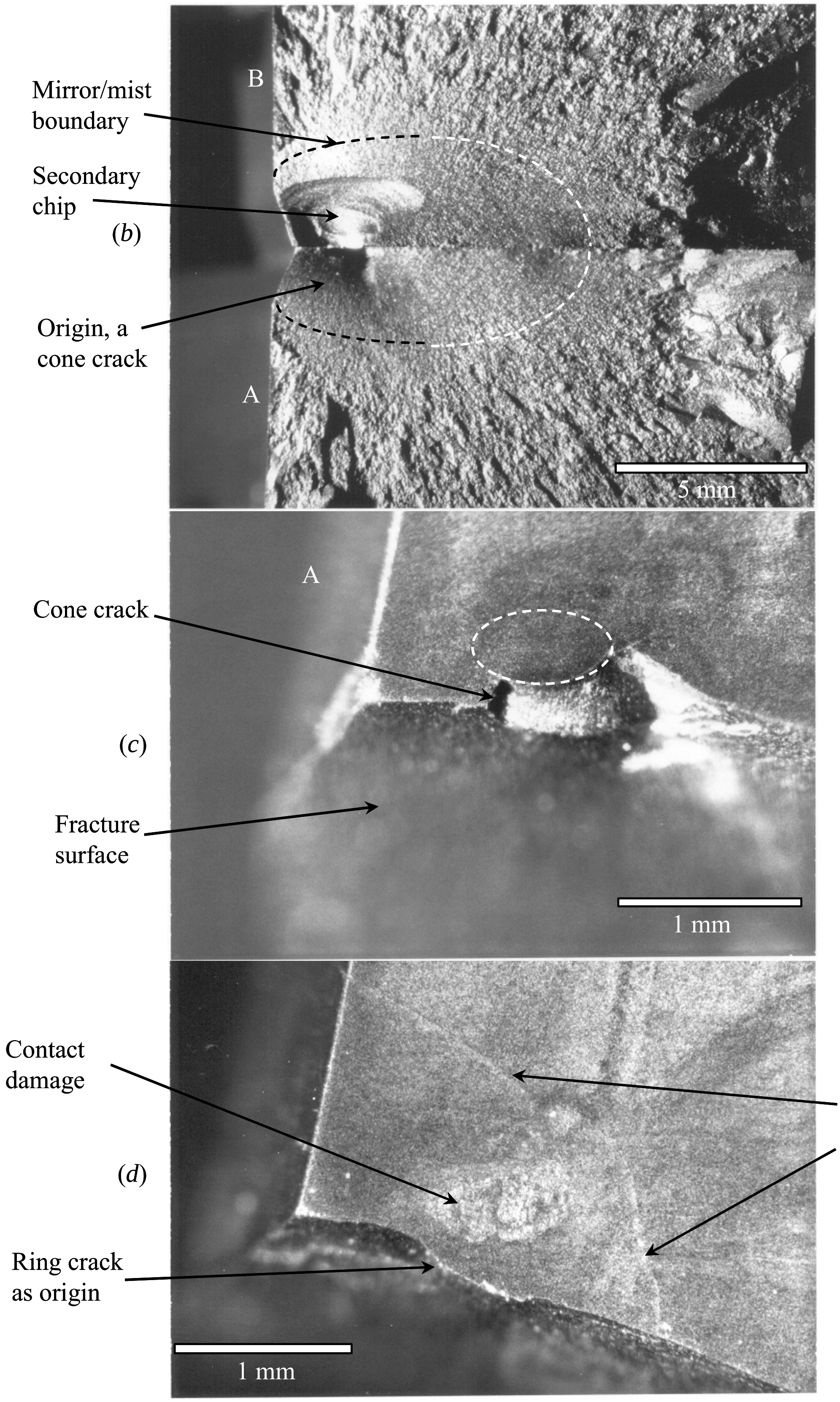

Figure A.4.4.5 (cont.) - Mechanical seal fracture showing (b) matching fracture faces with a clear mirror region, (c) the origin, which is part of a Hertzian cone crack, and (d) a similar secondary fracture origin.

Endnote

In the cases described above, emphasis has been placed on the initial stages of the diagnosis, i.e. assembling the fragments, determining the crack patterns and their relationship to the manner of use, and locating and tentatively identifying the origins. Each case could have been taken much further with additional time and effort. The circumstances of failure were documented and therefore each case would be amenable to stress distribution estimation based on formulae for stresses in spinning rings. This would permit an estimate of stress at the site of failure, which, using an approximation for the material's fracture toughness, can be correlated with the observed defect size. Comparison with behaviour in conventional flexural strength tests could provide information on material performance limits for the particular application.